ROSA FABIANA ZABALAGA DAVILA

MATHEMATICAL MODELING OF DRYING PROCESS OF UNRIPE BANANA SLICES

São Paulo
2016

ROSA FABIANA ZABALAGA DAVILA

MATHEMATICAL MODELING OF DRYING PROCESS OF UNRIPE BANANA SLICES

Thesis submitted to Escola Politécnica of University of São Paulo for the degree of Doctor in Science

São Paulo
2016

ROSA FABIANA ZABALAGA DAVILA

MATHEMATICAL MODELING OF DRYING PROCESS OF UNRIPE BANANA SLICES

Thesis submitted to Escola Politécnica of University of São Paulo for the degree of Doctor in Science

Concentration area:
Chemical Engineering

Advisor: Prof. Carmen C. Tadini

São Paulo
2016

Este exemplar foi revisado e corrigido em relação à versão original, sob responsabilidade única do autor e com a anuência de seu orientador.

São Paulo,___de_____de___

Assinatura do autor: _____

Assinatura do orientador: _____

Catalogação-na-publicação

Dávila, Rosa Fabiana Zabalaga
Mathematical modeling of drying process of unripe banana slices / R. F. Z. Dávila -- versão corr. -- São Paulo, 2016.
152 p.

Tese (Doutorado) - Escola Politécnica da Universidade de São Paulo. Departamento de Engenharia Química.

1.Secagem convectiva 2.Modelagem matemática 3.Banana verde 4.Amido resistente I.Universidade de São Paulo. Escola Politécnica. Departamento de Engenharia Química II.t.

To my little piece of heaven and my husband Ignácio

To my parents Oscar and Ayvi my siblings Jaencarla and Will

AKNOWLEGEMENTS (*In portuguese*)

Primeiramente agradecer infinitamente a Deus pelas continuas bênçãos, porque sem ele eu não estaria neste momento totalmente agradecida com a vida. A minha maravilhosa família que sem eles não poderia continuar. Ao meu esposo Aldo pelo apoio incondicional durante estes quatro anos.

À Profa. Carmen Cecilia Tadini, pela oportunidade de trabalhar no LEA e pela confiança depositada em mim, pelos conhecimentos transmitidos, incentivos, comentários, sugestões para melhorar o presente trabalho.

Ao Prof. Reinaldo Giudici pela atenção, ensinamentos e transmissão do conhecimento.

Ao Prof. José Luis Pires Camacho pelas tardes de estudo e sugestões, comentários para aperfeiçoar o trabalho, em especial pela amizade e as palavras certas no momento certo.

Ao CNPq, pela ajuda financeira recebida durante a realização deste trabalho.

A FAPESP pelo apoio financeiro na aquisição do secador através do processo 11/23599-0.

Aos meus queridos amigos no Brasil, Nedher, Ana, Mario, Hector, Lily, Sandra, Juancho, Roxana, Juanito, Jenny, que não só encontre amizade, mas sim uma irmandade e fraternidade; sinto saudade de cada domingo juntos.

Ao pessoal do LEA, Vanessa e Ivan pela ajuda e apoio nestes anos.

RESUMO

A farinha de banana verde (UBF) produzida de bananas não submetidas ao processo de maturação é uma alternativa interessante para minimizar as perdas dos frutos relacionadas ao manejo inadequado e a alta perecibilidade do produto. A UBF pode ser considerada um ingrediente funcional em formulações alimentícias, pois pode reduzir o índice glicêmico e o nível de insulina plasmática no sangue, demonstrando eficácia no controle da saciedade e da resistência à insulina. O objetivo deste trabalho foi estudar o processo de secagem de fatias de banana verde (*Musa cavendishii, Nanicão*) e desenvolver um modelo de secagem transiente através da modelagem matemática com transferência de massa e energia simultânea. Inicialmente, foi realizada a caraterização físico-química da matéria prima que foi submetida ao processo de secagem em escala piloto, a 40 ºC, 50 ºC e 60 ºC, com termopares inseridos no produto monitorando sua temperatura, a velocidade do ar de secagem foi de 4 $m \cdot s^{-1}$. Com a cinética de secagem e a temperatura interna da fatia foi possível validar o modelo de difusão baseado na 2ª Lei de Fick e Fourier. Para este propósito, foram medidas durante o processo: as isotermas de sorção ajustadas ao modelo do GAB permitindo estimar a umidade de equilíbrio (X_e), 1.76 [g H_2O/100g d.b.] a 60 ºC e 10 % de umidade relativa (*RH*) e as propriedades físicas e termofísicas (k, C_p, α) para serem inseridas no modelo. Consideraram-se cinco casos: i) Propriedades termofísicas constantes; ii) Variáveis; iii) Estimativa do coeficiente de transferência de massa (h_m) de calor (h) e difusividade efetiva (D_e) parâmetros importantes que controlam a taxa de secagem, 134 $W \cdot m^{-2} \cdot K^{-1}$, 4.91×10^{-5} $m^{-2} \cdot s^{-1}$ e 3.278×10^{-10} $m \cdot s^{-2}$ para uma temperatura de 60 ºC, respectivamente; iv) Estimativa do D_e como função do teor de umidade (M) apresentando um comportamento polinomial de terceira ordem; v) O encolhimento teve influência no modelo matemático, em especial nas primeiras três horas de secagem, a espessura da banana verde experimentou uma redução de (30.34 ± 1.29) %, encontrando dois períodos de taxa de secagem decrescentes (DDR I e DDR II), os D_e estimados para estes dois períodos foram 3.28×10^{-10} $m \cdot s^{-2}$ e 1.77×10^{-10} $m \cdot s^{-2}$, respectivamente. As simulações no COMSOL Multiphysics foram possíveis de serem realizadas através dos dados estimados pelo modelo matemático.

Palavras-chave: Secagem convectiva, Modelagem matemática, Banana verde, Amido resistente.

ABSTRACT

Unripe banana flour (UBF) production employs bananas not submitted to maturation process, is an interesting alternative to minimize the fruit loss reduction related to inappropriate handling or fast ripening. The UBF is considered as a functional ingredient improving glycemic and plasma insulin levels in blood, have also shown efficacy on the control of satiety, insulin resistance. The aim of this work was to study the drying process of unripe banana slabs (*Musa cavendishii, Nanicão*) developing a transient drying model through mathematical modeling with simultaneous moisture and heat transfer. The raw material characterization was performed and afterwards the drying process was conducted at 40 ºC, 50 ºC e 60 ºC, the product temperature was recorded using thermocouples, the air velocity inside the chamber was 4 $m \cdot s^{-1}$. With the experimental data was possible to validate the diffusion model based on the Fick's second law and Fourier. For this purpose, the sorption isotherms were measured and fitted to the GAB model estimating the equilibrium moisture content (X_e), 1.76 [g H_2O/100g d.b.] at 60 ºC and 10 % of relative humidity (*RH*), the thermophysical properties (k, C_p, α) were also measured to be used in the model. Five cases were contemplated: i) Constant thermophysical properties; ii) Variable properties; iii) Mass (h_m), heat transfer (h) coefficient and effective diffusivity (D_e) estimation 134 $W \cdot m^{-2} \cdot K^{-1}$, 4.91×10^{-5} $m^{-2} \cdot s^{-1}$ and 3.278×10^{-10} $m \cdot s^{-2}$ at 60 ºC, respectively; iv) Variable D_e, it presented a third order polynomial behavior as function of moisture content; v) The shrinkage had an effect on the mathematical model, especially in the 3 first hours of process, the thickness experienced a contraction of about (30.34 ± 1.29) % out of the initial thickness, finding two decreasing drying rate periods (DDR I and DDR II), 3.28×10^{-10} $m \cdot s^{-2}$ and 1.77×10^{-10} $m \cdot s^{-2}$, respectively. COMSOL Multiphysics simulations were possible to perform through the heat and mass transfer coefficient estimated by the mathematical modeling.

Keywords: Convective drying, Mathematical modeling, unripe banana, resistant starch.

LIST OF FIGURES

LIST OF TABLES

ABREVIATIONS

AOAC Association of official Analytical chemists

B1 Atomizer Nozzle

CEAGESP Companhia de entrepostos e Armazéns Gerais do Estado de São Paulo

CNPq Conselho nacional de Desenvolvimento Científico e Tecnológico

d.b. Dry basis

DDR Decreasing Drying Rate Period

DVS Dynamic Vapor Sorption

FAO Food and Agriculture Organization of the United Nations

PID Proportional Integral Derivative

PVC Polyvinyl chloride

R1 Electrical heater 1

RS Resistant Starch

TEMP1 Temperature controller 1

TEMP2 Temperature controller 2

TH1 Thermo-hygrometer

UBF Unripe Banana Flour

UR1 refrigeration unit

V1 Induction Fan 1

V2 Induction Fan 2

VSA Vapor Sorption Analyzer

w.b. Wet basis

SYMBOLS

a_0, a_1, a_2, a_3 and a_4 Constants for Eq. 5.11	[-]
a_w Water activity	[-]
A Constant to determine $p_{v0}(T)$ in Antoine correlation Eq. (5.11)	[-]
B Constant to determine $p_{v0}(T)$ in Antoine correlation Eq. (5.11)	[-]
C Energetic constant related to first layer GAB model	[-]
C_1 and C_2 Constants in Eq. (6.3)	[-]
C_{air} Moisture content in the drying air	[kg·kg^{-1}dry ar]
C_{air} Outside air moisture concentration	[mol·m^{-3}]
C_b Moisture concentration of banana slab	[mol·m^{-3}]
C_{sur} Water content (liquid water film) at the surface	[kg·kg^{-1}dry ar]
C_p Specific heat capacity	[J·kg^{-1}·K^{-1}]
C_0 Initial moisture content of banana slab	[mol·m^{-3}dry ar]
D Constant for water to determine $p_{v0}(T)$	[-]
d Unripe banana slice diameter	[m]
D_e Effective diffusivity	[m^2·s^{-1}]
D_1, D_2 and D_3 Constants in Eq. (6.4)	[-]
E_a Energy of activation	[kJ·mol^{-1}]
h Heat transfer coefficient	[J·s^{-1}·m^{-2}·K^{-1}]
h_m Mass transfer coefficient	[m·s^{-1}]
k_∞ Thermal conductivity of the drying air	[W·m^{-1}·K^{-1}]
k Thermal conductivity	[J·s^{-1}·m^{-1}·K^{-1}]

K Parameter (difference of chemical potential between the multilayer and bulk water in the food) GAB Eq. (3.1)	[-]
L Food thickness	[m]
L_0 Initial thickness	[m]
m_b Weight of the sample	[g]
m_f Weight of the glass pycnometer	[g]
m_{t+s} Weight of the glass pynometer plus the sample and solvent	[g]
M moisture content during drying	[kg·kg^{-1} db]
$\overline{M}$ Average moisture content	[kg·kg^{-1} db]
M_0 Initial moisture content	[kg·kg^{-1} db]
M_r Dimensionless moisture content	[-]
M_w Moisture content (wet basis)	[kg·kg^{-1} wb]
$\overline{MW_{H_2O}}$ Molecular weight	[kg·kmol^{-1}]
N Number of discretizations	[-]
r Food radius during drying	[m]
r_0 Food initial radius	[m]
R Ideal gas constant	[Pa·m^{-3}·mol^{-1}·K^{-1}]
RH Relative Humidity	[%]
p_c Critical pressure of water for Eq. (5.11)	[bar]
p_v Water vapor pressure	[Pa]
p_{v0} Vapor pressure of pure water	[Pa]
P Total pressure	[Pa]
P_1, P_2, P_3 and P_4 Constants in Eq. (6.1)	[-]
RH Relative humidity	[%]
S_b Shrinkage during drying	[-]

t Time of drying process	[s]
T Absolute temperature	[K]
T_0 Initial temperature	[K]
T_a Absolute temperature	[K]
T_{air} Air drying temperature	[K]
T_c Critical temperature of water	[-]
T_{sur} Surface temperature of banana slice	[K]
$\vec{v}$ Solid phase displacement	[m·s^{-1}]
V_0 Initial food volume	[m^3]
V_A Apparent volume	[m^3]
V_{A0} Initial apparent volume	[m^3]
V_f Volume of the glass pycnometer	[m^3]
V_t Food volume during drying	[m^3]
V_T True volume	[g·cm^3]
W_1, W_2 and W_3 Constants in Eq. (6.2)	[-]
X Moisture content for GAB model	[kg·kg^{-1} db]
X_e Equilibrium moisture content	[kg·kg^{-1} db]
X_m Moisture content of the monolayer	[kg·kg^{-1} db]
y Component-specific constants	[-]

Greek symbols

α Thermal diffusivity	[m^2·s^{-1}]
β_1 Shrinkage coefficient in Eq. (3.7)	[-]
β_2 Shrinkage coefficient in Eq. (3.7)	[-]
γ_1 Constant of shrinkage during drying in Eq. (3.6)	[-]

γ_2 Constant of shrinkage during drying in Eq. (3.6)	[-]
ε Porosity	[-]
η_1 Constant of shrinkage during drying in Eq. (3.5)	[-]
η_2 Constant of shrinkage during drying in Eq. (3.5)	[-]
Θ Constant for water to determine $p_{v0}(T)$	[g·m^{-3}]
κ Empirical constant (Eq. 3.4)	[-]
λ Heat of vaporization (Latent heat)	[J·kg^{-1}]
μ_∞ Drying air viscosity	[Pa·s]
v_∞ Drying air velocity	[m·s^{-1}]
ρ Food density	[g·m^{-3}]
ρ_T True volume	[g·m^{-3}]
υ_e Specific volume of air	[m^3·kg^{-1} dry air]
$\vec{\nabla}$ Vector differential operator	[-]
Ω_1 Ω_2 Ω_3 Ω_4 Boundaries in COMSOL Multiphysics	[-]
ω Empirical constant (Eq. 3.4)	[-]

TABLE OF CONTENTS

1. INTRODUCTION

Transporting energy and mass across interfaces is of crucial importance in food processing. In many ways, food processing is about preserving, creating, or manipulating food structures. Drying is an important aspect of the production of various types of food and this process can be very challenging: the appearance of the product can be enhanced, the original flavor encapsulated and nutritional value maintained. Nowadays drying is extensively used on a large scale in order to produce more desirable foods that can be distributed and enjoyed by people globally (DATTA, 2008).

Process modeling is one of the key activities in process engineering. A model is an imitation of reality and a mathematical model is a particular form of representation. It is a significant activity driven by application areas as process optimization, design and control. In the process of model building, a real world problem is translated into an equivalent mathematical problem whose solution attempt to interpret for control, optimization or possibly safety uses (HANGOS; CAMERON, 2001). The main feature of the system is its ability to predict moisture and temperature inside the product, which is a very important way of providing structural knowledge of food and quality. The goal is to keep as many details of the process as possible, without creating unnecessary computational complexity or time commitment. Therefore, it is necessary, in process engineering area to model and interpret the behavior and the characteristics of the system under study.

Brazil, one of the greatest worldwide banana producers, with 6.9 million of MT harvested in 2012 (FAO, 2013), is also responsible for consuming and wasting this fruit. The background data states that this activity is one of the greatest in the harvest area, collaborating with a considerable percentage of the total agricultural production. Banana exports nearly doubled from 2001 to 2006 and the highest export amount corresponds to 2006 with almost 380 thousand tons (AGRIANUAL, 2012). However, Brazil is still weak in banana exportation, despite being one of the largest world producers. Amounts between 20 % and 40 % of all banana harvested is discarded in different ways (production/weather conditions, harvesting, packing, transport, handling). Rejected bananas are normally disposed improperly (INFORME AGROPECUARIO, 2005; SILVA *et al.,* 2003; SPRICIGO, 2011; TORRES, 1999).

According to Zhang *et al.* (2005) a successful industrial use of the culled bananas would alleviate the problem and the production of unripe banana flour, which is considered as a functional ingredient, that is, its regular consumption can confer health benefits in humans. Unripe banana pulp contains up to 70–80 % of starch on d.b., a percentage comparable to that in the endosperm of corn grain and the pulp of white potato.

Resistant starch (RS) contained in the unripe banana flour may be used as a source of dietary fiber, since it presents similar physiological effects. Due to its low energy content might be used as a supplement in the formulation of products with reduced fat/sugar content (MENEZES *et al.,* 2010).

It is important to notice that producing unripe banana flour with high RS content and considering it as a functional ingredient requires the differentiation of the stages of banana ripeness. Ripeness may influence technical aspects of the processing and results in different chemical compositions.

According to Mustaffa *et al*. (1998), bananas at different stages of maturation have significant differences in their physicochemical characteristics and firmness. The soluble solids content increases along the ripening, while the pulp firmness decreases with maturity due to the action of enzymes involved in the degradation of starch.

The production of unripe banana flour with high RS, in laboratory and pilot scale, was developed by Tribess *et al.* (2009) carrying out drying at different conditions: concluding that the RS is thermo-sensitive modifying its structure at temperatures above 70 °C. Thermal analysis presented peak gelatinization temperatures from (67.9 ± 0.3) ºC to (68.6 ± 0.3) ºC.

The fundamental study of drying becomes very difficult throughout the process of biological materials, due to the complexity of their structure. For this reason, the modeling/simulation is mostly employed to simplify this kind of complex biological systems. In this way, it will be possible to study the main variables affecting the product quality.

2. OBJECTIVE

To develop a transient drying model through mathematical modeling of unripe banana slabs (*Musa cavendishii, Nanicão*) with simultaneous moisture and heat transfer.

To achieve the objective the following steps of the study were proposed:

- To study the transport phenomena during the drying process of unripe banana slices, considered as a homogenous material;
- To develop a one-dimensional mathematical model considering the banana slice as a slab, applying numerical resolution with and without shrinkage;
- To determine the thermal properties behavior of unripe banana during convective drying;
- To conduct experimental tests in order to establish the drying kinetics and to validate the model;
- To perform a simulation with the parameters found in the mathematical model using COMSOL Multiphysics.

3. LITERATURE REVIEW

3.1 Banana

Banana (*Musa* spp.), one of the most consumed fruit in the world, is cultivated in several tropical countries. Native from the Indo-Malaysian, Asian, and Australian regions; nowadays, this fruit is found throughout the tropical and subtropical regions and it can be industrialized at different stages of maturation. Rich in vitamins (A, B and C), minerals (Ca, Fe and K) and containing about 70 % of water, provides a low amount of fat and energy to the body and good digestibility (NELSON; PLOETZ; KEPLER, 2006; SOUZA; BORGES, 2004).

Unripe banana as well as mature are very nutritive, its composition consists of carbohydrates, protein, fiber, vitamins, low fat content and considerable content of minerals like potassium, calcium and magnesium. Moreover, the unripe banana has a considerable content of a complex carbohydrate type: resistant starch (RS) (MOTA *et al.,* 2000).

3.1.1 Taxonomy

Cavendish bananas are a subgroup of the triploid (AAA) cultivars of Musa acuminate, named 'Dwarf Cavendish' cultivar, distinguished by height and features of the fruits. The Cavendish cultivars produce fruits that are used in international market; they are major export commodities in Central America, South America, the Caribbean, West Africa, and the Philippines. In total, Cavendish cultivars are the most popular and valuable, comprising over 40 % of these fruit that are produced worldwide. The Dwarf Cavendish varieties known in Brazil are: *Nanica, Nanicão*, characterized by the thinness, size and the curvature of the fruits (PLOETZ, *et al.,* 2007).

3.1.2 General characteristics

Bananas are produced in large quantities in tropical and subtropical areas. World production of Musa in 2003 was estimated to be about 102 million MT of which about 68 % was classified as bananas and 32 % as plantains (FAO, 2012).

Developed countries are the usual destination for exporting bananas (ZHANG, *et al.* 2005). Production, as well as exports and imports of bananas, are highly concentrated in a few countries. Ten major banana producing countries accounted for about 75 % of total production in 2012 with India, Ecuador, Brazil, and China accounting for half of the total.

The most important varieties grown in Brazil are: *Prata, Pacovan, Prata anã, Maçã, Mysore, Terra e D'Angola* of the genome group AAB; and *Nanica, Nanicão* of the genome group AAA. To a lesser extent *Figo cinza* and *Figo vermelho* of the genome group ABB; *Ouro* of the genome group AA; *Caru verde Caru roxa* of the group AAA are grown (SOUZA; BORGES, 2004).

The low height varieties (*Nanica*) are more resistant to the wind than the higher size varieties (*Nanicão*). The banana varieties traditionally used for export and industrialization are the *Nanica* and *Nanicão*, traditionally grown in the Northeast and Southeast regions of Brazil (Table 3.1).

Table 3.1 - Brazilian production of banana in 2012.

Region	Harvest area [ha]	Yield [t]	Participation [%]
North	70 576	829 959	**12.02**
Northeast	197 295	2 424 974	**35.13**
Southeast	139 811	2 298 477	**33.30**
South	53 307	1 077 263	**15.61**
West-center	20 127	271 511	**3.93**
BRAZIL	**481 116**	**6 902 184**	**100.00**

IBGE - National agricultural production, 2012

In certain regions, the post-harvest lost could reach 40 % of all production. Most of these losses are due to excessive handling, improper transport and packing (SOUZA; BORGES, 2004).

3.1.3 Ripening stages

During the ripening process, the banana experiments great changes and depending on its application, there has been an interest on the ripening stage to support its proper processing. As banana ripens, its pulp gets softer, in this way, the degree of ripeness may be evaluated through the force required to penetrate the

pulp, measured by a texturometer express in Newton [N] (DITCHFIELD; TADINI, 2002; TRIBESS, 2009).

These changes and the different ripening stages are illustrated in Figure 3.1, in which the last stage 8, yellow with many brown spots was introduced and described by Lii *et al.* (1982) and Ditchfield; Tadini (2002). The first stage (all green) and the last ripening stage are characterized by the high content of starch and accumulation of sugars, respectively.

Figure 3.1 - Evolution of the different ripening stages of banana with the incorporation of the last stage (EMBRAPA, 2008).

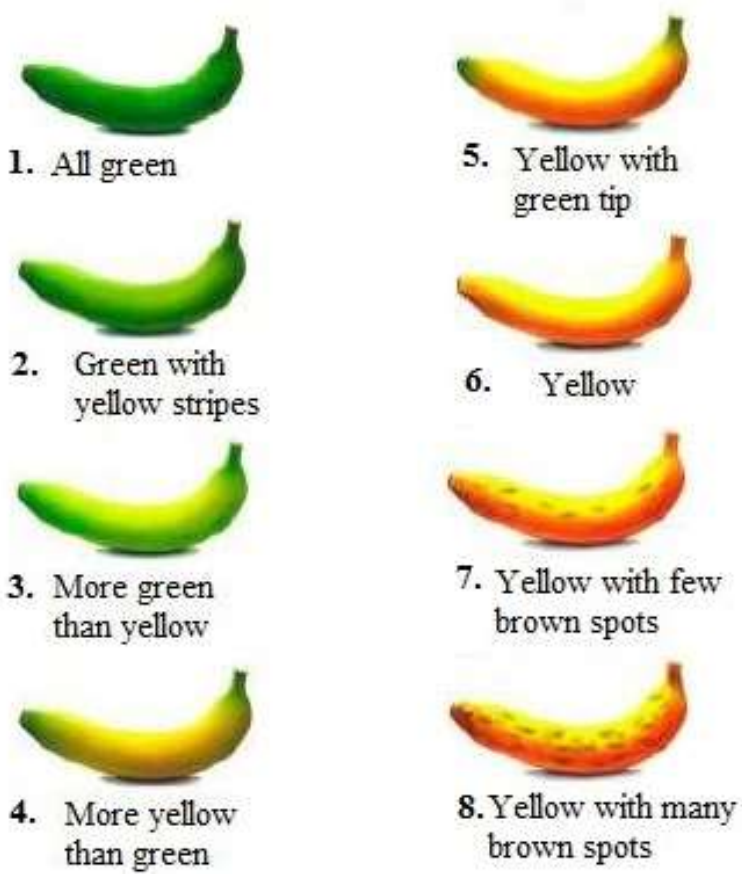

Different authors performed physicochemical analysis on each ripening stages of banana *Nanicão*, presented in Table 3.2.

Table 3.2 - pH, soluble solids, titratable acidity and firmness measured in banana pulp during the ripening process.

Ripening stage	pH	Soluble solids [ºBrix]	Tritable acidity[(1)] [g/100 g]	Firmness [N]
1	5.3 ± 0.1[a] 5.3 ± 0.1[b]	5 ± 2[a] 3.5 ± 0.1[b]	0.24 ± 0.03[a] 0.37 ± 0.09[b]	26 ± 3[a] 25.8 ± 2.4[b]
2	4.8 ± 0.1[a]	7 ± 1[a]	0.44 ± 0.03[a]	14 ± 2[a]
3	4.5 ± 0.1[a]	20 ± 1[a]	0.63 ± 0.03[a]	5 ± 1[a]
4	4.6 ± 0.1[a]	21 ± 1[a]	0.51 ± 0.09[a]	3.1 ± 0.3[a]
5	4.7 ± 0.2[a]	21 ± 2[a]	0.50 ± 0.09[a]	2.6 ± 0.2[a]
6	4.9 ± 0.1[a]	22 ± 1[a]	0.44 ± 0.03[a]	2.2 ± 0.2[a]
7	5.2 ± 0.1[a]	21 ± 1[a]	0.35 ± 0.05[a]	1.5 ± 0.2[a]
8	5.44 ± 0.07[a]	21 ± 2[a]	0.27 ± 0.06[a]	0.8 ± 0.2[a]

[(1)] As malic acid
[a] Ditchfield (2004)
[b] Tribess (2009)

Ditchfield (2004) and Tribess (2009) concluded that banana passes through major changes during the ripening process, which can be observed by changes in the physicochemical analyses. According to these authors, the best parameter to determine the stage of maturation of the banana is the firmness.

3.1.4 Resistant starch

It is well known that starch is present in all seeds (wheat, corn, etc.), tubers (potatoes), roots (cassava), and to a lesser proportion in plant leaves. Starch is a mixture of polysaccharides (amylose and amylopectin in different proportions) that are easily assimilated, making it of great importance in the food industry. However, other attractive characteristics of this material, such as natural availability, biodegradability, low cost, has led to various other applications (GUIMARÃES *et al.,* 2010).

Starch is the major dietary component in all human populations. In addition, this biopolymer constitutes an excellent raw material to modify food texture and consistency. Not only the amount of starch is important for the texture of a given food product, but starch type is equally critical (BILIADERIS, 1991).

Variable amounts of starch in food can escape digestion in the human small intestine and pass into the colon. This fraction is referred to as resistant starch (RS) well defined as the fraction that does not provide glucose to the organism, fermented in the large intestine, producing gases and short-chain fatty acids. Because of this, its behavior can be compared with food fiber.

Faisant *et al.* (1995) studied the digestibility of banana starch granules in the human small intestine. Starch breakdown in the human small intestine and structural features of RS were investigated. These studies are important for an assessment of the digestibility and nutritive value of starch.

Starch is the principal component of unripe bananas, according to literature its flour may present (61.3–76.5) g/100 g of starch (d. b.) and also has a fiber content of (6.3 - 15.5) g/100 g (d.b.) (JUAREZ-GARCIA *et al.,* 2006; MOTA *et al.,* 2000). Moreover, great part of the starch found in green banana flour is the resistant starch type 2 (RS2 – 52.7 - 54.2 g/100 g d.b.) (FAISANT *et al.,* 1995). Its granules were ellipsoid or spherical, varying in diameter from (10 to 50) μm as shown in Figure 3.2A.

Figure 3.2 - Scanning electron micrographs of starch granules: (A) green Valery bananas (Kayisu; Hood, 1981). Photograph of green banana starch granules: (B) under polarized light (Lii *et al.*, 1982).

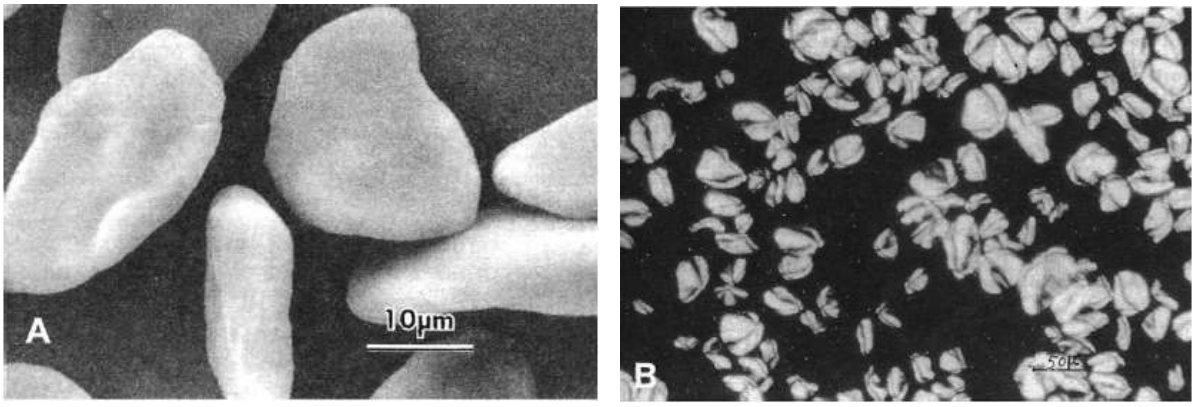

RS escapes digestion in the human upper gastrointestinal tract and is classified into four general subtypes called RS1–RS4. Resistant starch type 2 (RS2) describes starch granules such as found in unripe banana or raw potato (Table 3.3), that provides a moderate increase in glucose and insulin plasma after a meal allowing a slow intake of glucose into the bloodstream (MENEZES *et al.,* 2004).

A summary of the different types of resistant starch, their classification criteria, and food sources are outline in Table 3.3.

Table 3.3 - Classification of types of resistant starch (RS), food sources, and factors affecting their resistance to digestion in the colon (SAGILATA; SINGHAL; KULKARNI, 2006).

Type of RS	Description	Food sources
RS_1	Physically protected	Whole- or partly milled grains and seeds, legumes
RS_2	Ungelatinized resistant granules with type B crystallinity, slowly hydrolyzed by α-amylase	Raw potatoes, green bananas, some legumes, high amylose corn
RS_3	Retrograded starch	Cooked and cooled potatoes, bread, cornflakes, food products with repeated moist heat treatment
RS_4	Chemically modified starches due to cross-linking with chemical reagents	Foods in which modified starches have been used (for example, breads, cakes)

Carson (1972) compared the functional properties of the isolated starch to those of banana flour obtained from green banana pulp and observed that they were similar. Different authors (CARSON, 1972; LII, 1982; MENEZES *et al.,* 2010; SUNTHARALINGAM; RAVINDRAM, 1993) stated that there is a potential to convert exceeding or rejected green banana fruits into flour.

3.2 Equilibrium moisture

Knowledge of the thermodynamic equilibrium state between the surrounding air and the solid is a basic requirement for drying, as it is for any similar mass transfer situation. The first stage to model and simulate a drying process is to estimate the equilibrium moisture (X_e), which is an important information to delineate the drying curves as a function of time. Data on moisture isotherms are essential in modeling and to simulate this unit operation being able to optimize the drying equipment (MARINOS-KOURIS; MAROULIS, 2006).

The sorption isotherm is needed to calculate the moisture changes that may occur during storage and also to predict shelf-life stability of foods. A distinction can be made between the isotherms depending if the moisture levels within the products are increasing or decreasing.

Brunauer *et al.* (1940) classified the sorption isotherms into five different types. The sorption isotherms of the hydrophilic polymers, such as natural fibers and foods,

are of type II that shows asymptotic approaching to the saturation pressure, which means that equilibrium is attained at infinite dilution.

In the literature, several models describe sorption isotherms. For the well-known (two parameters) BET model, it was assumed that formation of multilayers occurs on a homogeneous surface. Moreover, heat of adsorption occurs only in the first layer and there are no interactions between adsorbed molecules. Anderson (1946) modified the BET equation assuming that the heat of adsorption in the second to ninth layers is lower than the heat of liquefaction. Anderson's equation was later kinetically and statistically derived by de Boer (1953) and Guggenheim (1966), and it is called the GAB equation. In this way, the GAB model is recognized as the fundamental equation for the characterization of water sorption of food materials.

The effect of temperature on the sorption isotherm is of great importance since food materials are exposed to a range of temperatures during processing and storage resulting in water activity changes.

The relationship between the water activity and the equilibrium moisture content of the food at constant temperature and pressure is given by the water sorption isotherm (LEWICKI, 2009).

Five classic types of sorption isotherms (Figure 3.3) are described by Brunauer; Emmett; Teller, (1940) and found in scientific studies.

Figure 3.3 - Five main types of sorption isotherms (BRUNAUER; EMMETT; TELLER, 1940).

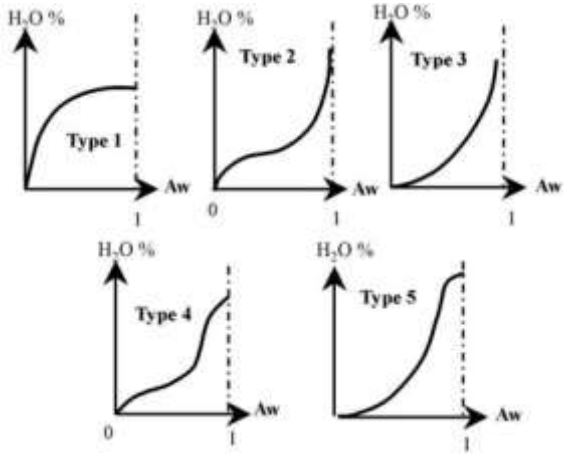

The two isotherms most frequently found for food products are Types 2 and 4 isotherms. The best-known and most widely used mathematical representation of the

complete sorption phenomenon in biological materials is given by the BET / GAB equation (Eq. 3.1).

$$X = \frac{X_m C a_w}{(1 - a_w)(1 + a_w (C - 1))} \quad (3.1)$$

The GAB isotherm equation (Eq. 3.2) is an extension of the two-parameter BET model which takes into account the modified properties of the adsorbate/desorbate in the multilayer region and bulk liquid (“free” water) properties through the introduction of a third parameter:

$$X = \frac{X_m C K a_w}{(1 - K a_w)(1 - K a_w + C K a_w)} \quad (3.2)$$

Wherein: X is the amount of water and X_m represents the moisture content of the monolayer, both generally expressed in dry basis $kg \cdot kg^{-1}$; a_w is the water activity [-]; C is an energetic constant related to first layer net heat of sorption; and K is a parameter that takes into account the difference of chemical potential between the multilayer and bulk water in the food.

The constants in the GAB equation (K and C) are temperature dependent, from which it can be extracted information to construct and refer to sorption isotherms at different temperatures.

3.3 Drying of foodstuff

Drying is an important method of food preservation, which is defined as a process of moisture removal due to simultaneous heat and mass transfer (OKOS *et al.,* 1992). Drying differs from other separation techniques due to the movement of the molecules, which in this case is obtained by a mass transfer of the liquid and/or vapor due to the difference in partial pressure of the steam between the surface of the solid to be evaporated and the air that surrounds it. In the case of foods, water must be removed from the moist material up to a level where deterioration provoked by microorganisms can be minimized (DELGADO; BARBOSA DE LIMA, 2014).

Drying is an energy intensive operation consuming (9 – 25) % of national industrial energy in the developed countries (MUJUMDAR, 1999). It appears to be a

complicated unit operation involving simultaneous, coupled heat and mass transfer phenomena, which occur inside the material being dried. The temperature and moisture distributions inside the moist solids during drying are of great importance in order to provide better design and performance analysis of the drying process. Due to intricate coupling between the primary variables and in combination with non-linearities as a result of variation of physical properties, the use of numerical simulation has become an essential tool in this regard (PAKOWSKI *et al.,* 1996).

Drying of fruits and vegetables demands special attention, considered as important source of vitamins and minerals, essential for human health. Fruits have certain morphological features quite distinct from other natural materials that greatly influence their behavior during drying and preservation. Fruits are generally characterized by high initial moisture content, high temperature sensitivity (i.e. color, flavor, texture and nutritional value subject to thermal deterioration), and shrinkage during drying.

Moreover, the transfer of energy (heat) depends on the air temperature, air humidity, air flow rate, exposed area of food material, and pressure. The physical nature of the food, including temperature, composition, and in particular moisture content, governs the moisture transfer (OKOS *et al.,* 1992).

The required amount of thermal energy to dry a particular product depends on many factors, such as, initial moisture content, desired final moisture content, temperature, relative humidity of drying air and air flow rate (KARIM; HAWLADER*,* 2005a).

Currently, most dehydrated fruits are produced by the technique of hot air drying, which is the simplest and most economical of the various methods. Several other drying techniques have been proposed, such as a combination of osmotic dehydration with hot air drying or a combination of freeze drying followed by air drying or superheated steam (FERNANDES *et al.,* 2011).

The thermophysical properties of food play an important role in the project of equipments and processes that involve heat and mass transfer, such as drying, because their knowledge are necessary in the calculation of thermal charges, energetic dispends and equipment dimensions. Properties such as density, thermal diffusivity, specific heat and thermal conductivity of the food material are used to

estimate the energetic demand and also to predict the microbiological and biochemical spoilage, representing a tool for food safety and quality control. The food thermophysical properties are strongly dependent on the temperature and chemical composition, including moisture content. It is almost impossible to determine experimentally and tabulate the thermal properties of foods and beverages for all the conditions and compositions possible.

3.3.1 Mathematical modeling and simulation of food drying

The principle of modeling is based on having a set of mathematical equations, which can adequately characterize the process. Modeling and simulation are necessary for dryer system design, selection of suitable drying conditions, and prediction of mass and heat transfer during the process.

Modeling coupled heat and mass transfer can be divided into three different approaches, depending on the level of details desired, as shown in Figure 3.4. In the simplest formulation, **1**, only the rate of heat/mass transfer between a surface and a fluid is described, without detailed information on the temperature profile in a fluid. In formulation **2**, the detailed temperature/mass profile in the fluid is available at the expense of fairly intensive computations. In formulation **3**, at the expense of a still greater level of complex computations, details of the temperature/mass profile are available not only for the fluid, but also for its immediate surroundings.

Figure 3.4 - Formulations of convective heat transfer with increasing complexity from left to right.

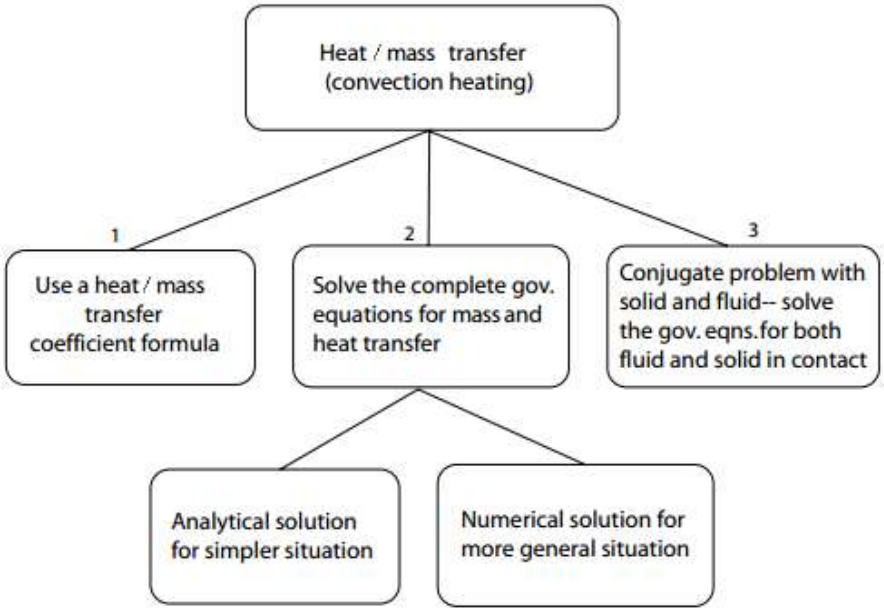

Source: Datta (2007)

Due to the availability of powerful computational fluid dynamics (CFD) software, convection formulations **2** and **3** are primarily solved numerically. For formulation **1**, analytical solutions exist for simple situations. When a food-processing situation can be simplified such that analytical solutions can be used, the analytical solutions are generally encouraged because they can provide more insight into the problem with less effort. Using the surface heat/mass transfer coefficient, the temperature and the moisture content in the solid can be calculated (DATTA, 2007).

The visualization of drying mechanisms in two- or three-dimensional is not straightforward. To visualize the underlined physics more easily, it will be described only one-dimensional conditions (Fig. 3.5). The perfect flat and smooth surface is at the start a simplification. Using liquid diffusion alone is not enough to be able to explain the process of air drying. Eventually, a vapor concentration profile has to be established within the porous material being dried. As an improvement from the pure liquid diffusion model with an effective diffusivity (or diffusivity function against temperature and water content), the mechanisms of drying are the liquid water diffusion and water vapor diffusion.

Figure 3.5- A simple schematic diagram showing the system considered in this study (the shaded background represents the complex nature of the microstructures inside the solid being dried).

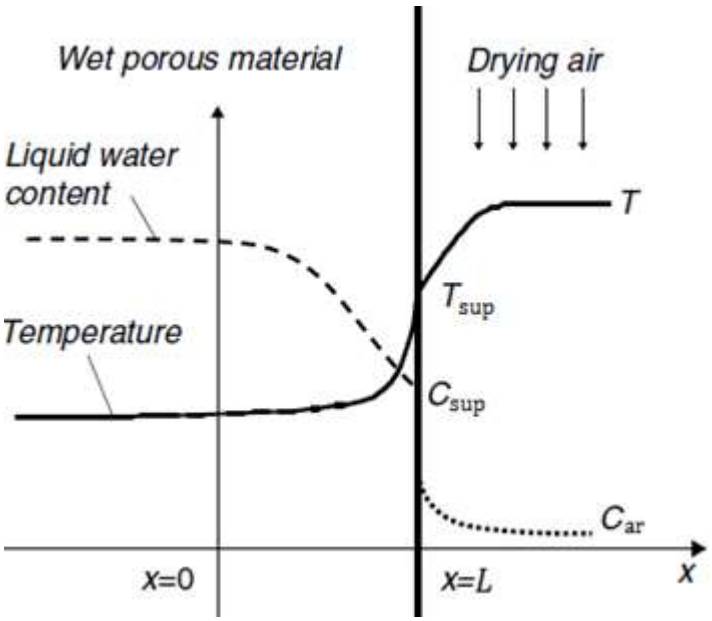

Source: Chen (2007)

The investigation of process dynamics requires the modeling in transient regime based on the mass and energy balances and constitutive equations, creating a nonlinear system. From this, a series of simulations are done to verify the behavior of the involved variables in this process. In order to scale up the experimental results obtained in the laboratory, certain process parameters need to be optimized and reliable mathematical models are necessary to predict the influence of the key parameters.

According to Datta (2008), observation based models provide a starting point but they are primarily empirical in nature. In contrast, a physical based model should describe the presumed physical phenomena, even in the absence of experimental data. Mathematical drying models are categorized as theoretical, semi-theoretical, and empirical models. Theoretical models are based on analytical or numerical solutions of mass and energy equations. Various semi-theoretical and empirical models have been used to describe the drying process (LEMUS-MONDACA *et al.,* 2013).

Two main categories of models have been developed, with regard to the major transport mechanisms: in the first, convection by Darcy flow and diffusion is considered, accounting for capillary and pressure driven water flow and diffusion inside the drying material.

Drying kinetics process of bio-products and food, have been studied considering the mass transfer by using the second category, Fick's diffusion accounts for the water transport inside the product, by adopting an effective diffusion coefficient that is often obtained experimentally in a semi-empirical manner (thin-layer equation) (CORZO *et al.,* 2008; GOYAL *et al*., 2006; LEMUS-MONDACA *et al.,* 2009). Fick's Second Law allows obtaining the drying parameters such as the water effective diffusion coefficient, the activation energy and the drying curve. Lemus-Mondaca *et al.* (2009) studied and modeled the drying kinetics of the blueberry at three different temperatures. Diffusional and empirical models were applied in the modeling of the drying kinetics of this fruit. The mass diffusion coefficient, evaluated by an Arrhenius-type equation, and kinetic parameters of each model showed dependence on temperature.

Diffusion-based models can be further distinguished in two main categories, namely, conjugated and non-conjugated models described by Defraeye, (2014),

Lemus-mondaca; Vega-gálvez; Moraga, (2011). In conjugated models, the fully coupled unsteady transport equations for both the drying air and the product are solved (CURCIO, 2010; DATTA, 2012; HALDER; KURNIA, 2013; SABAREZ, 2012). These models offer high accuracy and extended applicability; however, the complexity of the non-linear mathematical models makes the solution procedure complicated and computationally very demanding. In non-conjugated models, the calculations of the heat and mass transfer inside the product are performed independently from the flow field calculations. The general aspects of the various models proposed for convective drying of agricultural products using non-conjugated heat and mass transfer are summarized in Table 3.4.

Table 3.4 - Summary of studies on convective drying of foodstuff using non-conjugated approach (Tzempelikos *et al*., 2015).

Authors	**Product**	**Dimension**	**HTC**	**MTC**	**Evaporation term in heat equation**
Aversa *et al*., (2012)	Rectangular carrot	2D	Empirical	HMTA	Yes
Barati; Esfahani (2012)	Cylindrical carrot	1D	Empirical	HMTA	Yes
da Silva *et al*., (2012)	Cylindrical banana	1D	-	ORA	No
Lemus-Mondaca *et al*., (2013)	Rectangular papaya	3D	TDC	TDC	Yes
Maroulis *et al*., (1995)	Potato	1D	ORA	ORA	Yes
Oztop; Akpinar (2008)	Rectangular apple & potato	2D	Constant Akpinar; Dincer (2005)	Constant Akpinar; Dincer (2005)	No
Villa-Corrales *et al*., (2010)	Rectangular mango	2D	TDC	TDC	No

HTC: heat transfer coefficient
MTC: mass transfer coefficient
TDC: time-dependent coefficient
HMTA: heat and mass transfer analogy
ORA: optimization and regression analysis

Some studies conducted by Hussain; Dincer (2003a), Nilnont (2011), Oztop; Akpinar (2008) have reported computational simulations of drying fruits and vegetables considering the unsteady bi-dimensional thermal conduction equations and mass diffusion coupled.

Zare (2006) developed a computer program for simulating the drying process of rough rice in a deep bed batch dryer. The model consisted of four non-linear partial differential equations as a result of the heat and mass balances, together with an appropriate solution procedure using the finite difference method. Validation of the computer simulation was found in a good agreement with the measured values along the depth of the dryer bed during the drying process. In the available literature, there are important alternatives to treat heat and mass convective transfer coefficients, especially when they vary in space (HALDERA; DATTA, 2012; VITRAC; TRYSTRAM, 2005).

3.3.2 Effective moisture diffusivity of foodstuff

The moisture effective diffusivity, D_{eff}, is an important transport property in food drying processes modeling, being a function of temperature and material moisture content. However, due to the complex food composition and physical structure, accurate estimates of this property are difficult to obtain, thus leading to the need of experimental measurements, as reported by Vagenas; Karathanos (1993). According to these authors, when the parameter is considered to vary, it is calculated through the application of the slopes method (empirical model).

Mathematical models have been proved useful to understand the physical mechanism, optimize energy efficiency, and improve product quality (KUMAR *et al.,* 2012). Mathematical models can be either empirical or fundamental models. Empirical expressions are common and relatively easy to use (KUMAR; KARIM; JOARDDER, 2014). Many empirical models for drying have been developed and applied for different products; for instance, banana (SILVA; HAMAWAND; SILVA, 2014; ZABALAGA; CARBALLO, 2014), apple (WANG *et al.,* 2007), rice (CIHAN; KAHVECI; HACIHAFIZOGLU*, 2007*) carrot (CUI; XU; SUN, 2004), cocoa (HII; LAW; CLOKE, 2009), etc. Erbay; Icier (2010) reviewed empirical models for drying and found that the best fitted model is different for different products. However, these empirical models are only applicable in the range used to collect the experimental parameters (KUMAR *et al.,* 2012).

Calculation of the effective diffusivity is crucial for drying models because it is the main parameter that controls the process with a higher diffusion coefficient, implying an increased drying rate. The diffusion coefficient changes during drying

due to the effects of sample temperature and moisture content (BATISTA; DA ROSA; PINTO, 2007). Alternatively, some authors considered effective diffusivity as a function of shrinkage or moisture content (KARIM; HAWLADER, 2005b), whereas others postulated it as temperature dependent (CHANDRA MOHAN; TALUKDAR, 2010). In the case of a temperature dependent effective diffusivity value, the diffusivity increases as drying progresses. On the other hand, effective diffusivity decreases with time in the case of shrinkage or moisture dependency. This latter behavior is ascribed to the diffusion rate decreasing as the moisture gradient drops.

3.3.2.1 Variable effective diffusivity

There are limited studies comparing the influence of temperature-dependent and moisture-dependent effective diffusivity. Recently, Silva; Hamawand; Silva (2014) considered effective diffusivity as a function of both temperature and moisture together (i.e., $D_e=f(T, M)$), not temperature or moisture dependent diffusivities separately. Therefore, it was not possible to compare the impact of considering temperature and moisture-dependent effective diffusivities. Moreover, they did not report the impact of variable diffusivities on material temperature. A comparison of drying kinetics for both temperature- and moisture-dependent effective diffusivities can play a vital role in choosing the correct effective diffusivity for modeling purposes. Though there are several modeling studies of food drying, there are limited studies that compare the impacts of temperature dependent and moisture-dependent effective diffusivities.

The estimation of moisture diffusivity from drying experiments is a challenging method. A generalized procedure (numerical solution-regression analysis) has been discussed by Marinos-Kouris; Maroulis (2006). This method uses an experimental drying apparatus and estimates the heat and mass transport properties as parameters of a drying model, which is fitted to experimental data.

Some results concerning the diffusion coefficient of food products were presented by Jayas (1991) and Zogzas; Maroulis; Marinos-Kouris (1996). This coefficient is described by different mathematical relationships connecting it to the water content and to the temperature of the product. The diffusivity increases with temperature according to an Arrhenius law.

As denoted by Azzouz *et al.* (2002) the effective mass diffusivity varies with moisture content as a third order polynomial function, on the drying of grapes of two varieties, in this case the expression of the mass diffusivity of water is written under the following form:

$$D_e(M) = D_0(T)\exp\left(-D_1(T)M\right) \tag{3.3}$$

The coefficient D_0 increases with the air temperature according to an Arrhenius type law, wherein the energy of E_a activation is a parameter to adjust. Some authors consider that E_a is variable and function of the content in water (KECHAOU, 1989). The expression of the coefficient of water diffusion in grape proposed by Azzouz *et al.* (2002) was:

$$D_e(M) = D_0 \exp\left(-\frac{E_a}{RT_a}\right)\exp\left(-(\omega T_a + \kappa)M\right) \tag{3.4}$$

wherein, M corresponds to the moisture content in dry basis, ω and κ are the empirical constants. The authors performed drying tests at 45 ºC, 55 ºC, 60 ºC, 65 ºC with two varieties (Sultanin and Chasselas).

Kiranoudis *et al.* (1993) determined, as well, the D_e as a function of moisture content and temperature, the results presented on application to some vegetables as: onions, pepper, potato and carrot, at five different air temperatures (60 ºC, 65 ºC, 70 ºC, 75 ºC, and 80 ºC) and air humidities ranging from 6 to 22 $g \cdot kg^{-1}$ d.b. The effective moisture diffusivity is assumed to be a function of material moisture content and temperature, and it is described by the following equation:

$$D_e = D_0 \exp\left(-\frac{A_0}{M}\right)\exp\left(-\frac{B_0}{T}\right) \tag{3.5}$$

wherein: M the material moisture content (dry basis, d.b.), T the material temperature and D_0, A_0, and B_0 are adjustable constants.

The authors concluded that the moisture diffusivity is nearly constant at high moisture content, but it decreases sharply as the moisture content decreases. The effect of the temperature is not obvious; the results of the proposed method are presented in Table 3.5.

Table 3.5 - Parameter estimates by Kiranoudis *et al.* (1993) for the proposed correlation (Eq. 3.4).

Vegetable	D_0 [$m^2 \cdot s^{-1}$]	A_0 [K]	B_0 [$kg \cdot kg^{-1}$ db]
onion	3.72	7.11×10^{3}	8.63×10^{-2}
pepper	7.33×10^{-3}	4.71×10^{3}	1.05×10^{-2}
potato	2.94×10^{-7}	1.57×10^{3}	6.72×10^{-2}
carrot	4.37×10^{-7}	1.65×10^{3}	8.06×10^{-2}

3.3.3 Mass and heat transfer coefficients estimation

The heat and mass transfer coefficients (h and h_m, respectively) are usually considered in food engineering literature as “standard” parameters that can be determined using a classical Nusselt number or correlation. The Sherwood number or correlation is simply a substitution of the Nusselt number correlation using the Schmidt number for mass transfer. These correlations are related to the Reynolds number, the Prandtl number, air-drying velocity, density, viscosity, thermal diffusivity and the mass effective diffusivity.

The determination of the convective heat transfer coefficient is important for several studies on heat transfer processes, although the available data are rare, mainly regarding food thermal processes. The optimization methodology and numerical simulations for determining the h between fluids with variables properties and bodies with irregular geometries are successfully used in the literature (SANTANA; AUGUSTO; CRISTIANINI, 2011; AUGUSTO; CRISTIANINI, 2011; PORNCHALOEMPONG *et al.,* 2003). As stated by Verboven *et al*. (1997), boundary conditions (convective heat transfer in this case) need to be well known for heat transfer calculations to be interpreted correctly, small deviations in heat transfer coefficient may result in large deviations especially when surface heat transfer coefficient is small. This especially might be the case when the air, as a fluid medium, was applied in different processing conditions.

Silva; Silva; Gama (2012) presented an algorithm that minimizes the errors produced by the optimization routine to calculate the parameters h, h_m using analytical solutions for cooling process for the one-dimensional diffusion equation in a cylindrical geometry, for (Biot number), $N_{Bi} = 0.5$ the estimated h_m was 4.49×10^{-6} $m \cdot s^{-1}$, wherein, the $N_{Bi} = hL/k$, the h estimation will depend on the properties of the material being cooled.

Miketinac; Sokhansanj; Tutek (1992) used five models to simulate simultaneous heat and mass transfer while drying a layer of barley. They found that the mass transfer coefficient was 1.08 x 10^{-6} $m \cdot s^{-1}$ for all of the models studied.

3.3.4 Mathematical modeling considering shrinkage

In the case of food products with high moisture content, changes in the volume are significant. Therefore, the moisture gradient within the particle that induces microstructure stresses, leading to shrinkage (MAYOR; SERENO, 2004).

Further, shrinkage will decrease the diffusion path of heat transfer processes and is extremely important in drying because it produces a variation in the distance required for the movement of water molecules (HERNANDEZ; PAVON; GARCIA, 2000).

3.3.4.1 Review of shrinkage models

Shrinkage is one of major changes taking place during the drying process. During drying, the shape and size of the food particles are constantly changing as a result of water removal and internal collapse. These dimensional changes are variable during drying: some changes are observed in dimension or shape and occasional cracking of the product may take place. Reduction in diameter and length of dried fruits reduces the volume itself. Normally, an empirical fitting through experimental test is used to find an equation for shrinkage (CHEMKHI; ZAGROUBA; BELLAGI, 2005; LIMA *et al.,* 2002; QUIROZ; NEBRA, 2001; SIMAL 1998).

A comprehensive mathematical model describing shrinkage phenomenon of materials undergoing drying processes was firstly proposed by Kowalski (1996). The model was based on the methods of continuous mechanics and on the principles of thermodynamics of irreversible processes. Hernandez *et al*. (2000) presented a mathematical description of food drying kinetics taking into account the effect of shrinkage. The authors validated the model consistency by performing various experiments under different drying conditions for fruits available in two shapes. Several empirical models were also formulated to fit the experimental results collected during drying of different foods and expressing the variation of samples volume vs. its moisture content (AVERSA *et al*., 2012).

In order to quantify the effect of shrinkage of potato, Wang and Brennan (1995) fitted the thickness, length and width, correlated by a linear relationship with moisture as:

$$L = \eta_1 + \eta_2 * M \qquad (3.6)$$

In which *L* is the thickness of the sample, η_1 and η_2 are constants and the equation (3.6) is fitted with the experiment data. This method was also used by Quiroz; Nebra (2001), who proposed a shrinkage equation by fitting the mean radius *r* of the banana as a function of the moisture content from an initial radius r_0 by a linear regression, as:

$$\frac{r}{r_0} = \gamma_1 + \gamma_2 * M \qquad (3.7)$$

De Lima; Quiroz; Nebra (2002), for the drying of banana, and Simal *et al.* (1998), for the drying of kiwi, included shrinkage into the model using a correlation that relates volume and average moisture content $\overline{M}(t)$, processing during 20 h to 30 h, as:

$$\frac{V_t}{V_0} = \beta_1 + \beta_2 * \overline{M} \qquad (3.8)$$

Wherein β_1 and β_2 are shrinkage coefficients obtained by fitting the equation (3.8) with the experiment result.

Mayor; Sereno (2004) reviewed a number of shrinkage models for food material with different geometries (cylinder, sphere, ellipsoid, slab, and cube) and different reduced dimensions (volume, radius, thickness, width, length, diameter, and surface area). Empirical models (linear and nonlinear) and fundamental models (linear, deviations of linear behavior, and explicit variation of porosity) were discussed in this review. These models usually present a good fit with experimental data, but their wider predictive use is limited because of their dependence on the drying conditions and material characteristics.

Baini and Langrish (2007) included shrinkage for fresh bananas as a relation between radius and volume:

$$\frac{r}{r_0} = \left(\frac{V}{V_0}\right)^{1/2} = \left(0.6\frac{M}{M_0} + 0.4\right)^{1/2} \qquad (3.9)$$

Typically, empirical fitting through experiments is used to correlate the shrinkage phenomenon, as those used by the authors above, equations (3.6-3.9). Using these conditions, the thickness or radius of the sample is adjusted at each time step during the calculation of the governing equations for heat and mass. This approach is one of the limitations used; detailed experimental results on specific tropical fruits were used to find the empirical shrinkage equation before mathematical modeling is solved.

In the early stage of drying, the properties of material surface layer do not differ much from the center. As drying proceeds, the surface deforms due to viscoelastic behavior of the solid food particles.

Hassini *et al.* (2007) reported that shrinkage effect could not be neglected when moisture diffusivity determination for highly shrinking materials, like vegetables and fruits, had to be determined. The extent of shrinkage strongly depends on matrix mobility; in particular, it was proved that shrinkage is more significant during the constant and the falling rate periods.

In this way, Katekawa; Silva (2007) observed that the reduction of banana volume actually corresponded to the volumetric amount of liquid water removed from the sample (ideal shrinkage).

4. MATERIALS AND METHODS

The present study was developed in steps: raw material characterization, study of drying process under conditions described by Tribess (2009), termophysical properties measurement, mathematical modeling of drying process, study of shrinkage in real time.

4.1 Raw material characterization

The unripe banana (*Mussa cavendishii* var. Nanicão) from Vale do Ribeira, São Paulo, Brazil, was purchased from a local market (CEAGESP) and characterized as green banana (first stage of maturation); they were harvested at the commercial stage and were not submitted to maturation chamber.

The characterization of green banana was developed through physicochemical analyses and firmness.

4.1.1 Physicochemical analyses

- **pH:** measured, in duplicate, using a pH-stat (RADIOMETER, mod. PHM290, France), according to the method described by Zenebon; Pascuet (2005).
- **Titratable acidity:** was determined, in triplicate, according to the AOAC (1995) conducted in the pH-Stat (RADIOMETER, mod. PHM290, France).
- **Soluble solids**: determined, in duplicate, by a Refractometer (CARL-ZEISS JENA, mod. 711849, Germany). In order to obtain liquid (one drop) from the unripe banana structure, it was necessary to squeeze the pulp on the refractometer.
- **Moisture content**: determined, in triplicate, by gravimetric method after dehydration at 70 °C, at low pressure (≤ 20 kPa) until constant weight according to Zenebon; Pascuet (2005).

4.1.2 Firmness

To evaluate the firmness of green banana pulp, in triplicate, it was used a TA-Tx*plus* texture analyzer (Stable Micro Systems, UK). Penetrometry tests were performed along the long axis of the peeled banana at: stem end, the central point

and the distal end, as shown in Figure 4.1a. The probe was a cylinder with a flat base of 6 mm diameter (P/6 model). Fruit penetration velocity was of 1.0 $mm.s^{-1}$ and penetrated until 20 mm deep, according to Ditchfield (2004) and Tribess (2009) (Figure 4.1b).

Figure 4.1- Firmness analysis for unripe banana pulp in TATxplus texture analyzer, (Stable Micro Systems, UK) (a) and central point penetrometry test (b).

a) b)

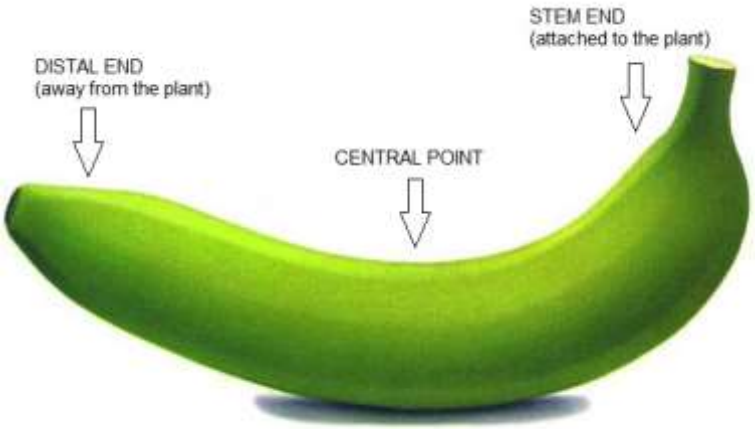

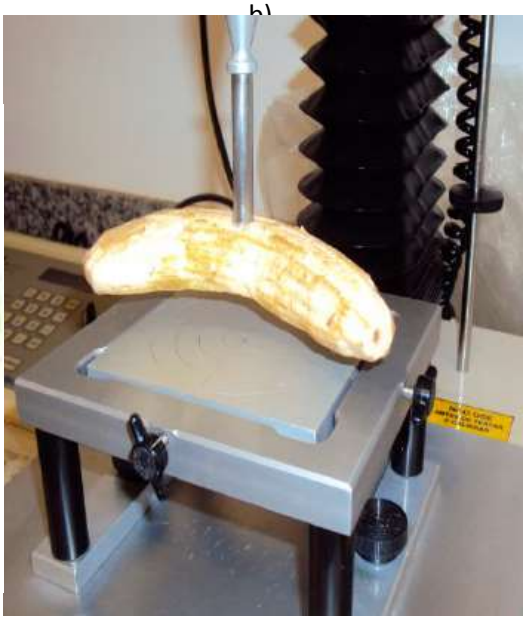

4.1.3 Moisture sorption isotherms

The adsorption and desorption curves of fresh unripe banana were obtained with a fully-automated and highly sensitive Vapor Sorption Analyzer (VSA, DECAGON, USA). The method chosen was the Dynamic Vapor Sorption (DVS) to determine static or equilibrium moisture, which the sample is exposed to different controlled humidities and temperatures.

The unripe bananas were peeled and cut into cylindrical slices (5 mm aprox. of thickness). Approximately 2 g were submitted to pre drying tests in an open oven at 40 ºC during 45 min or until the material achieved a water activity of 0.90.

After that, samples were transferred to a stainless steel sampling cup and inserted into the sample chamber (VSA), which is subsequently airtight sealed. The sorption isotherms measurements were conducted at four temperatures: 25 ºC, 40 ºC, 50 ºC and 60 ºC, in three replicates. These temperatures were chosen to avoid

the gelatinization temperature of the starch which is about (68.4 ± 0.3) ºC (TRIBESS *et al.,* 2009).

After obtaining the sorption isotherms, the moisture content of the banana sample was determined, according to gravimetric method proposed by Zenon; Pascuet (2005).

4.2 Fitting models

As stated before, the experimental behavior of sorption isotherms was fitted to GAB model (Eq. 3.1) , which was developed using the curve fitting tool of MATLAB® program, estimating the parameters (*C, K,* X_m) known as specific to each product, describing the behavior during adsorption or desorption.

The experimental behavior of physicochemical properties and the apparent volume during drying process of banana slices were fitted to different equations using the nonlinear regressions of the Statgraphics Centurion v.15.0 program (StatPoint®, Inc., USA).

4.3 Drying equipment

Drying experiments were carried out in a pilot scale LM-ES.20 (LabMaq, Brasil) dryer under conditions described by Tribess (2009). The equipment has been designed and constructed for unripe banana drying, in order to preserve the RS through the air-drying control, mainly by the relative humidity inside the drying chamber to ensure that the superficial temperature of the material does not increase, it is composed with two modules (Fig. 4.2).

Figure 4.2- Drying equipment LM-ES.20 constructed with two modules.

Module 1

- The chamber measures 0.6 m (width), 0.6 m (length) and 0.4 m (height).
- The drying chamber is constructed with stainless steel AISI 304, with 4 trays resting on a load cell, of maximum weight of 5 kg.
- On the top of the drying chamber (Fig. 4.3), there is a quartz glass characterized: high transparency, thermal resistance, high purity. In order to perform image acquisition for shrinkage measurements
- Next to the quartz glass, there is a temperature sensor for measuring and control the drying process temperature.
- At the bottom – back two ducts are connected to the chamber for the air-drying inlet and outlet, respectively.
- There are two chamber doors, the internal made of tempered glass and the outer of polycarbonate.

Figure 4.3- Chamber drying upper view showing: a) Quartz glass; b) Temperature sensor.

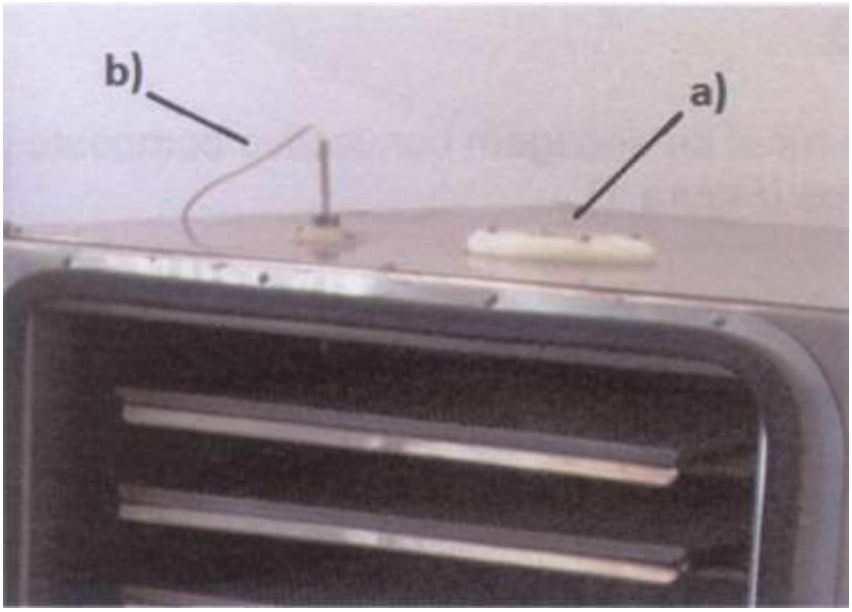

Module 2

This module is responsible for the equipment control, consisting of:

- Two fans with a flow rate of 24 $m^3 \cdot min^{-1}$, in order to ensure an air-drying velocity of 5 $m \cdot s^{-1}$ across the drying trays.
- Air temperature is controlled by means of an 3500 W electrical heater regulated by a proportional integral derivative (PID) controller.
- A refrigeration unit of 0.19 kW in order to control air humidity.
- A humidification unit with a peristaltic pump (Fig. 4.4a), atomizer nozzle (Fig. 4.4b) and a compressed air pressure regulator (Fig. 4.4c) to humidfy the drying air.

Figure 4.4 - Humidification unit: a) Peristaltic pump; b) Atomizer nozzle; c) Compressed air pressure regulator.

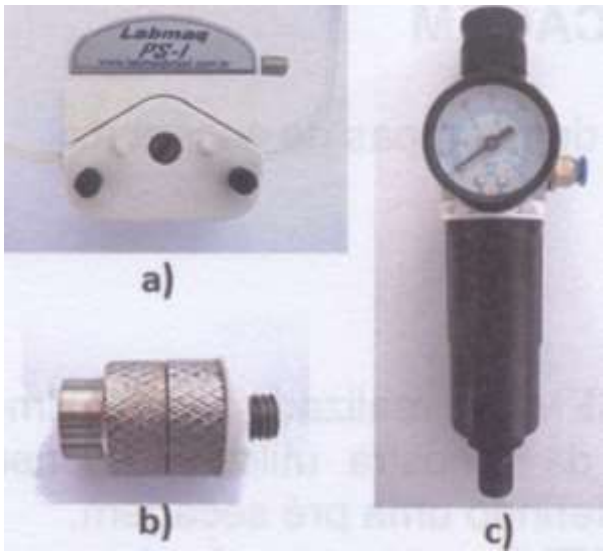

- A temperature sensor and thermo-hygrometer for measuring and controlling the temperature and humidity, it is worth to notice that there are two points where the air-drying temperature can be controlled.
- The automation unit is basically controlled by a frequency converter, the air-temperature, humidity and velocity by means of a proportional integral derivative (PID).
- Flask (1 L) positioned on the holder, to humidify the air-drying with the peristaltic pump and the atomizer nozzle (Fig. 4.5).

Figure 4.5 - Flask of 1 L of volume positioned on the holder.

4.3.1 Flowchart

The flowchart is summarized in the Fig. 4.6 presenting the dryer flowchart. It begins with the air inlet through the induction fan (V1) of 1.5 kW, next, it passes into the electrical heater (R1) of 3.5 kW; the temperature might be controlled at this point (TEMP2). Then, the hot air enters to the drying chamber across the four trays; it is worth to notice that inside the chamber there is another temperature sensor (TEMP1) to measure and control the temperature. In the initial stage of the process, the outlet air cools down and it becomes more humid, however, in the final stages of the process, the air-drying presents lower humidity.

The outlet air-drying goes into the air duct which conducts either to the induction fan (V2) and then to the refrigeration unit (UR1) to cool down or otherwise it will be conducted to the electrical heather (R1). If the air-drying is too dry, measured by the thermo-hygrometer (TH1), it will be humidified with the atomizer nozzle (B1).

Figure 4.6 - The air-drying fluid dynamics in the pilot scale LM-ES.20 dryer.

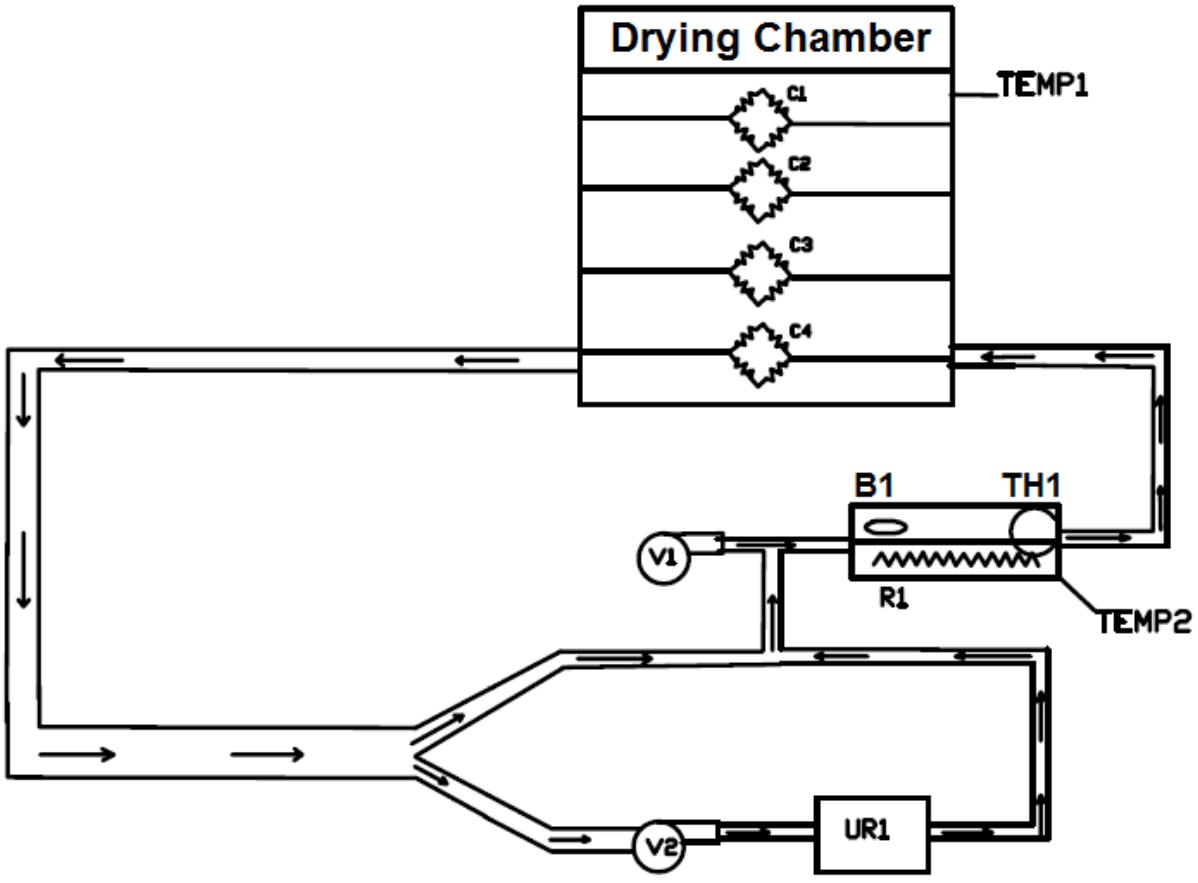

Source: LabMaq do Brasil, 2014

4.4 Drying experiments

The stages of the drying process of the unripe banana are represented in Figure 4.7, according to Tribess (2009).

Figure 4.7 - Drying process diagram.

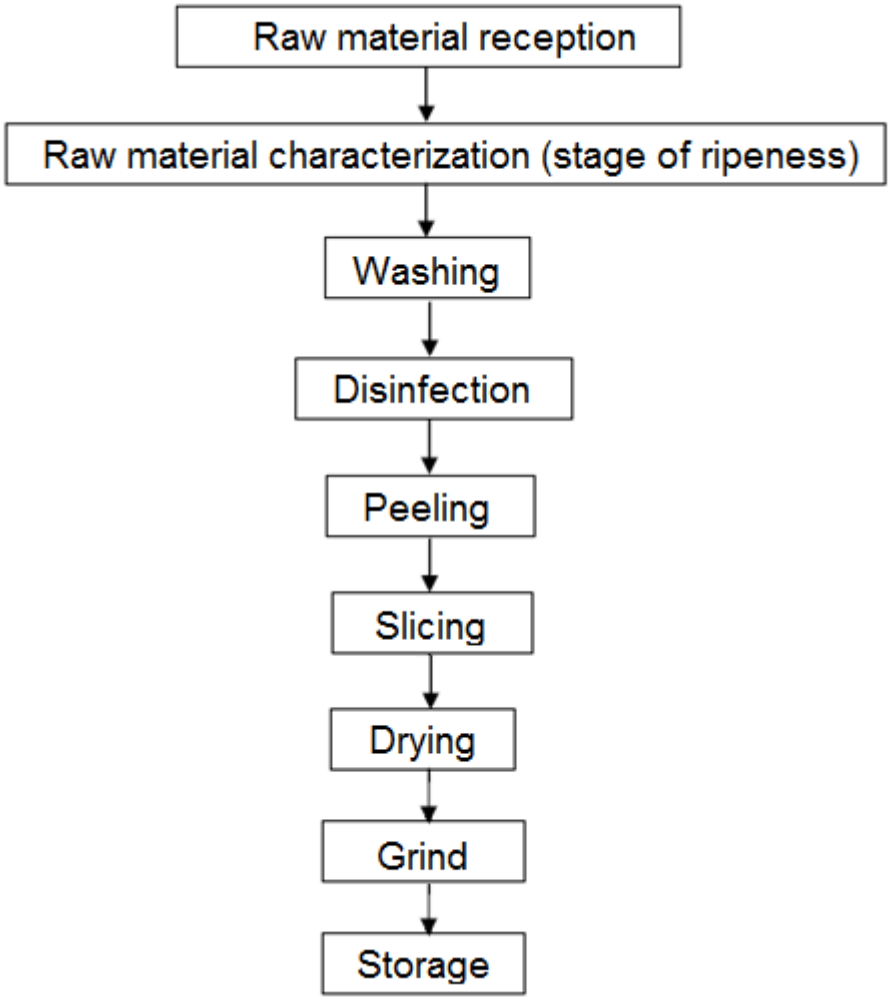

Source: adapted TRIBESS, 2009

The drying process was initiated with the reception of green banana fruits ensuring the maturation stage 1. Then, the unripe bananas were peeled and cut into 10 mm slices.

The banana slices were placed gently on the oven tray, and submitted to the drying process in triplicate at 60) ºC, 10 % of relative humidity and 4 $m \cdot s^{-1}$ of velocity in order to validate the mathematical modeling. During the dehydration process the weight loss relative humidity and temperature of the air-drying inside the chamber were track and save in an USB drive. The product temperature was recorded using

thermocouples inserted in two regions: at the surface and at the middle (0.5 cm of thickness).

The drying kinetics curve was constructed through the weight loss traduced to moisture content as a function of time.

4.4.1 Thermophysical properties measurement during drying process

The thermophysical properties were measured during drying process, because in the literature the thermal conductivity, specific heat capacity, and thermal diffusivity present strong dependence with the moisture content of the foodstuff.

The dehydration process was carried out in a laboratory open oven with forced ventilation (Nova Etica, Brazil), using three temperatures, 40 ºC, 50 ºC and 60 ºC.

At 50 ºC and 60 ºC of drying temperature, every 15 min during the first two hours of process and after that every 30 min, five banana slices were taken off, packed with PVC film and stored for at least 24 h in a desiccator at ambient temperature to avoid moisture loss and to ensure a uniform water concentration distribution. Because of the drying process of banana slices at 40 ºC was slower; five banana slices were taken off every 15 min during the first three hours. This procedure was done in duplicate.

The thermal conductivity (k), specific heat capacity (C_p) and thermal diffusivity (α) of banana slices were directly measured using KD2-PRO thermal properties analyzer (Decagon Devices, Inc), using the SH-1 (Dual Needle Sensor) compatible with most solid and granular materials. It uses transient line heat source method to measure k, C_p and α. The measurement is made by heating a needle that is placed in the sample and monitoring the temperature of the needle. In the case of the SH-1 sensor, one needle heats while the other one monitors. The heat input is made as small as possible to avoid thermally driven redistribution of moisture in the sample. The temperature change from heating may therefore be only a few tenths of a degree. The algorithms in the KD2 Pro are several orders of magnitude less sensitive to these errors than the conventional approach (plotting temperature vs. log time during heating and looking for a linear portion of the graph). This fully mathematical solutions delivers the measurement within ±10 %.

4.4.2 Physical properties during drying process

For these determinations, the samples geometry was standardized. For this purpose the bananas were cut into cylindrical slices with 26 mm of radius and 10 mm of thickness, as shown in Figure 4.8.

Figure 4.8 – Determination of physical properties of unripe banana cut into slices of 26 mm of radius and 10 mm of thickness.

At 40 ºC and 50 ºC of drying temperature, the banana slices were taken off every 45 min. The total drying time was about 600 min or until reaching moisture content closer to the equilibrium moisture content (X_e).

4.4.2.1 Apparent volume

The apparent volume (V_a) was measured through the volume displacement method. A glass pycnometer calibrated with distilled water at ambient temperature (V_f) was used to determine the toluene density (ρ_L).

The samples were weighed precisely and then transferred into a flask half filled with toluene, where the banana slices had to be cut into six small pieces to fit inside the glass pycnometer, as shown in Figure 4.9. After that the flask was then filled completing the volume, being carefully adjusted to ensure consistency, and weighed (MOHSENIN, 1968).

Figure 4.9 - The six small pieces of banana slice to determine its apparent volume.

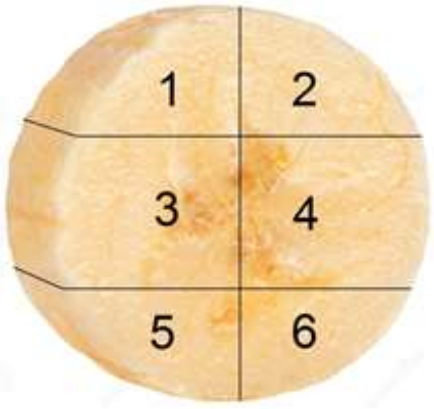

The volume of sample was calculated using Eq. 4.1:

$$V_A = V_f - \frac{m_{t+s} - m_f - m_b}{\rho_L} \qquad (4.1)$$

Wherein: V_f is the volume of the glass pycnometer; m_{t+s} is the weight of the glass pynometer plus the sample and the solvent; m_f is the weight of the glass pycnometer; m_b is the weight of the sample and ρ_L is the density of toluene.

4.4.2.2 True volume

The true volume (V_T) was measured using a multi-volume gas pycnometer AccuPyc II 1340 (Micromeritics Instrument Corp., Norcross, USA) with helium. The drying samples were taken as explained previously and the volume was measured in triplicate. A nominal sample chamber volume of 10 cm^3 was selected and the gas helium pressure adjusted to 134 kPa.

4.4.2.3. Shrinkage and porosity

Porosity (ε) is defined as the volume fraction of air in the sample. It can be calculated using Eq. (4.2)

$$\varepsilon = 1 - \frac{\rho}{\rho_T} \qquad (4.2)$$

Wherein, ρ is the apparent density and ρ_T is the true density of the unripe banana. Thus, the determination of porosity requires the measurement of both apparent and true volumes.

4.4.3 Shrinkage measurement

The dehydration process, for measuring the shrinkage phenomenon, was executed in the LM-ES.20 dryer specially designed for this purpose, as explained in section 4.3-Module 1.

Usually, the shrinkage is expressed as a function of decreasing volume and often as a function of the change of selected dimensions of the samples, measured with vernier or digital calipers.

The shrinkage data was measured using the stereo microscope (Leica S6D Greenough, Singapore) with 6.3:1 zoom and integrated video/photo port which allows easy and fast documentation.

As the unripe banana was being dried the shrinkage was proceeding, a single slab was under study, as soon as the process was started the slab was placed right under the quartz glass The shrinkage was measured with intervals of 1 h during 7 h, as drying process was carried out, with an electronic indicator (manual operation) adapted exclusively for the shrinkage measurement in the axial axis, shown in Fig. 4.10, which traduces the modified distance in micron (thousandth millesimal precision).

Figure 4.10 - Electronic indicator with manual operation for measuring shrinkage.

As soon as the process was started it was necessary to establish and set the focus to 0.000 in the electronic indicator, focusing a small part of the unripe banana with the maximum magnification corresponding to 4.0x. Every hour of drying the slab went out of focus due to the height diminution, requiring to be readjusted, (see Fig. 4.11). Such readjustment, at each hour of processing, was traduced in distance measured in microns by the electronic indicator. This procedure was repeated each hour until the material has not shown shrinkage in the axial axis and the thickness remained constant.

This part needed all the patience and accuracy, adjusting the objective, finding the focus and taking pictures every measurement, to track the phenomenon.

Figure 4.11 - Schematic diagram to measure the shrinkage data during drying process.

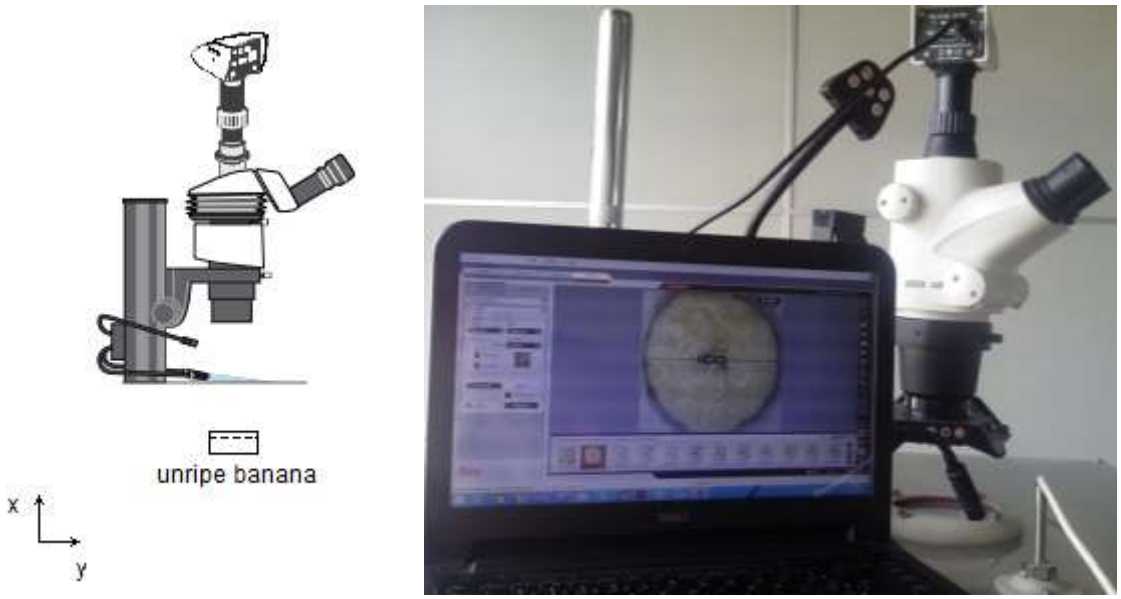

As a result, the height diminution was quantified making possible to obtain a correlation of the shrinkage behavior as a function of drying time, this correlation was inserted in the mathematical modeling.

The camera (Leica MC170 HD, Singapore) used to take the pictures was a HD Digital microscope camera with c-mount interface providing live image with a resolution of 5 Mpixels (see Fig. 4.12). The camera was used in PC mode offering full

compatibility with software installed in the PC providing an interactive measurement of the material being dried.

Figure 4.12 - Greenough Leica S6D stereo microscope with main objective, camera, illumination.

Source: www.leica-microsystems.com/

5. MATHEMATICAL MODELING

It was assumed that the banana slices were two-phase system, in which the solid phase would be the food matrix with some adsorbed water and the liquid phase a solution that includes the major part of water and solutes present in the food (FITO *et al.,* 1996).

Initially, the considered hypotheses are:

i. The initial distribution of moisture content and temperature of the banana are uniform;
ii. The water vaporization takes place only at the surface;
iii. During drying, the temperature of the banana slice is considered to be uniform at a fixed drying time;
iv. The shrinkage is negligible.
v. Physical and thermal properties are constant during drying process;
vi. The moisture transport phenomenon within the banana during drying can be described by the second Fick's law;
vii. The mass transfer mechanism is considered unidirectional;
viii. Air-drying conditions are considered constant during process.

Model Development

The model developed in this research considered the unidirectional mass transfer mechanism and the geometry of the food product as shown in Fig. 5.1.

Figure 5.1 - (a) Geometry of the sample slice and (b) simplified 2D axisymmetric model domain.

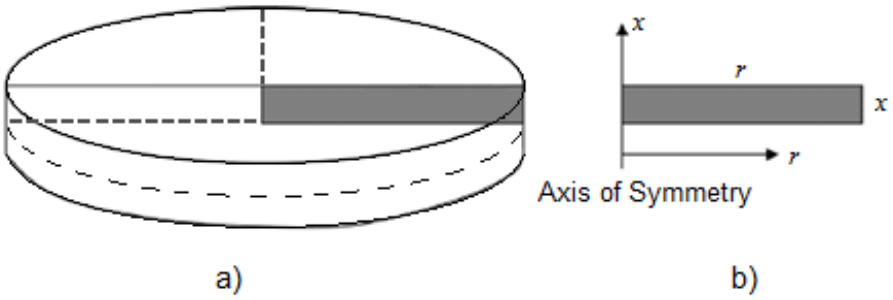

Source: KUMAR; MILLAR; KARIM, 2015

In a second step, this research project continued with the development of a more complex model, considering:

a) The physical and thermal properties changing during drying process;
b) The estimation of heat and mass transfer coefficients;
c) The estimation D_e as a function of moisture content;
d) The study of the shrinkage effect.

Then, the model validation with experimental data obtained in the dryer was carried out.

5.1 Mass and heat balance equation

For general heat and mass transfer a simple model of moisture and heat distribution during the drying of unripe banana slices is considered. The physical problem involved a single slice of banana of thickness 2*L*, initially at uniform temperature T_0 and uniform moisture content M_0. Drying is taken as effective only at the surfaces $x = \pm L$. The surface of the drying material is in contact with drying air, providing a convective boundary condition for moisture content *M*, at constant air temperature T_{air}, as shown in Figure 5.2.

Figure 5.2 - Schematic representation of a banana slice considering a unidimensional model during process study.

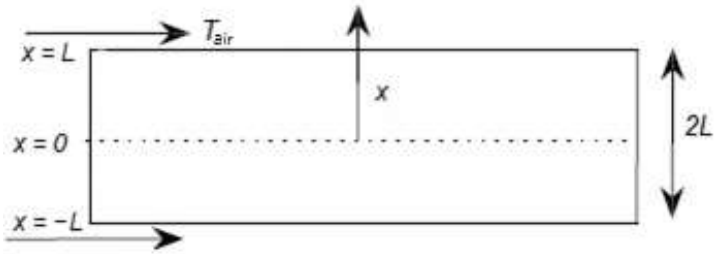

Source: Adapted from Shahari; Hibberd (2012)

During drying, heat is transferred mainly by convection from air to the product surface and by conduction from the surface towards the product center. Such mechanism provides the basis for a simultaneous heat and moisture transfer model.

The equation of mass conservation could be written as follows (BIRD *et al.,* 1960; CARSLAW; JAEGER, 1959):

$$\rho\left\{\frac{\partial M}{\partial t}+\vec{v}\ \vec{\nabla}M\right\}=\vec{\nabla}\left(\rho\ D\ \vec{\nabla}M\right) \qquad (5.1)$$

The equation of heat conservation could be written as follows:

$$\rho\left\{\frac{\partial\left(C_pT\right)}{\partial t}+\vec{v}\ \vec{\nabla}\left(C_pT\right)\right\}=\vec{\nabla}\left(k\ \vec{\nabla}T\right) \qquad (5.2)$$

The displacement , denoted as $\vec{v}$, is neglected. For a one-dimensional geometry (axial direction) with constant effective diffusivity D_e and constant thermophysical properties, considering the hypotheses described in the previous section, the governing physical equations for the simultaneous heat and moisture transfer problem become:

$$\rho\frac{\partial M}{\partial t}=\frac{\partial}{\partial x}\left(D_e\ \rho\frac{\partial M}{\partial x}\right);\qquad 0<x<L \qquad (5.3)$$

$$\rho C_p\frac{\partial T}{\partial t}=\frac{\partial}{\partial x}\left(k\frac{\partial T}{\partial x}\right);\qquad 0<x<L \qquad (5.4)$$

At the beginning of the drying process, the moisture content, temperature and the thickness of the product are taken as uniform; therefore, the initial conditions are:

$$M=M_0,\qquad T=T_0,\qquad L=L_0\quad \text{at}\quad t=t_0 \qquad (5.5)$$

Imposing symmetry, there are no temperature and moisture concentration gradients at the center of the product, therefore the boundary conditions are:

$$\frac{\partial M}{\partial x}=0\qquad \text{and}\qquad \frac{\partial T}{\partial x}=0;\qquad \text{at } x=0 \qquad (5.6)$$

At the surface, a driving gradient from the surface to the air that involves partial pressure and temperature is considered as drying boundary condition. The driving force for the water vapor flux from the wetted surface to the air is the difference between absolute humidity in the air (C_{air}) and the water content in the form of liquid water film at the surface (C_{sur}). In this case, the boundary condition at the surface becomes:

$$-D_e \rho \frac{\partial M}{\partial x} = h_m \left(C_{\text{sur}} \overline{MW}_{H_2O} - C_{air} \frac{1}{\upsilon_e} \right); \qquad \text{at} \qquad x = L \qquad (5.7)$$

wherein: h_m is the mass transfer coefficient $m \cdot s^{-1}$.

Heat transfer at the surface boundary occurs by convection, typically modeled through the use of a heat transfer coefficient (h). Some heat is also absorbed by the moisture in transferring to a vapor phase, and the boundary condition at the surface is given by:

$$k \frac{\partial T}{\partial x} - \lambda D_e \rho \frac{\partial M}{\partial x} = -h\left(T_{\text{sur}} - T_{air}\right) \qquad \text{at} \qquad x = L \qquad (5.8)$$

wherein: λ is the heat of vaporization of water (latent heat).

In this model the moisture is removed from the surface when the air temperature $T_{air} \gg T_0$, in which the gradient of temperature permitted to dry the unripe banana slab.

5.1.1 Estimation of C_{air} and C_{sur}

Boundary conditions (5.6 and 5.7) link the surface condition directly to the surface temperature and incorporate surface water concentrations under local psychometric conditions. As denoted in hypotheses (viii) the air-drying conditions (temperature, relative humidity (RH), velocity) are assumed constant, in this way, the absolute humidity (C_{air}) is determined through the psychometric chart in kg $H_2O \cdot$kg dry air^{-1}, as shown in Table 5.1.

Table 5.1 - Air-drying water concentration C_{air} far from the sample at different drying conditions.

Air-drying conditions		**Psycrometric chart**
Temperature [°C]	*RH* [%]	C_{air} * [kg H_2O·kg dry air^{-1}]
40	10	0.0050
50	10	0.0085
60	10	0.0130

* Data taken from the psycrometric chart at P = 0.926 bar

Thermodynamic equilibrium relationship between the air humidity and the moisture surface of food has been used to calculate C_{sur}, according to the desorption isotherm at the process temperature and the a_w definition stated as the ratio of the partial pressure of water in the headspace of a product (p_v) to the vapor pressure of pure water ($p_{v0}(T)$) at the same temperature (Eq. 5.9). In the estimation, it has been considered that the thermodynamic equilibrium in the sorption isotherms can be correlated with the drying process, as it is necessary to know the C_{sur} at each moment to model the process:

$$a_w = \frac{p_v}{p_{v0}(T)} \qquad (5.9)$$

Considering the air as an ideal gas (at low pressure) in thermodynamic equilibrium with the water film at food surface and the water activity relationship, the following relationship can be considered (FELDER; ROUSSEAU, 2000):

$$C_{sur} = \left(\frac{a_w p_{v0}(T)/P}{1-\left(a_w p_{v0}(T)/P\right)} \right) \frac{P}{RT} \overline{MW}_{H_2O}\, \upsilon_e \qquad (5.10)$$

For this purpose it was necessary to determine the vapor pressure of pure water at drying temperature ($p_{v0}(T)$) from Antoine modified equation (REID; PRAUSNITZ; SHERWOOD, 1977):

$$\ln\left(\frac{p_{v0}}{p_c}\right) = a_0\ \left(a_1 + a_2 + a_3 + a_4\right) \qquad (5.11)$$

wherein: $a_0 = (1-y)^{-1}$

$a_1 = A\,y$

$a_2 = B\,y^{1.5}$

$a_3 = \Theta\,y^3$

$a_4 = D\,y^6$

$y = 1-\left(\frac{T}{T_c}\right)$

This correlation uses the T_c and $p_{c,}$ which corresponds to the critical temperature and pressure for saturated vapor of 647.3 [K] and 221.2 [bar], respectively. The parameters a_o to a_4 and y are component-specific constants.

5.2 Mass and heat balance equation considering shrinkage

An interesting shrinkage approach was published by Shahari; Hibberd (2012), in which, the authors considered the drying process as a simultaneous heat and mass transfer, similarly with this study. They introduced a complex factor for the solution related to a changing region of the sample, with an interface decreasing with drying. To track the interface position, it is convenient to fix its location within a changing coordinate grid. Using the transformation $\xi=\frac{L(t)}{L_0}$, the surface interface corresponds to a fixed value ξ=1, a revised formulation for equations (5.3) and (5.4), in the form of independent state variables (ξ, t), replacing (x, t), become

$$\rho\frac{\partial M}{\partial t} = \frac{1}{L^2(t)}\frac{\partial}{\partial \xi}\left(D_e\,\rho\frac{\partial M}{\partial \xi}\right)+\frac{1}{L_0}\frac{dL}{dt}\frac{\partial M}{\partial \xi}; \qquad (5.12)$$

$$\rho C_p\frac{\partial T}{\partial t} = \frac{1}{L^2(t)}\frac{\partial}{\partial \xi}\left(k\frac{\partial T}{\partial \xi}\right)+\frac{1}{L_0}\frac{dL}{dt}\frac{\partial T}{\partial \xi}; \qquad (5.13)$$

For the boundary condition at the surface for mass and heat, respectively:

$$-D_e\rho\frac{\partial M}{\partial \xi} = h_m L_0\left(C_{\text{sur}}-C_{air}\right); \qquad \text{at} \quad x = L(t) \qquad (5.14)$$

$$k\frac{\partial T}{\partial \xi} - \lambda D_e \rho \frac{\partial M}{\partial \xi} = -hL_0\left(T_{sur} - T_{air}\right) \qquad \text{at} \qquad x = L(t) \qquad (5.15)$$

The thermodynamic equilibrium relationship between water concentration in the air and water concentration on the external surface of food, C_{sur}, and C_{air} were estimated as explained in section 5.1.1.

5.3 Computational formulation

A numerical solution was obtained using the method of lines (SCHIESSER, 1991). Discretizing the fixed integration region $0 \leq \xi \leq 1$ into N sub-intervals, gives a system of $2N$ ordinary differential equations for $M_j(t)$, $T_j(t)$. This system of equations was then solved numerically using MATLAB ODE45 solver, which is based on an order-5 Runge Kutta-Fehlberg Method (RK45).

Discretizing equation (5.3) with a central difference approximation becomes:

$$\frac{\partial M_j}{\partial t} = D_e\left[\frac{M_{j+1} - 2M_j + M_{j-1}}{\Delta x^2}\right] \qquad j = 2,3...,N-1$$

at general index point j with $M_j = M(x_j)$ for j=1,...,N-1 com $\Delta x = \frac{L}{N-1}$

Applying the symmetry condition (there are no temperature and moisture concentration gradients at the center of the product), using the central difference approximation of Eq. 5.6 and boundary condition of Eq. 5.7:

$$x = 0; \qquad \frac{M_{j+1} - M_{j-1}}{2\Delta x} = 0 \qquad j = 1$$

$$x = L; \qquad \frac{\partial M_j}{\partial x} = -\frac{h_m}{D_e \rho}\left(C_{sup} - C_{air}\right) \qquad j = N$$

For the heat balance equation (5.4) discretizing with a central difference approximation becomes:

$$\frac{\partial T_j}{\partial t} = \alpha \left[\frac{T_{j+1} - 2T_j + T_{j-1}}{\Delta x^2} \right] \qquad j = 2,3...,N-1$$

at general index point j with $T_j = T(x_j)$ for j=1,...,N-1 com $\Delta x = \frac{L}{N-1}$

Applying the symmetry condition using the central difference approximation of Eq. 5.6 and Eq. 5.8:

$$x = 0; \qquad \frac{T_{j+1} - T_{j-1}}{2\Delta x} = 0 \qquad j = 1$$

$$x = L; \qquad k\left(\frac{T_{N+1} - T_{N-1}}{2\Delta x}\right) - \lambda \rho D_e \left(\frac{M_{N+1} - M_{N-1}}{2\Delta x}\right) = -h\left(T_{sup} - T_{air}\right) \qquad j = N$$

5.4 Input parameters

5.4.1 Case I – Constant properties

The input parameters used in case I for the drying simulation are summarized in Table 5.2. with the generic drying conditions for unripe banana slices.

Table 5.2 - Input parameters used in the simulations of drying unripe banana slices.

Parameter	Symbol	Range of value	Units
Food density	ρ	1045	$kg \cdot m^{-3}$
Effective diffusivity[a]	D_e	3.054×10^{-10}	$m^2 \cdot s^{-1}$
Length	L	0.005	m
Mass transfer coefficient[b]	h_m	4×10^{-4}	$m \cdot s^{-1}$
Heat transfer coefficient[b]	h	80	$W \cdot m^{-2} \cdot K^{-1}$
Thermal conductivity[c]	k	0.894	$J \cdot s^{-1} \cdot m^{-1} \cdot K^{-1}$
Thermal diffusivity[d]	α	1.8×10^{-7}	$m^2 \cdot s^{-1}$
Specific heat capacity	C_p	4854	$J \cdot kg^{-1} \cdot K^{-1}$
Latent heat evaporation	λ	2.345×10^6	$J \cdot kg^{-1}$
Ideal gas constant	R	8.3144	$Pa \cdot m^3 \cdot mol^{-1} \cdot K^{-1}$
Parameter of desorption isotherm[e]	C	5.4	-
Parameter of desorption isotherm[e]	K	0.93	-
Parameter of desorption isotherm[e]	X_m	0.053	$kg \cdot kg^{-1}$

Source: [a] Zabalaga; Carballo (2009)
[b] Shahari; Hibberd (2012)
[c] Perussello; Mariani; Mendes (2010)
[d] Erdoğdu (2008)
[e] Present work

In this stage (Case I) the heat and mass transfer coefficients used were taken from the available literature for foodstuff (BIALOBRZEWSKI, 2007; ERDOĞDU, 2008; HUSSAIN; DINCER, 2003b). The thermal properties used were measured at the beginning of the process and taken as constants.

5.4.2 Case II – Variable thermophysical properties

It is vital to have accurate thermal property data for foods for modeling and design purposes. Thermophysical properties are needed in food process design and optimization involving heat transfer, such as drying, cooking, and freezing. Although highly desirable, a generic model to predict thermophysical properties of foods does not exist.

There are many studies available in the literature about thermal conductivity data for minimally processed foods such as fruits and vegetables (CHOI AND OKOS, 1986; ERDOĞDU, 2014; MARIANI; MENDES, 2010; PERUSSELLO; RAHMAN, 1995).

According to Sweat (1994) there is a strong linear correlation between specific heat and moisture content, especially over the highest range of water content. Alvarado (1991) used exponential form of equation to correlate the specific heat of fruit pulps which water content varied from (0 to 95) g/100g moisture content w.b.

The density and porosity are important physical properties characterizing the texture and the quality of dry and intermediate moisture foods (WANG; BRENNAN, 1995). Experimental values of these properties are also essential in modeling and design of various heat and mass transfer operations. Marousis and Saravacos (1990) investigated the density and porosity in drying starch materials. A polynomial function of moisture content was fitted to the density data.

In this study, the physical and thermophysical properties were estimated during the drying process determining empirical correlation used in the mathematical model, as explained on sections 4.4.1 and 4.4.2,

5.4.3 Case III – Estimation of heat and mass transfer coefficients

In this case the estimation of h and h_m were performed through a nonlinear optimization routine in Matlab, in which, the modeling process involved iterative

process minimizing the error sum of the squares (ESS) of the experimental data (moisture content and temperature of the slab) against the calculated from the model (partial differential equations).

In order to perform the estimation, it was necessary to calculate the *h* and h_m as an initial input parameter, according to Holman (1986) by:

$$h = \frac{Nu\ k_\infty}{d} \qquad (5.16)$$

wherein: Nu is Nusselt number, k_∞ is the drying air thermal conductivity $W \cdot m^{-1} \cdot K^{-1}$ and d is the unripe banana slice diameter [m].

Nu was calculated by Eq. (5.17) (HOLMAN, 1986), a correlation between Reynolds number (Re) and Prandlt number (Pr), which is applied to the fluid flow through cylinders, valid for $Pr \geq 0.7$ and $0.4 \leq Re \leq 4x10^5$.

$$Nu = 0.683 Re^{0.466} Pr^{1/3} \qquad (5.17)$$

Re and Pr were calculated according to Incropera; Dewitt (1990) by

$$Re = \frac{\rho_\infty v_\infty d}{\mu_\infty} \qquad (5.18)$$

and

$$Pr = \frac{Cp_\infty \mu_\infty}{k_\infty} \qquad (5.19)$$

wherein: μ_∞ is the drying air viscosity [Pa·s], v_∞ is the air-drying velocity $m \cdot s^{-1}$ and k_∞ is the thermal conductivity $W \cdot m^{-1} \cdot K^{-1}$.

The convective mass transfer coefficient, h_m $m \cdot s^{-1}$, was calculated according to Holman (1986) by:

$$h_m = \frac{h}{\rho_\infty Cp_\infty \left(\frac{\alpha_\infty}{D_\infty} \right)^{2/3}} \qquad (5.20)$$

wherein: α_∞ is the air thermal diffusivity $m^2 \cdot s^{-1}$ and D_∞ is the water diffusivity on air $m^2 \cdot s^{-1}$, available in Incropera; Dewitt (1990).

In Table 5.3 the parameters used in the correlations for Nu, Re and Pr are shown to estimate the heat and mass transfer coefficients.

Table 5.3 - Parameters used in the correlation for *Nu, Re and Pr* numbers

Parameter	Symbol	Value	Units
Density of air [b]	ρ_∞	1.086	$kg \cdot m^{-3}$
Thermal conductivity of air [a]	k_∞	0.0207	$W \cdot m^{-1} \cdot K^{-1}$
Viscosity of air [a]	μ_∞	1.664×10^{-5}	$Pa \cdot s$
Specific heat of air [a]	$C_{p\infty}$	1005.04	$J \cdot kg^{-1} \cdot K^{-1}$
Water diffusivity on air [b]	D_∞	2.418×10^{-9}	$m^2 \cdot s^{-1}$
Thermal diffusivity of air [b]	α_∞	26.63×10^{-6}	$m^2 \cdot s^{-1}$
Air-drying velocity	v_∞	4	$m \cdot s^{-1}$
Unripe banana diameter	d	28×10^{-3}	m
Nusselt number	Nu	23.7	-
Prandtl number	Pr	0.702	-
Reynolds number	Re	411	-
Coefficient of heat transfer	h	146	$W \cdot m^{-2} \cdot K^{-1}$
Coefficient of mass transfer	h_m	2.7×10^{-3}	$m \cdot s^{-1}$

Source: [a] Incropera; Dewitt (1990)
[b] Holman (1986)

5.4.4 Case IV – D_e as a function of moisture content

Through the estimation of h and h_m performed in the Case III, it was possible to estimate the D_e behavior denoted in section 3.3.2.

Two approaches were used: the first model (Eq. 3.4) was tested in carrot, potato, onion and pepper by Kiranoudis *et al.* (1993). The second model used corresponds to a polynomial equation presented in Eq. (5.21).

$$D_e = \psi_1 M^3 + \psi_2 M^2 + \psi_3 M + \psi_4 \qquad (5.21)$$

wherein: M is the moisture content in dry basis $kg \cdot kg^{-1}$ and the D_e is expressed in $m^2 \cdot s^{-1}$ and Ψ_i are the parameters estimated in the nonlinear regression, through an optimization routine, as performed in the previous section 5.3.3.

5.4.5 Shrinkage condition

As explained shrinkage is a complex phenomenon, which, reduces the thickness of the sample and so affects the transfer of heat to the medium and the transfer of moisture to the surface. At this point, the major challenge was to highlight the effect of shrinkage; initially, it was assumed that no gas phase (air or vapor) is present and the material consists only of solid and liquid phases.

In Eqs. 5.12 and 5.13, the last term describes the shrinkage phenomenon (thickness reduction) through the $\frac{dL}{dt}$, this reduction was measured during the process with the stereomicroscope every hour.

5.5 COMSOL modeling

Simulation was performed by using COMSOL Multiphysics 4.4, finite element–based engineering simulation software. The software facilitated all steps in the modeling process, including defining geometry, meshing, specifying physics, solving, and then visualizing the results. COMSOL Multiphysics can handle the variable properties, which are a function of the independent variables. Therefore, this software was very useful in drying simulation where material properties changed with temperature and moisture content. The simulation methodology and implementation strategy followed in this project shown in Fig. 5.3. The simulation does not model the convective velocity field outside the unripe banana slab because the coefficients for convective heat and moisture transfer to the surrounding air are given.

Figure 5.3 - Simulation strategy in COMSOL Multiphysics.

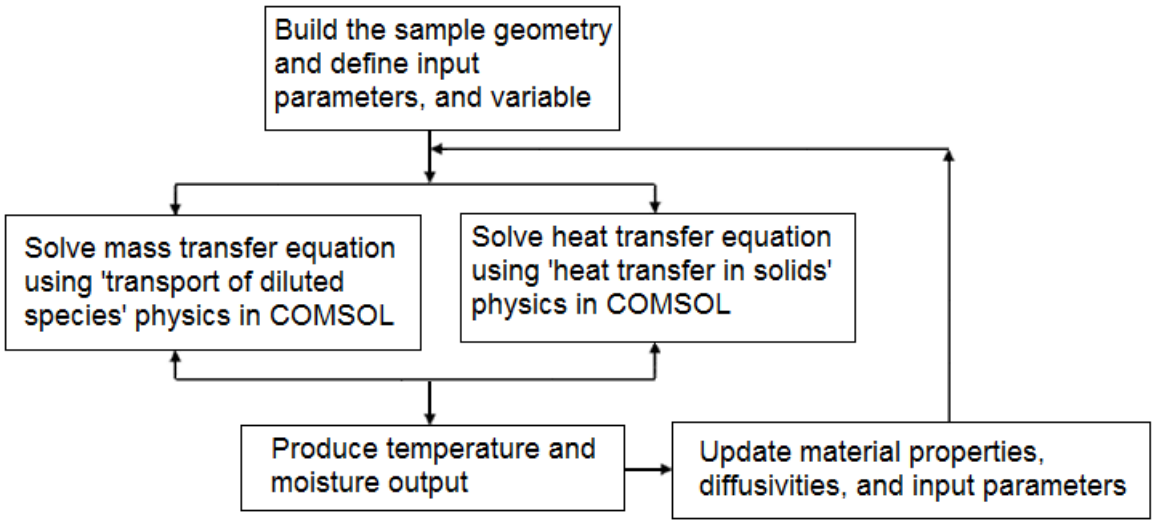

Adapted from (KUMAR; MILLAR; KARIM, 2015)

5.5.1 Model definition

COMSOL Multiphysics couples time-dependent interfaces describing the temperature and the moisture concentration, respectively. Inside the slab, diffusive processes describe both heat transfer and moisture transport. Fig. 5.4 depicts the slab geometry, which is simple and allows for 2D-axisymmetric modeling of its cross section. Additional symmetry in the cross section makes it possible to model just one quarter of the cross section.

Figure 5.4 - Geometry considered for the unripe banana slab.

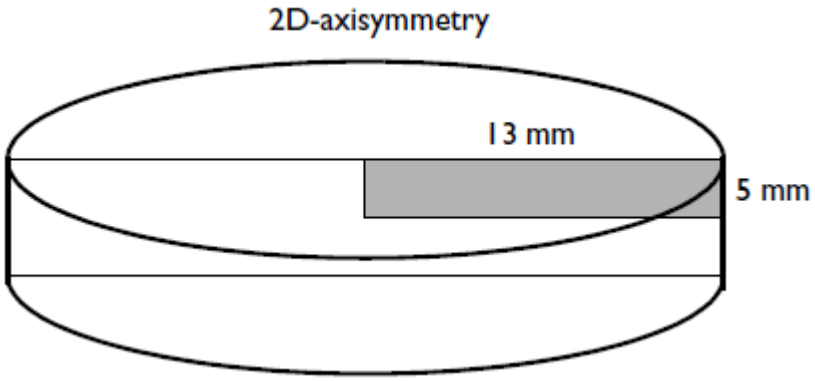

These simplifications result in a simple rectangular domain with the dimension 13 mm by 5 mm. Figure 5.5 describes the boundary numbering used when specifying the boundary conditions.

Figure 5.5 - Model domain and boundary numbering.

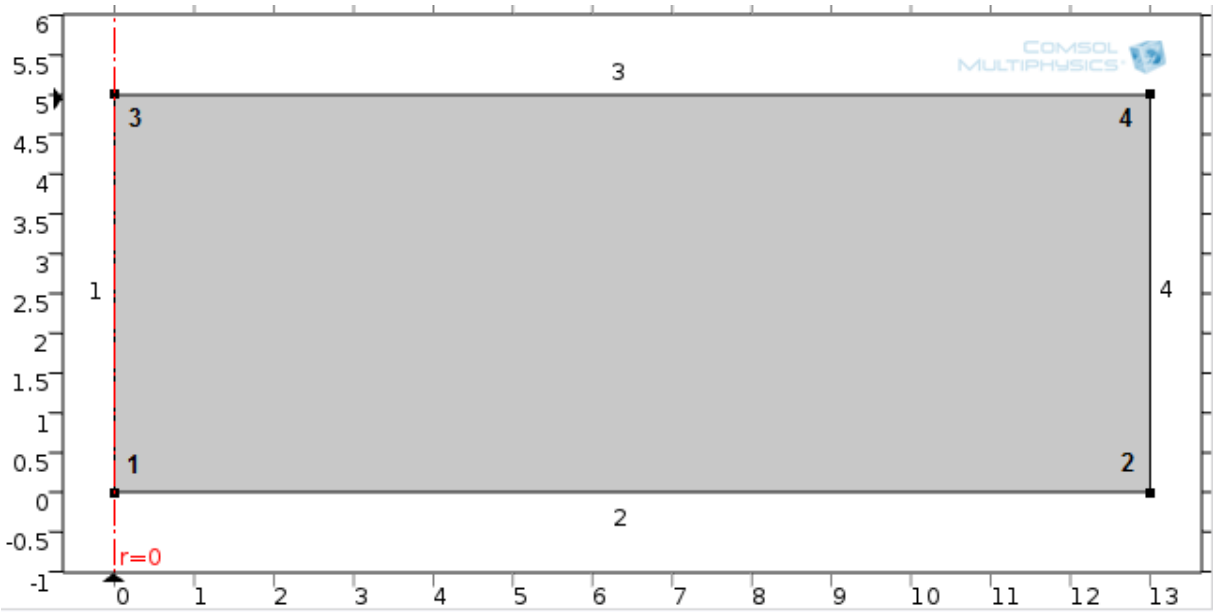

The vaporization of water at the slab outer boundaries generates a heat flux out of the patty. This heat flux is represented with the term $D_e\lambda\nabla C$ in the boundary conditions for boundaries 3 and 4. Assume symmetry for the temperature field on boundaries 1 and 2. Air convection adds heat in the boundaries 3 and 4.

COMSOL considers the next system of boundary conditions for heat transfer according to the assumptions made earlier, add a term for the heat flux out of the slab due to moisture vaporization in the boundaries 3 and 4.

$$(-k\nabla T) = 0 \qquad \text{at } \partial\Omega_1 \text{ and } \partial\Omega_2 \qquad (5.22)$$

$$(k\nabla T) = h(T_{air} - T) + (D_e\lambda\nabla C) \qquad \text{at } \partial\Omega_3 \text{ and } \partial\Omega_4 \qquad (5.23)$$

wherein: h is the heat transfer coefficient $W\cdot m^{-2}\cdot K^{-1}$, T_{air} is the air-drying temperature and Ω denotes the boundary in the model domain.

The boundary conditions for the diffusion are:

$$(-D_e\nabla C) = 0 \qquad \text{at } \partial\Omega_1 \text{ and } \partial\Omega_2 \qquad (5.24)$$

$$(D_e\nabla C) = h_m(C_{air} - C_b) = 0 \qquad \text{at } \partial\Omega_3 \text{ and } \partial\Omega_4 \qquad (5.25)$$

wherein: h_m is the mass transfer coefficient m·s^{-1}, C_{air} denotes the outside air moisture concentration mol·m^{-3} and C_b moisture concentration of banana slab.

The computational domain considered by the COMSOL is represented by a cylinder in Fig. 5.6, as explained previously. The initial and boundary conditions for the heat transfer were defined as: homogeneous temperature in the beginning of the process (Eq. 5.22), convection on the surface of the material (Eqs. 5.23 and 5.25) and null heat flux in the symmetry region (Eq. 5.24).

Figure 5.6 - Computational domain considered by COMSOL.

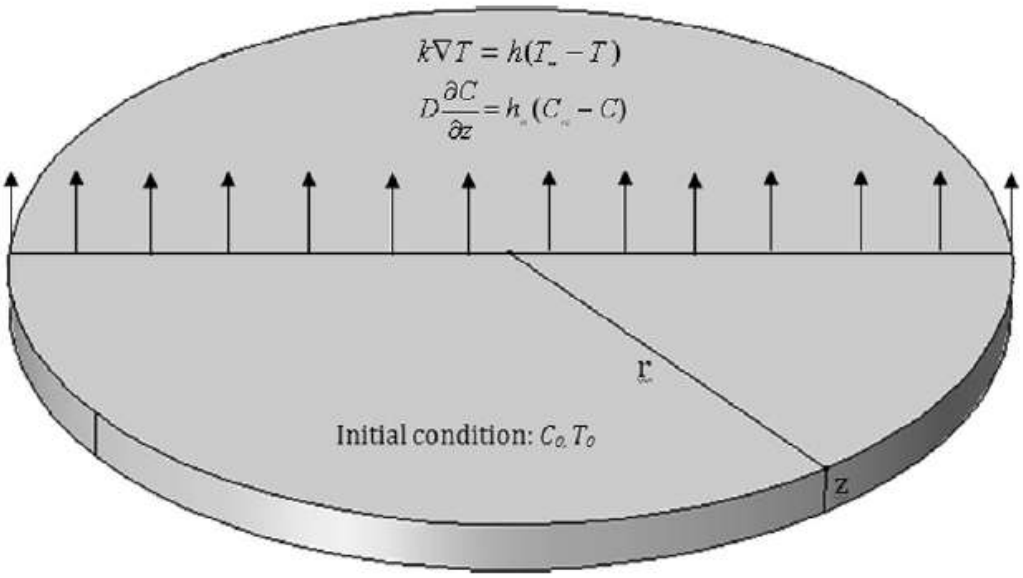

Addapted from: (Perussello *et al.,* 2013)

It was assumed that the unripe banana slab initial temperature was 22 ºC, as considered previously in the mathematical modeling using Matlab. The moisture concentration of the air (C_{air}) was 733 mol·m^{-3} on wet basis.

The meshing was performed in the rectangular domain with the dimensions of 13 mm and 5 mm. The software permitted to perform a smaller mesh at the surface which is in contact with the drying air, as shown in Figure 5.7.

Figure 5.7 – Model domain and mesh of the geometry considered in COMSOL.

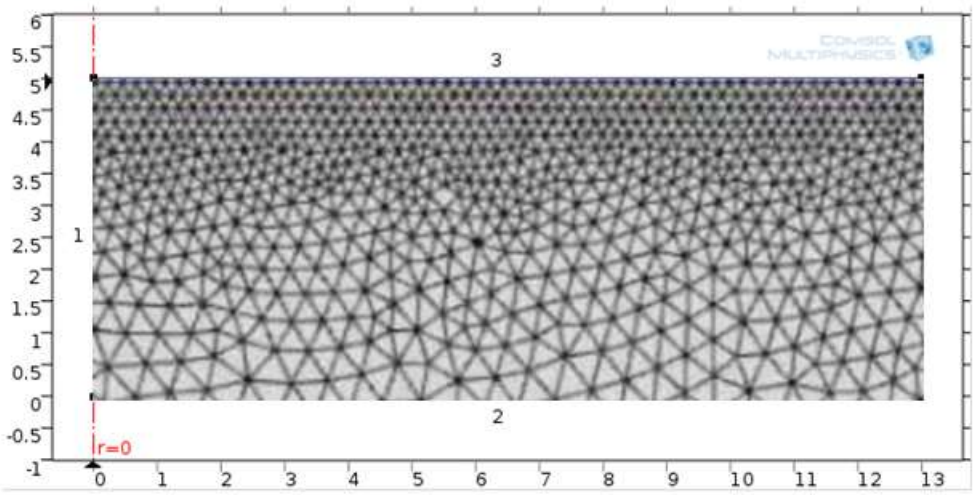

6. RESUTS AND DISCUSSION

6.1 Raw material characterization

The unripe banana characteristics are summarized on Table 6.1 and they were compared with results obtained by: Ditchfield (2004), Tribess (2009) and Mendez (2013).

Table 6.1 - Physico-chemical characterization and firmness of green banana in comparison with literature data.

Physico-chemical property	Results	Data from literature	
Titratable acidity (g.100 g^{-1})[1]	0.28 ± 0.03	0.24 ± 0.03[a]	0.37 ± 0.09[b]
Soluble solids (°Brix)	7.3 ± 0.5	3.5 ± 0.8[a]	5.3 ± 2.0[b]
Firmness (N)	30.9 ± 4.1	31.5 ± 1.5[b]	30.8 ± 5.3[c]
Moisture content (wb) (kg $H_20 \cdot kg^{-1}$)	0.707 ± 0.012	0.70 ± 0.01[b]	0.715 ± 0.010[c]
Ph	5.9 ± 0.1	5.3 ± 0.1[b]	5.6 ± 0.3[b]

[1] expressed as malic acid
[a] Ditchfield, (2004)
[b] Tribess, (2009b)
[c] Mendez, (2013)

The ripeness stage characterization through the visual peel color has its limitations due to the different perception on green and yellow leading to incorrect results. The main limitation consists on the fact that small color changes may carry on variations in the unripe banana composition, mostly in the resistant starch content.

The physico-chemical properties of the unripe banana were determined throughout September-2013 and October-2014; the results obtained are similar compared those reported in the literature, while the soluble solids obtained in this study presented a difference in comparison with literature data. The firmness is considered as the main characteristic to describe the ripeness stage, according to Ditchfield; Tadini (2002) and Tribess (2009), which in this study was found to be 30.9 ± 4.1 N, indicating that the ripeness of the unripe banana used in this study could be classified as stage 1.

It is worth to declare that the physico-chemical properties as soluble solids [°Brix], titratable acidity g·100g^{-1} and pH show variation during the year, due to the weather changes, temperature and relative humidity. According to Tribess (2009), the ambient temperature affects the firmness justifying the significant standard deviation of this property.

Therefore, with the physico-chemical results in Table 6.1 agree with the ripeness stage 1 stated by Ditchfield (2004), can be concluded that the unripe banana used in this study may present high resistant starch content.

6.2 Sorption isotherms

The water adsorption and desorption isotherms data of fresh unripe banana at studied temperatures (25, 40, 50 and 60) °C modeled with the GAB equation (Eq. 3.1) are shown in the Figs. 6.1 and 6.2, respectively.

Figure 6.1 - Adsorption isotherms for fresh unripe banana, at temperatures of 25 ºC, 40 ºC, 50 ºC and 60 ºC, at an interval of a_w between 0.1 and 0.9. Lines correspond to the GAB model.

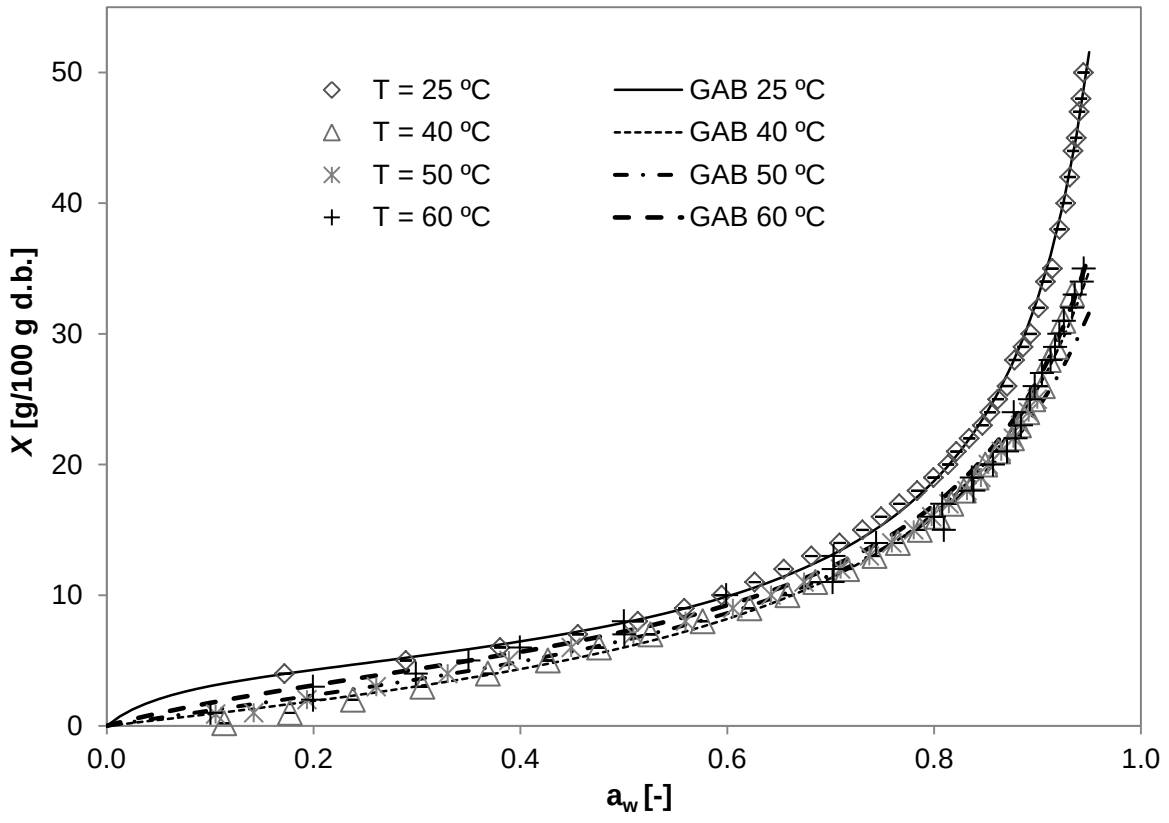

Figure 6.2 - Desorption isotherms of fresh unripe banana, at temperatures of 25 ºC, 40 ºC, 50 ºC and 60 ºC, at an interval of a_w between 0.1 and 0.9. Lines correspond to the GAB model.

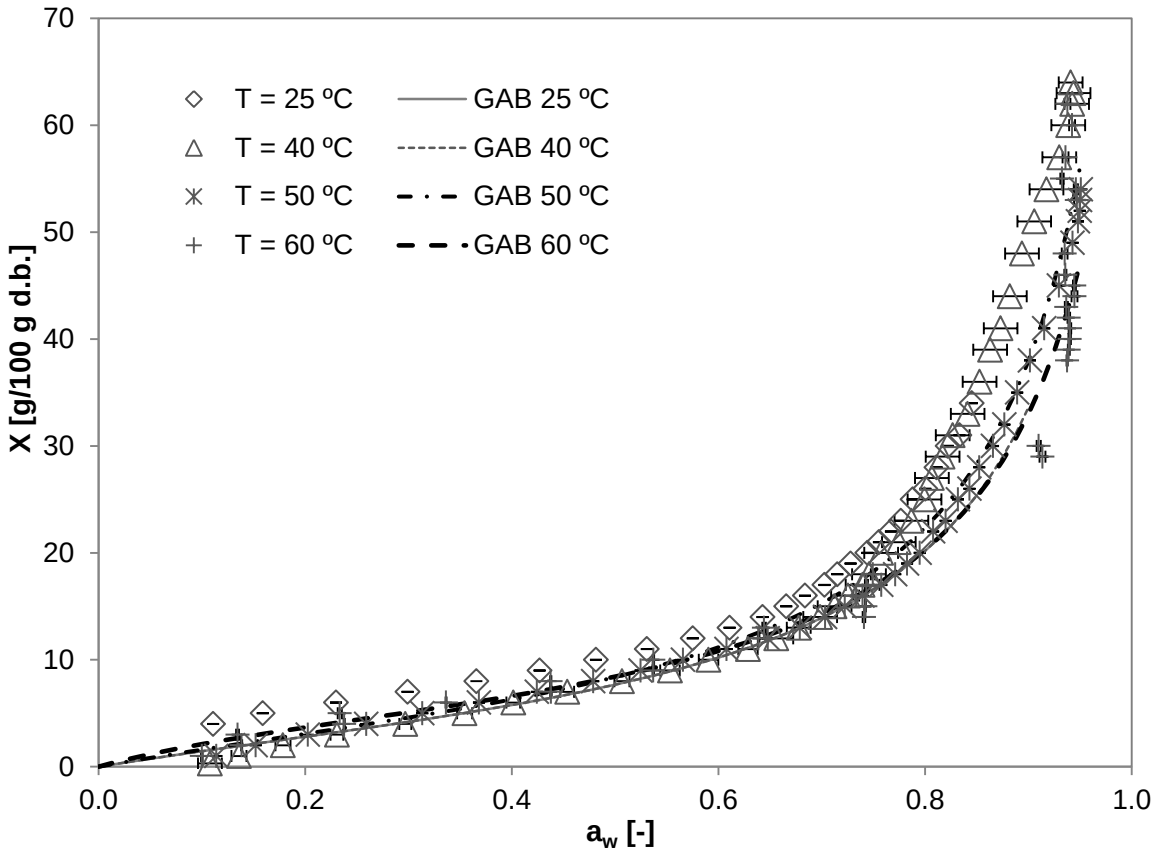

Moisture content increased as water activity increased for all studied temperatures. It is clearly observed that the isotherms of unripe banana describe multilayer adsorption and can be identified as type II, showing asymptotic approaching the saturation pressure, with two different regions (Fig. 6.1). At low and intermediate water activities, the so-called multilayer sorption region, the moisture content increased linearly with water activity, whereas at high water activity levels, the so-called capillary condensation region, moisture content increased nonlinearly with water activity.

This behavior is very common in foodstuff as previously reported to: banana (AGUIRRE *et al.,* 2010; CARDOSO; PENA, 2014), corn (IGLESIAS; CHIRIFE, 1994), potato (KIRANOUDIS, 1993; WANG; BRENNAN, 1991) and carrot (KIRANOUDIS, 1993).

For all water activity values, the equilibrium moisture content of the studied systems decreased with increase of temperature. This means that unripe banana

becomes less hygroscopic, which can be explained that the kinetic energy associated with water molecules present increases with increase in temperature.

As a consequence, there are a decrease of the attractive forces and escape of water molecules (FIGURA; TEXEIRA, 2007; IGLESIAS; CHIRIFE, 1994).

GAB model parameters (X_m, *k and C*) at studied temperatures and the statistical parameters (r^2, SE, and RMSD) are listed in Table 6.2. In both cases (desorption-adsorption), this model well fitted the experimental data, confirmed by the high coefficients of determination ($r^2 > 0.98$), low values of standard error (SE < 2.4 %).

The monolayer moisture content (X_m) is the minimum moisture content covering hydrophilic sites on the material surface, and it is an important data for achieving storage with minimum quality loss for long time. Therefore, at a given temperature, the maximum shelf stability of dehydrated material can be predicted by X_m determined from sorption isotherm.

The mean value of monolayer moisture content calculated by GAB model was (5.9 ± 0.2) g/100g d.b. (adsorption curve). This value is in accordance those reported in literature, for starchy foods (AL-MUHTASEB; MCMINN; MAGEE, 2004; SANTOS; FIGUEIREDO; QUEIROZ, 2004;). Below this value, none of the water is in the liquid phase anymore; therefore no free moisture is available for supporting any chemical, biochemical or biological activity (FIGURA; TEXEIRA, 2007).

Table 6.2 - Values for the parameters of GAB model (Eq. 3.1) and statistical coefficients (r^2, SE, and MAE) obtained by regression analysis from sorption isotherms of fresh unripe banana at different temperatures.

	Desorption isotherms				**Adsorption isotherms**			
Temperature [ºC]	**25**	**40**	**50**	**60**	**25**	**40**	**50**	**60**
X_m [g/100g db]	6.4 ± 0.1	6.1 ± 0.0	5.8 ± 0.1	5.3 ± 0.2	5.7 ± 0.0	5.6 ± 0.1	5.6 ± 0.1	4.9 ± 0.1
K	0.96 ± 0.01	0.98 ± 0.02	0.94 ± 0.00	0.93 ± 0.01	0.93 ± 0.01	0.9 ± 0.0	0.88 ± 0.03	0.91 ± 0.01
C	7.7 ± 1.1	1.8 ± 0.0	3.1 ± 0.0	5.4 ± 1.1	2.9 ± 0.2	1.8 ± 0.1	2.5 ± 0.1	4.9 ± 0.4
r^2	0.997	0.996	0.998	0.975	0.991	0.997	0.999	0.997
SE [g/100g db]	1.2	0.79	0.59	2.4	1.2	0.40	0.23	0.66
MAE	0.87	0.59	0.46	1.3	0.87	0.33	0.19	0.47

6.2.1 Equilibrium moisture content

The equilibrium moisture content (X_e) is a result of the interaction between the material and the environment. Under a given vapor pressure of water of the surrounding drying air, a food attains a moisture content, known as the equilibrium moisture content, useful in predictive drying models as well as in the design of drying equipment (FIGURA; TEXEIRA, 2007).

Considered as a significant factor in drying, it can provide a guideline for expediting drying and for terminating the drying process in a timely manner to save energy. Sometimes it is considered as zero to simplify the mathematical solution.

The X_e is dependent on the relative humidity and the temperature of the air. For example, ambient temperature and relative humidity of a region may prove to be associated with high equilibrium moisture and thus the materials may not dry in time when left in the field (HE *et al.,* 2013).

Assuming an infinite drying time, the relative humidity in the chamber will be equal to the water activity of the product; therefore the estimation of the X_e can be made using the GAB model for three constant *RH* (10, 20 and 30) % (Table 6.3).

Table 6.3 - Equilibrium moisture content (X_e) of unripe banana estimated through GAB model parameters at different temperatures and relative humidities.

Temperature [ºC]	**X_e [g $H_2O \cdot 100g^{-1}$ db]**			
	Relative Humidity [%]			**Tukey**
	10	**20**	**30**	**HSD 95 %**
25	3.2 ± 0.2^{aA}	5.1 ± 0.2^{bA}	6.8 ± 0.2^{cA}	0.3
40	1.4 ± 0.1^{aB}	2.9 ± 0.2^{bB}	4.4 ± 0.2^{cB}	0.3
50	1.5 ± 0.1^{aB}	2.9 ± 0.1^{bB}	4.4 ± 0.2^{cB}	0.2
60	1.7 ± 0.1^{aB}	3.2 ± 0.2^{bB}	4.7 ± 0.2^{cB}	0.3
Tukey HSD 95 %	0.2	0.3	0.4	

Means with same letters in the same row and capital letters in the same column are not significantly different (p>0.05)

The X_e increased with the decrease of temperature at a constant relative humidity, indicating that the banana slices becomes more hygroscopic. The values of equilibrium moisture content at different relative humidities found in this work, are

comparable those reported in the literature (BAINI; LANGRISH, 2007; CARDOSO; PENA, 2004).

Cardoso and Pena (2014) studying the hygroscopic behavior of banana flour based on the desorption mono-layer moisture content, concluded that the drying process of the 'Nanicão' banana with (2–9) ºBrix should not achieve a moisture content below 7.10 g $H_2O \cdot 100g^{-1}$ db to avoid unnecessary power consumption.

It is worth to note, that the X_e decreases as the drying temperature increases, as expected, since at higher temperatures the process of drying becomes easier. The water content in the product is more easily expelled from the inner structure.

6.3 Unripe banana properties

The values of the unripe banana physical and thermophysical properties are presented in Figs. 6.3 – 6.7 as a function of moisture content (wb). The experimental data of the thermophysical properties as a function of moisture content are presented in Appendix B.

6.3.1 Density and porosity

It can be observed that the unripe banana apparent density increases while moisture content decreases (Fig. 6.3).

Figure 6.3 - Unripe banana apparent densities (ρ) during drying at 60°C, 50°C and 40°C versus moisture content M_w (wb).

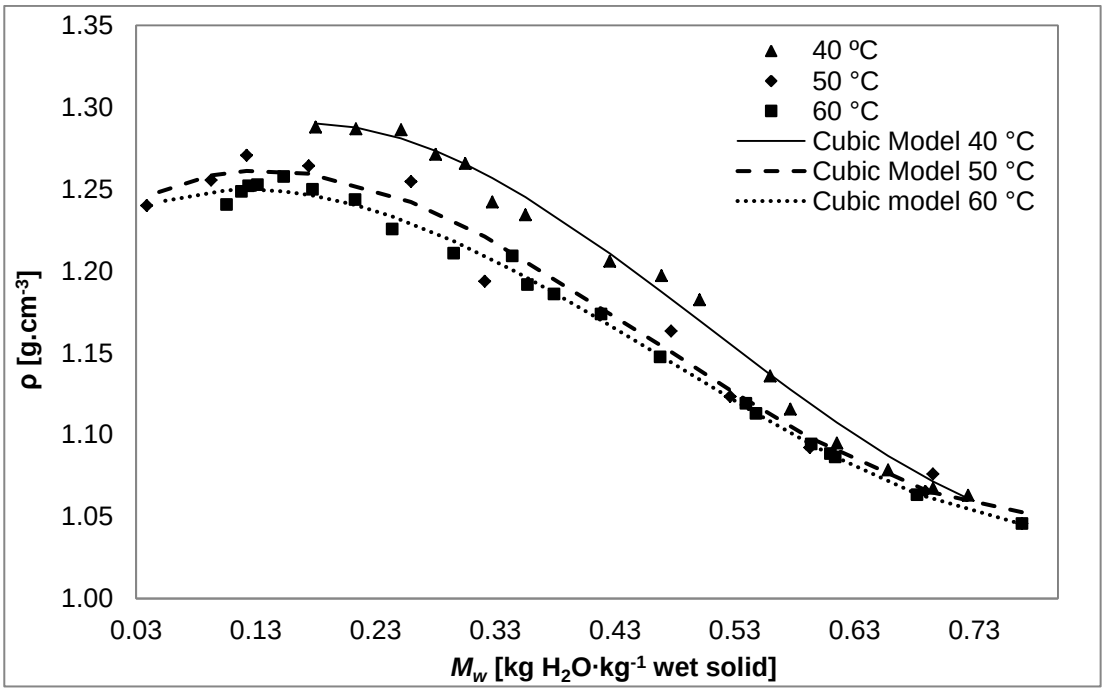

In the early stage of drying the density increased as moisture content decreased, reaching a maximum of 1.30 g·cm^{-3} at a moisture content of 0.2802 kg ·kg^{-1} w.b. at air drying of 40 °C. Marousis; Saravacos (1990), Wang; Brennan (1995) and Zhengyong; Sousa-Gallagher; Oliveira (2008) investigated the change of density of starch materials and fresh fruits during drying and found similar results. During the final stage of drying the volume of the sample does not change with the further loss of water. Therefore, the density of the material decreases with decreasing moisture content at low moisture contents.

It can also be observed in Fig. 6.3 that the drying air temperature has an effect on the density of unripe banana. Wang and Brennan (1995) declared that this difference is attributed due the out layers of the material becom more rigid and their final volume is fixed early in the drying. As a result, there is a lower density at high temperature than that at low temperature for a given moisture content.

The experimental data were correlated using the following equation of the form:

$$\rho = P1 \times M_w^3 + P2 \times M_w^2 + P3 \times M_w + P4 \qquad (6.1)$$

A multiple regression (Statgraphics®, Centurion XV, 2005) was performed to estimate the constants in Eq. 6.1 presented in Table 6.4, showing a good agreement at 95 % of confidence interval.

Table 6.4 - Estimated parameters of multiple regression for apparent density of unripe banana slices dried at different temperatures (Eq. 6.1).

Temperature [ºC]	**Estimated parameters**				**Statistics**	
	P_1	P_2	P_3	P_4	σ^*	r^2
40	1.68 ± 1.07	- 2.56 ± 1.11	0.74 ± 0.32	1.23 ± 0.09	0.0097	0.99
50	1.50 ± 0.99	- 2.08 ± 1.24	0.49 ± 0.43	1.23 ± 0.04	0.0135	0.98
60	1.21 ± 0.35	-1.72 ± 0.45	0.37 ± 0.17	1.23 ± 0.02	0.0050	0.99

* Standard deviation

Lozano *et al.* (1980) correlated the apparent and substance density of apple during air drying by an exponential equation for whole range of moisture content.

The authors mentioned that the apparent density increased linearly, until a given moisture content in dry basis, beyond that as moisture content decreased, the change in apparent density became steeper. Then, it showed a sharp decrease at low moisture content.

Ghiaus; Margaris; Papanikas (1997) expressed the apparent density of grapes as a function of moisture content ranging from (0.176 to 4.0) $kg \cdot kg^{-1}$ d.b., as a 3-degree polynomial function.

The behavior of the unripe banana porosity at 60 °C of air drying is presented in Fig. 6.4, as the simulation and the mathematical model of the process was performed with this temperature. It can be observed, as the moisture content increased (M_w) the porosity increased as well, showing an exact opposite behavior compared with the apparent density.

Figure 6.4 - Porosity of unripe banana slices on moisture content during convective drying at 60 ºC.

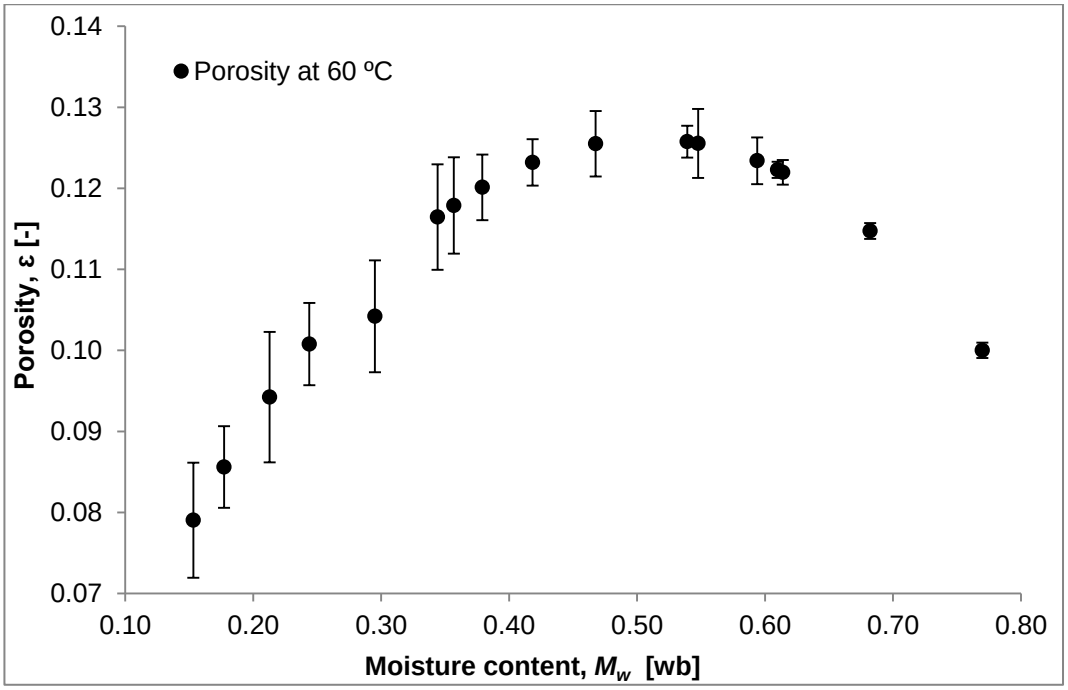

In the early stage of drying the porosity increased as moisture content decreased, reaching a maximum value at a moisture content of 0.46 kg·kg^{-1} w.b. Further reduction in moisture content resulted in a decrease of porosity of unripe banana (Fig. 6.4). As the drying proceeds, intracellular spaces (pores), previously occupied by water are replaced either by air or is compressed as result of shrinkage.

At this point, the porosity of the unripe banana slab decreased due to rupture of cell wall, this event has an influence in the thermophysical properties. This same behavior was reported, by Yan *et al.* (2008) for mango, pineapple and banana slices dried to moisture contents of 0.05 kg·kg^{-1} w.b. at 70 ºC, measuring the apparent density and the porosity.

As porosity and shrinkage are critical factors, influencing transport mechanism as well as product quality parameters, it becomes important to include this entire phenomenon in a single model to predict heat and mass transfer for better optimization of process, considering variable dimensions of the sample, porosity and shrinkage changes during the drying process.

Different authors have investigated the change in apparent density of starchy materials during drying and found similar results (MAROUSIS; SARAVACOS, 1990; WANG; BRENNAN, 1995; YAN *et al*., 2008). Shrinkage is responsible for the

increased apparent density at low moisture contents. During the final stage of the drying the volume of the sample does not change with the further loss of water. Therefore, the apparent density of the sample decreases with decreasing moisture content at low moisture contents (WANG; BRENNAN, 1995), which is completely correlated with the porosity behavior in Fig. 6.4.

6.3.2 Thermal conductivity

The thermophysical properties decreased with moisture content (wb). This means that as the moisture is removed from the product, the heat transfer turns more difficult; hence, the energetic demand for the process increases.

Thermal conductivity ranged from 0.894-0.154 $W.m^{-1}.K^{-1}$ with moisture content of 0.29 $kg.kg^{-1}$ db and 0.71 $kg.kg^{-1}$ db, respectively. There was no significant effect with the temperature, although *k* would be expected to increase with temperature, based on previous literature for homogenous foods (CHOI AND OKOS, 1986), however, the values for thermal conductivity found in this work (Fig. 6.5) are in good agreement with the results found from Rahman (1995) 0.698 $W{\cdot}m^{-1}{\cdot}K^{-1}$ for potato and 0.641 $W{\cdot}m^{-1}{\cdot}K^{-1}$ for fresh banana with moisture content of 0.84 $kg{\cdot}kg^{-1}$ and 0.76 $kg{\cdot}kg^{-1}$ wb, respectively.

Figure 6.5 - Unripe banana dimensionless thermal conductivity (k/k_0) during convective drying at temperature interval from (40 to 60) °C as a function of dimensionless moisture content (M_w/M_{w0}) and porosity (ε).

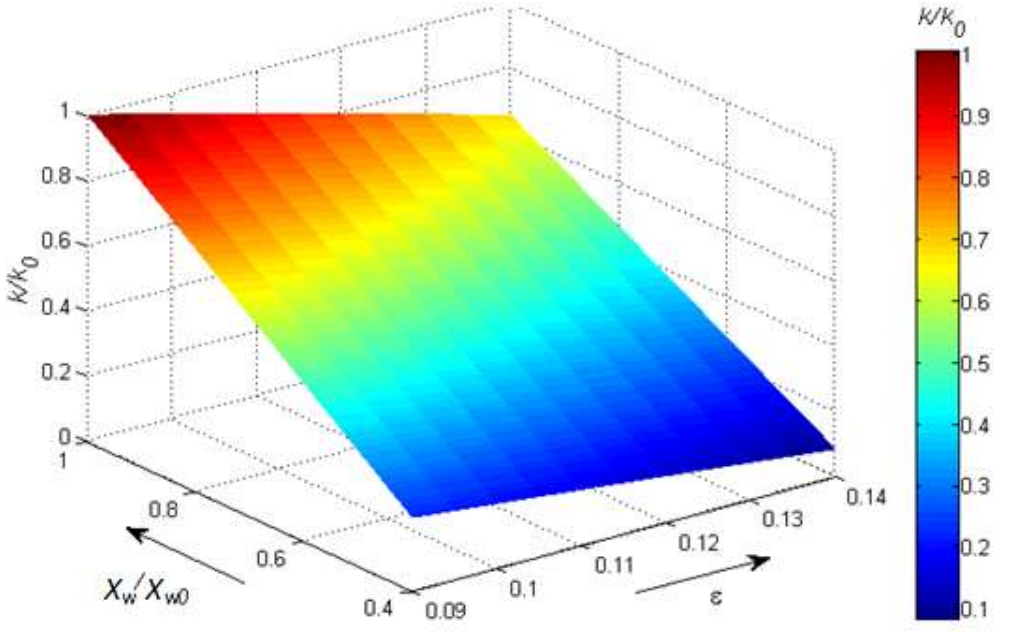

Erdoğdu et al. (2014) determined experimentally thermal conductivity-diffusivity of green and yellow Cavendish bananas with peel using analytical solution of heat transfer for cooling process, the estimated *k* for ripe and unripe bananas changed from (0.302 to 0.338) $W \cdot m^{-1} \cdot K^{-1}$, the authors concluded that the values found might present a difference compared with literature, due to the effect of peel and its composition. In food material, *k* is influenced by its composition, moisture content, temperature, and fiber arrangement. The same way as for the apparent density the experimental data were correlated (Statgraphics®, Centurion XV, 2005) obtaining the following equation of the form, in which linear and quadratic effects of temperature did not influence significantly ($p>0.05$) for all thermophysical properties:

$$\frac{k}{k_0} = A_1 + A_2 \frac{X_w}{X_{w0}} + A_3 \frac{1}{(1-\varepsilon)} \left(\frac{X_w}{X_{w0}} \right) \qquad (6.2)$$

The estimated parameters in Eq. 6.2 are presented in Table 6.5, showing a good agreement at 95 % of confidence interval. There was no significant effect with the temperature.

Table 6.5 - Estimated parameters of multiple regression for thermal conductivity of unripe banana slices dried at different temperatures (Eq. 6.2).

Estimated parameters				**Statistics**	
A_1	A_2	A_3	**Limits**	r^2	σ^*
-0.29 ± 0.05	7.37 ± 1.10	-5.53 ± 1.00	$0.4 \leq \frac{X_w}{X_{w0}} \leq 1$ $0.09 \leq \varepsilon \leq 0.14$	0.91	0.076

* Standard deviation

Water content is found to be the most important factor in determining thermal conductivity while the non-aqueous part of the most food is of lesser importance. It is common to find a linear relation between thermal conductivity and moisture content (MOHSENIN, 1980; PERUSSELLO; MARIANI; MENDES, 2010). The linear correlation is limited to small changes in moisture; hence a non-linear correlation is necessary to cover the whole range of moisture contents, which would correspond to an exponential, logarithm or inverse form (LOZANO; ROTSTEIN; URBICAIN, 1980, MATTEA; URBICAIN, ROTSTEIN, 1986).

Rahman; Potluri (1991) presented a more general form of correlation than Mattea; Urbicain; Rotstein (1986) and Lozano *et al.* (1980) for correlating their data on squid meat during air drying by normalizing both sides of correlation with initial water content before drying, as it is presented in this study.

6.3.3 Specific heat

The specific heat of unripe banana varied between (1800 to 3000) $J \cdot kg^{-1} \cdot K^{-1}$, decreasing along with drying time and as the moisture content decreases. The Fig. 6.6 shows the specific heat behavior at different moisture content, both expressed in dimensionless form.

Figure 6.6- Unripe banana dimensionless specific heat during convective drying at temperature interval from (40 to 60) °C as a function of dimensionless moisture content (M_w/M_{w0}) and porosity (ε).

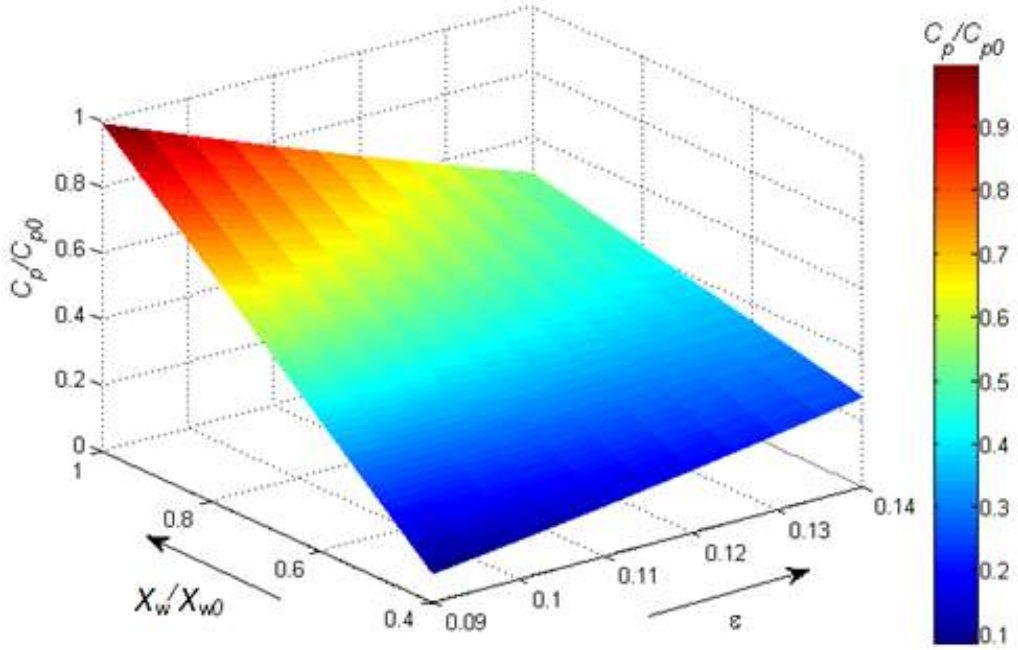

In fact, according to Sweat (1994) there is a strong linear correlation between specific heat and water content, especially over the highest range of water content. The very same result is observed in Fig. 6.6 (Statgraphics®, Centurion XV, 2005), in which specific heat varies almost linearly with moisture content until the value of 0.6 of dimensionless moisture content, after this the correlation becomes logarithmic (Eq. 6.3), and the estimated parameters are shown in Table 6.6

$$\frac{C_p}{C_{p0}} = B_1 + B_2 \frac{X_w}{X_{w0}} + B_3 \frac{1}{(1-\varepsilon)} + B_4 (1-\varepsilon)\left(\frac{X_w}{X_{w0}}\right) \qquad (6.3)$$

Table 6.6 - Estimated parameters of multiple regression for specific heat of unripe banana dried at different temperatures (Eq. 6.3).

Estimated parameters					Statistics	
B_1	B_2	B_3	B_4	Limits	r^2	σ^*
-11.60 ± 4.20	-19.32 ± 5.26	10.08 ± 3.72	22.9 ± 5.92	$0.4 \leq \frac{X_w}{X_{w0}} \leq 1$ $0.09 \leq \varepsilon \leq 0.14$	0.90	0.074

* Standard deviation

Mohsenin (1980) and Sweat (1986) both noted that the linear model gave significant deviation at the lower moisture content. This form of model can thus not be used to predict specific heat within the entire range of moisture content.

Alvarado (1991) used an exponential equation to correlate the specific heat of fruit pulps whose water content varied from (0 to 95) g/100 g of moisture content (w.b.), sustaining that the application of linear model is limited only above M_w = 0.50 (RAHMAN, 1995).

6.3.4 Thermal diffusivity

The thermal diffusivity (Fig. 6.7), by its turn, represents the speed of the product's temperature response as a function of the drying air temperature, and the values found were between (1.97 and 1.26)$\times 10^{-7}$ $m^2 \cdot s^{-1}$. It was observed that there was no dependence with temperature as with the other thermophysical properties.

Figure 6.7- Unripe banana dimensionless thermal diffusivity during convective drying at temperature interval from (40 to 60) °C as a function of dimensionless moisture content (Mw/Mw0) and porosity (ε).

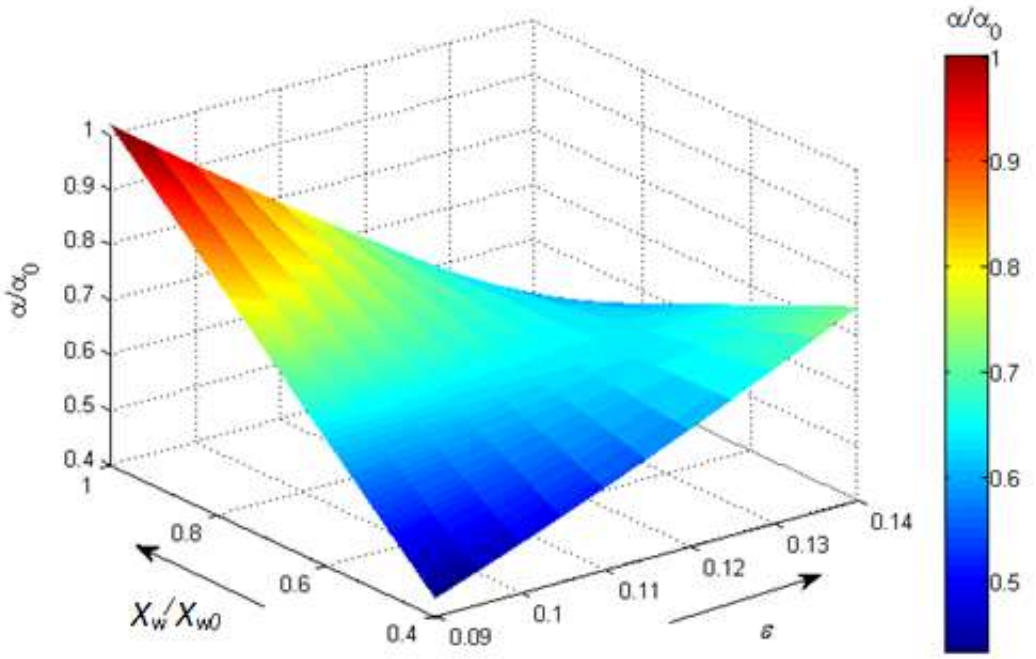

The nonlinear regression was performed (Statgraphics®, Centurion XV, 2005) and the parameters of Equation 6.4 are presented in Table 6.7.

$$\frac{\alpha}{\alpha_0} = C_1 + C_2\left(\frac{X_w}{X_{w0}}\right) + C_3\frac{1}{(1-\varepsilon)} + C_4(1-\varepsilon)\left(\frac{X_w}{X_{w0}}\right) \qquad (6.4)$$

Table 6.7 - Estimated parameters of multiple regression for thermal diffusivity of unripe banana dried at different temperatures (Eq. 6.4).

Estimated parameters					**Statistics**	
C₁	***C₂***	***C₃***	***C₄***	**Limits**	r^2	**σ***
-15.22 ± 1.93	-24.87 ± 2.42	13.89 ± 1.71	28.4 ± 2.7	$0.4 \le \frac{X_w}{X_{w0}} \le 1$ $0.09 \le \varepsilon \le 0.14$	0.91	0.034

* Standard deviation

Thermal diffusivity of a food material is affected by water content and temperature, as well as composition and porosity (SINGH, 1982). Several empirical models useful in predicting thermal diffusivity of foods have appeared in the literature. Riedel (1969) developed a model to predict thermal diffusivity as a function

of water content using a wide range of food products during sterilization. This model is valid for liquid and solid foods containing at least 40 g/100 g of water at a temperature range from (0 to 80) ºC.

The values of thermal diffusivity are also in good agreement with the results published by Andrieu *et al.* (1986) for potato 1.77×10^{-7} $m^2\cdot s^{-1}$ for fresh banana 1.46×10^{-7} $m^2\cdot s^{-1}$ with moisture content of 0.76 $kg\cdot kg^{-1}$ w.b., and for unripe and ripe banana from (1.442 to 1.500)$\times10^{-7}$ $m^2\cdot s^{-1}$ with moisture content of (0.72 and 0.76) $kg\cdot kg^{-1}$ w.b., respectively. Thermal diffusivity found using inversed method by Mariani; Barbosa; Santos (2008) and Mariani; Barbosa; Santos (2009) shows that a small change in moisture content of banana cause an abrupt change of the apparent thermal diffusivity, which decreases with as the moisture decreases.

6.4 Mathematical modeling

The analysis of transport phenomenon presented here is based on the time evolution, transient approach and the resolution of the well-known system of partial differential equations (Eqs. 5.3 – 5.8). For the simulation study it was considered the moisture transfer during drying of an unripe banana slab to predict the moisture profile inside the food. The simulations are divided into four Cases and the shrinkage phenomenon included in the last one.

6.4.1 Case I – Simulation considering constant properties

In Case I the system of partial differential equations (Eqs. 5.3 - 5.8) was solved with constant values of (see Table 5.2): specific heat, thermal conductivity, apparent density, diffusion coefficient, etc. The present model was used to predict the moisture distribution inside the solid. Moisture within the food is initially known as the initial moisture content, loosing moisture throughout drying time. Figure 6.8 shows the moisture distribution as a function of both position *N* (number of discretization) and drying time t, obtained from the simulations according to algorithm presented in Appendix A.

Simulation results show the highest moisture content in the center of the product, decreases monotonically to the lowest level at the surface of the product. The rate of moisture removal in the region near the surface is higher than the interior

of the banana slice because of the high initial moisture gradient in this region, which drives diffusion from the inside to the surface.

Moreover, in the early drying period, the moisture content reduces quickly. Due to the diffusion limitation of the drying process, the surface moisture content reaches the equilibrium value almost immediately and, as the drying period progresses, the rate of moisture removal becomes almost steady.

Figure 6.8 - Simulation of the moisture content (M_w) during drying time (t) of unripe banana slice at 60 °C considering thermal and transport properties constant (Case I).

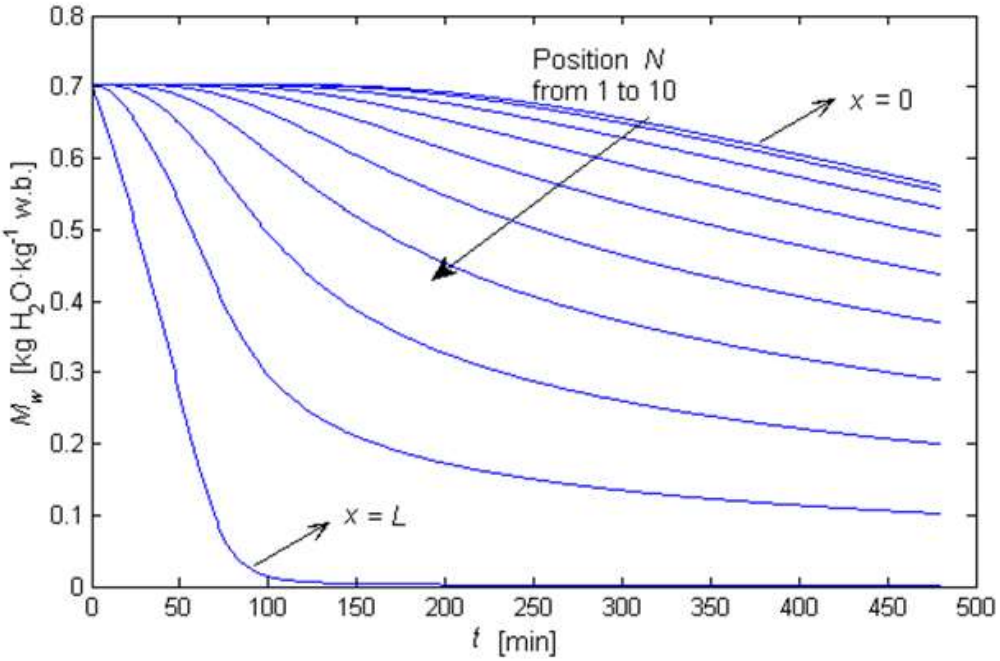

Simultaneously, the food temperature was calculated in different food regions. Figure 6.9 shows the temperature profile as a function of both position *N* (number of discretization) and time, during drying. Temperatures at each location increase with drying time, which is due to the higher drying air temperature. The temperature gradient between the center and the surface decreases along drying time. It was found that the temperature profile rises quickly in the early period of heating, due to the difference between air temperature and food temperature. As the heating period progresses, the rise in temperature attains an almost uniform profile. This arises because the surface has high moisture and most of the heat is used for evaporation near the surface. When the surface moisture becomes low, the increase on temperature becomes faster. Subsequently, only a small quantity of heat is used for evaporation and the increase in heat flux raises the food temperature.

Figure 6.9 - Estimation of the temperature (*T*) during drying time (*t*).

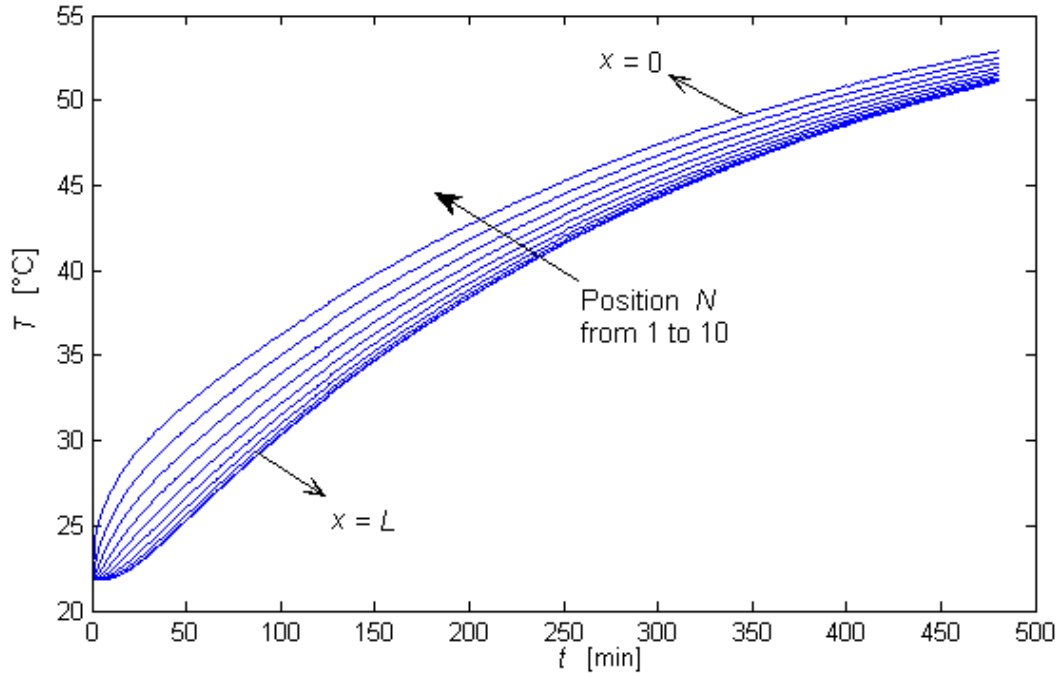

In order to compare the results of Case I (model) the average moisture content was calculated from the curves presented in Fig. 6.8 and plotted with the experimental drying curves determined through the mass loss at 60 °C of temperature, ··s^{-1} of air drying velocity and *RH* of 10 %, presented in Fig. 6.10.

Figure 6.10 - Experimental drying curve of unripe banana slice dried at 60 °C in comparison with the average moisture content estimated by the model Case I.

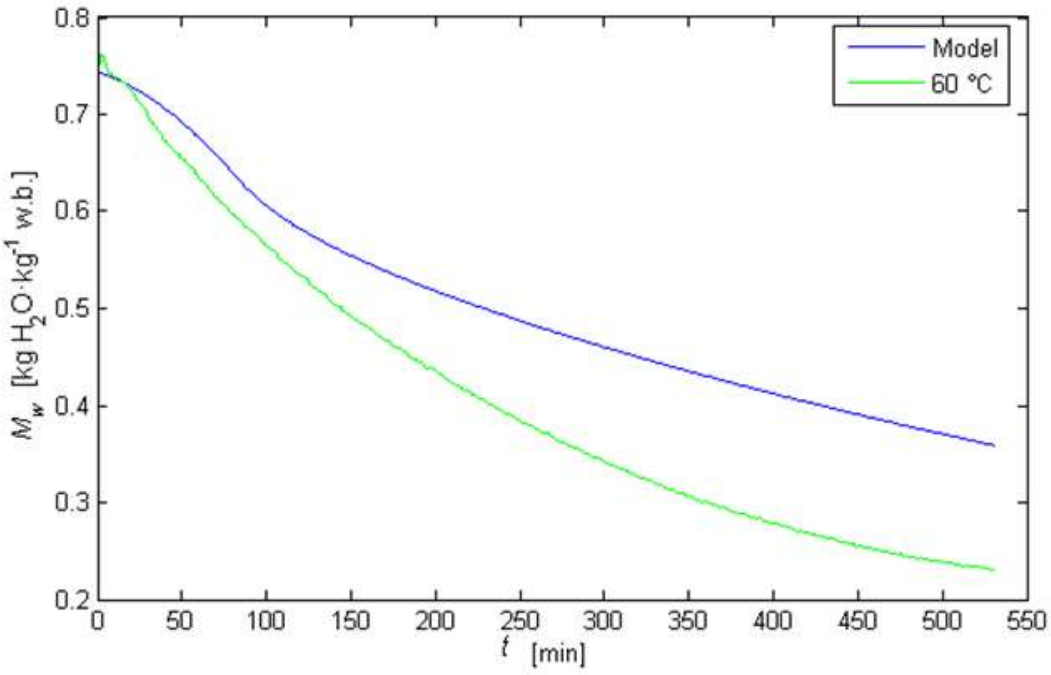

It can be observed that Case I model proposed does not describe adequately the drying phenomenon due to the variations throughout the drying time. The simulated curve (blue) showed that in 9 h of process the banana slab was dried close to 0.37 $kg \cdot kg^{-1}$ w.b., while the experimental curve indicates 0.21 $kg \cdot kg^{-1}$ w.b. It can be concluded that the model must be modified to ensure the accuracy of the moisture prediction.

The temperature inside the slab was measured at the center and at the surface. In Fig. 6.11, it is presented the average experimental temperature (green line) in comparison with the average temperature estimated by the model. It is possible to notice that the model agreement in this first case it is unsatisfactory, due to different factors: constant thermophysical properties, heat and mass transfer taken from the literature, constant effective diffusivity and disregarding the shrinkage effect.

This model predicts lower temperature and higher moisture content at any given time compared with the experimental values. For instance, necessarily the model had to be adjusted considering the distribution of air inside the drying chamber, the air velocity.

Figure 6.11 – Experimental average temperature curve of unripe banana slice dried at 60 °C in comparison with the average temperature estimated by the model-Case I.

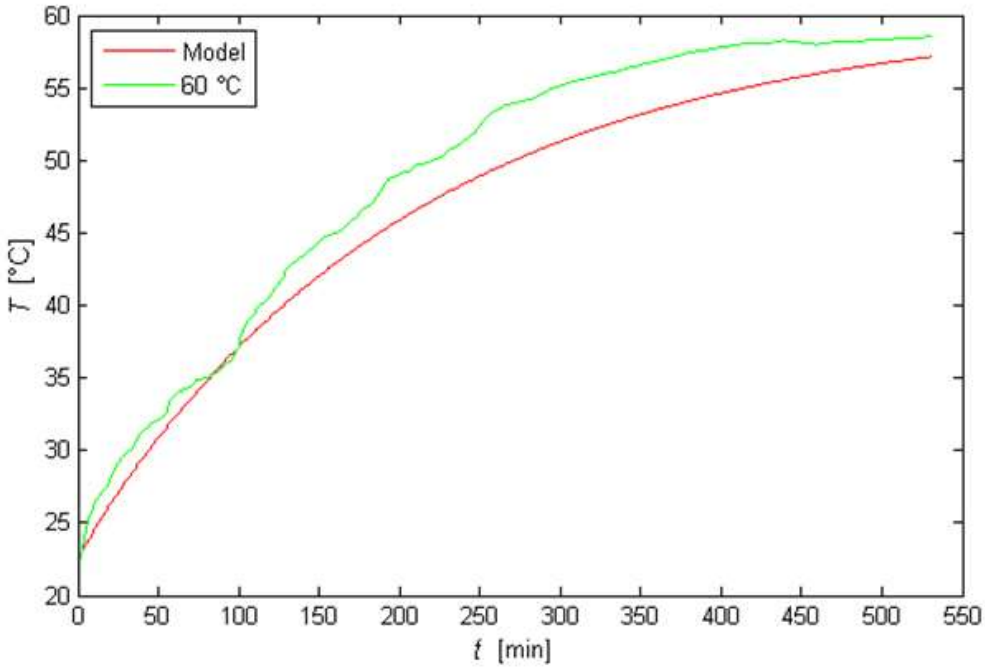

6.4.2 Case II – Variable thermophysical properties

According to Cai *et al.* (2014) there are little literature available about the effect on the thermophysical properties during the convective drying kinetics by taking the conjugated heat and mass transfer effects into account. Wang; Brennan (1995) applied the variable thermophysical properties in potato convective drying as a function of moisture content at the range studied from (3 to 0.8) $kg \cdot kg^{-1}$ d.b. It is important to denote that the authors performed temperature measurements during drying in different parts of the slab, and they found that there were no significant differences between the temperatures measured in the same position on the horizontal plane at 95 % of confidence interval. This may indicate that the heat is transferred only in the vertical direction, i.e. from the surface to the center of the sample. In this work, the temperature measurements were performed at the center and surface of the slab.

The simulation results of moisture and temperature profile inside the unripe banana slab, are presented in Figs. 6.12 and 6.14, using the apparent density and the thermophysical properties as a function only of moisture content, this because the porosity is strongly correlated to the apparent density as described in Eq. (4.2).

As it can be noticed comparing Fig. 6.10 and 6.12 the difference between them is perceptible, the variable thermophysical properties in the model had a slight effect on the moisture content behavior during drying. These properties had an influence on how the heat is being transferred from the outer air into the solid. Approximately, the first hour of drying the model describes properly the process behavior, after that, the experimental curve (green) decreases.

Figure 6.12 - Experimental drying curve of the unripe banana slice dried at 60 °C in comparison with the average moisture content estimated by model – Case II.

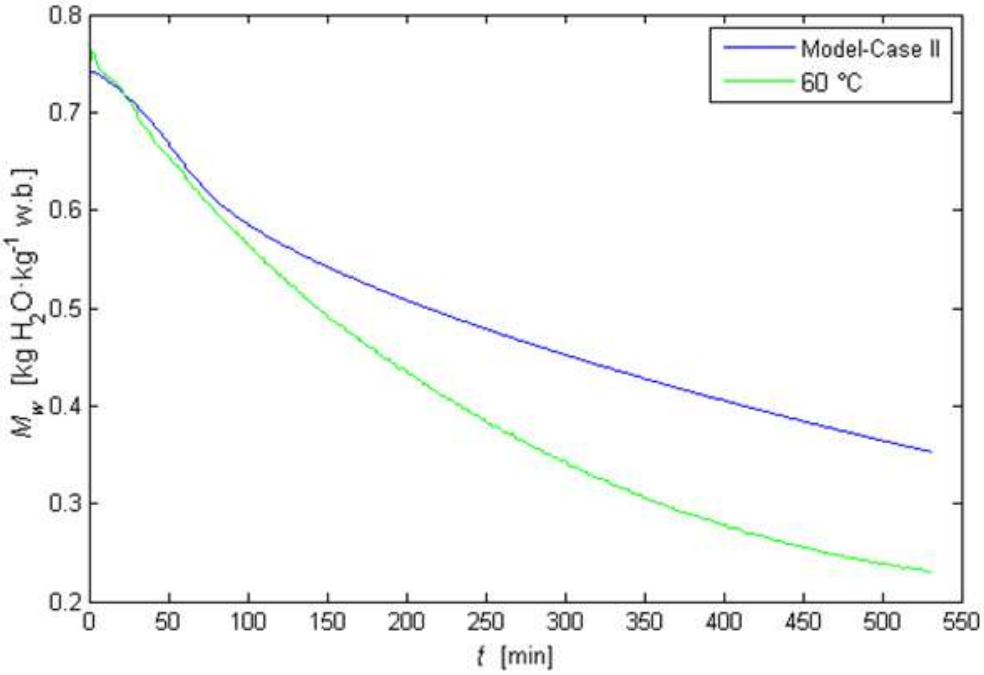

For better visualization in the Fig. 6.13 the moisture content simulated from both Case I and Case II models are compared, showing the contrast between them. Silva *et al.* (2010) proposed a method for the simultaneous determination of the convective mass transfer and the effective diffusivity, demonstrating that the influence of these two parameters had to be considered during the drying process. This fact could explain the limited effect on the results in moisture content, showing us the next approach to be taken.

Figure 6.13 - Experimental drying curve of the unripe banana slice dried at 60 °C in comparison with the average moisture content estimated by models: Case I (red) and Case II (blue).

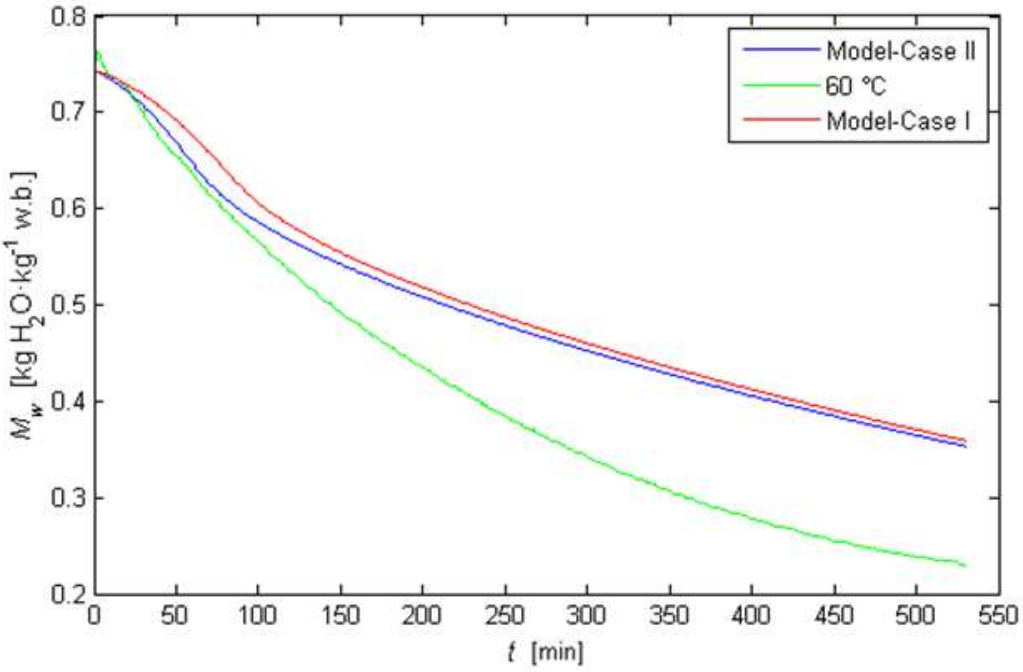

As described previously the thermophysical properties should have an effect on the temperature profiles inside the slab, this influence is appreciable showed in Figs. 6.14 and 6.15.

Figure 6.14 - Experimental average temperature curve of unripe banana slice dried at 60 °C in comparison with the average temperature estimated by the model-Case II.

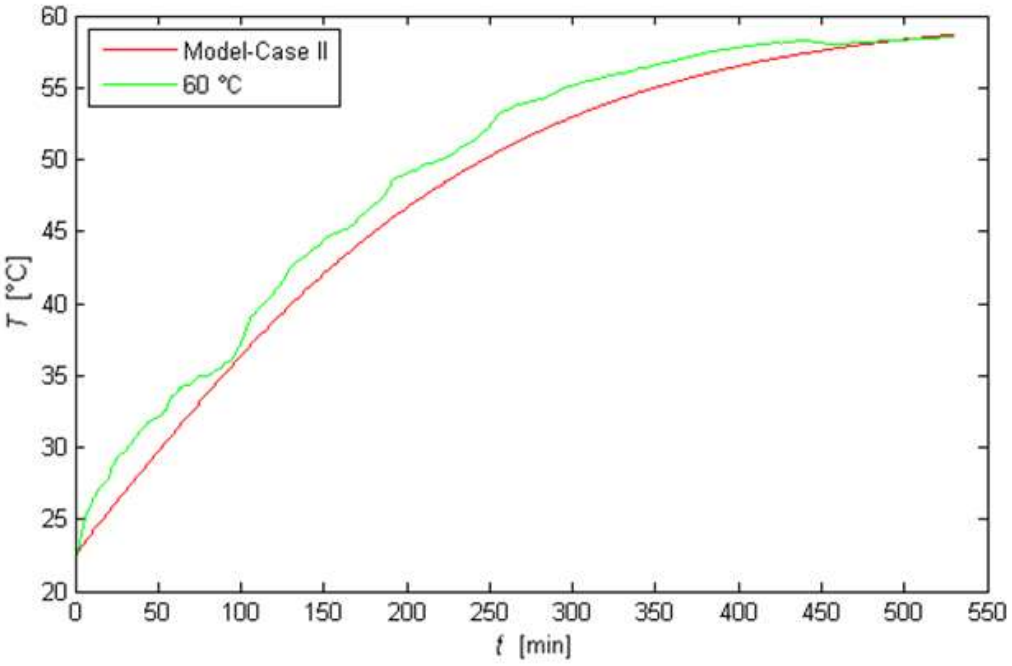

The Case II model describes reasonably the heat transfer behavior, as it can be observed the red curve is approaching to the experimental curve (green) comparing with Case I model (blue) in Fig. 6.15.

Figure 6.15 – Experimental average temperature curve (green) of the unripe banana slice dried at 60 °C in comparison with the average temperature estimated by models: Case I (red) and Case II (blue).

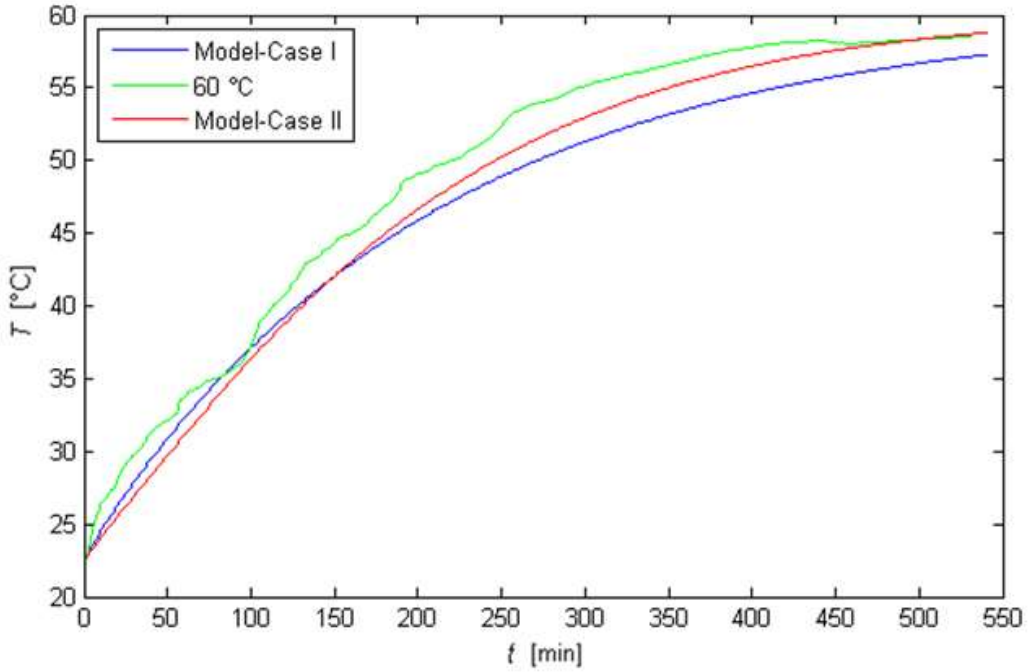

The first minutes of drying the slab is more dried according to the simulation for Case II (Fig. 6.13), this could explain why the temperature at the beginning of the process is lower comparing with Case I, as the thermophysical properties depends on the moisture content and they are directly proportional.

6.4.3 Case III – Estimation of heat and mass transfer coefficients

It is important to remember that the heat and mass transfer coefficients were not estimated at this point. Heat (heat transfer coefficient and thermal diffusivity values) and mass (mass transfer coefficient and diffusion coefficient values) transfer parameters are crucially important for characterization and modeling of food processing operations. Since they are important function and property of interest material and medium itself; experimental determination of these values would be valuable (ERDOĞDU, 2005).

Analytical solutions for regular geometries (infinite slab, infinite cylinder and sphere) have a broad use in experimentally determining these parameters, as in this

specific case for unripe banana. These solutions, with use of experimental data, might give a greater advantage over use of other methods, e.g. the lumped system approach or empirical equations. Effective use of numerical solution techniques with experimental data would enable simultaneous determination of the related parameters with the experimental data (ERDOĞDU, 2005).

The heat and mass transfer coefficients depend on the thermophysical properties of the medium, characteristics of the product (size, shape, surface temperature and surface roughness), characteristics of fluid flow (velocity and turbulence) and heat and mass transfer equipment (RAHMAN, 1995).

The initial input parameters to perform the h and h_m estimation, were calculated through expressions found in the literature (different *Nusselt* and *Sherwood* number correlations as a function of *Reynolds* and *Prandtl* numbers), as specified in section 5.4.3.

The h and h_m estimation improved greatly the model performance, however, during the first minutes of drying (120 min) still exists a gap between the experimental curve (green) and the estimated (blue), as can be seen in Fig. 6.16.

Figure 6.16 - Experimental drying curve of the unripe banana slice dried at 60 °C in comparison with the average moisture content estimated by model-Case III.

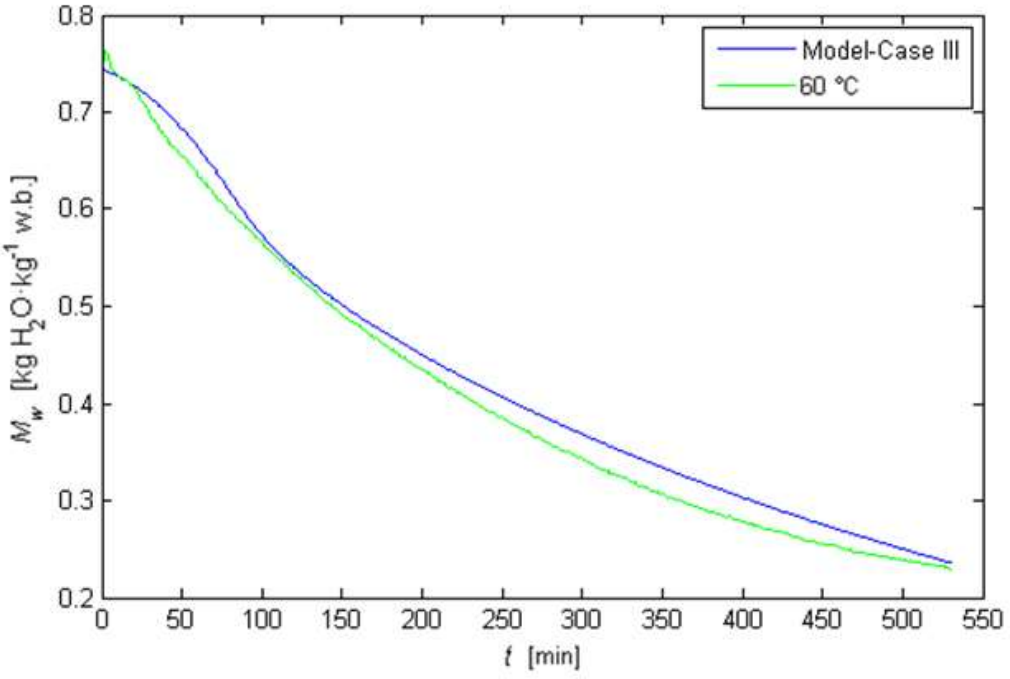

Comparing the simulated Case III model (black) with the previous Case II (red), it is possible to notice that after the first 120 min of process the Case III fits satisfactorily the experimental drying curve (green), these results are summarized in Fig. 6.17.

Figure 6.17 – Experimental drying curve (green) of the unripe banana slice dried at 60 °C in comparison with the average moisture content estimated by the models: Case II (red) and Case III (black).

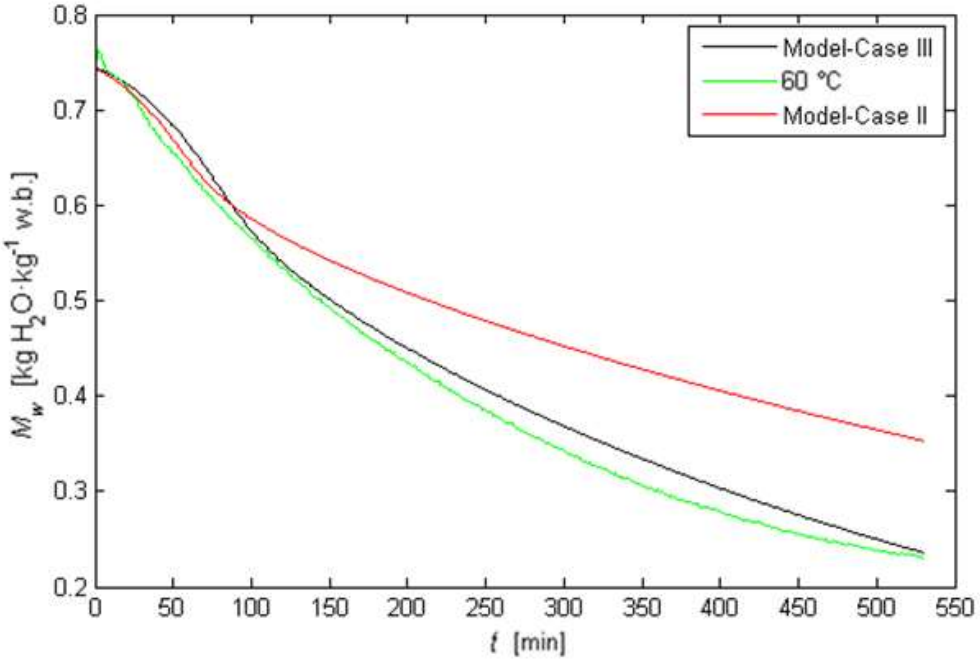

Although, the temperature profile was improved in Case III (see Fig. 6.18); the experimental curve of moisture content behavior was not fitted satisfactorily with the mathematical model, this might be due to the effective moisture diffusivity (D_e), which it should not be taken as constant and affects directly to the moisture transfer during the process and the drying kinetics. So far, in the Case III model the moisture diffusivity, heat and mass transfer coefficients were estimated, considering variable thermophysical properties updated overtime, shown in Table 6.8.

Table 6.8 - Estimated heat, mass transfer coefficients and effective diffusivity for unripe banana slice dried at 60 °C, 4 m·s^{-1} of air drying velocity and *RH* of 10 %.

Parameter	Symbol	Value	Units
Heat transfer coefficient	h	134	W·m^{-2}·K^{-1}
Mass transfer coefficient	h_m	4.91×10^{-5}	m·s^{-1}
Effective moisture diffusivity	D_e	3.28×10^{-10}	m^2·s^{-1}

Figure 6.18 – Experimental average temperature curve (green) of the unripe banana slice dried at 60 °C in comparison with the average temperature estimated by the modes: Case II (red) and Case III (black).

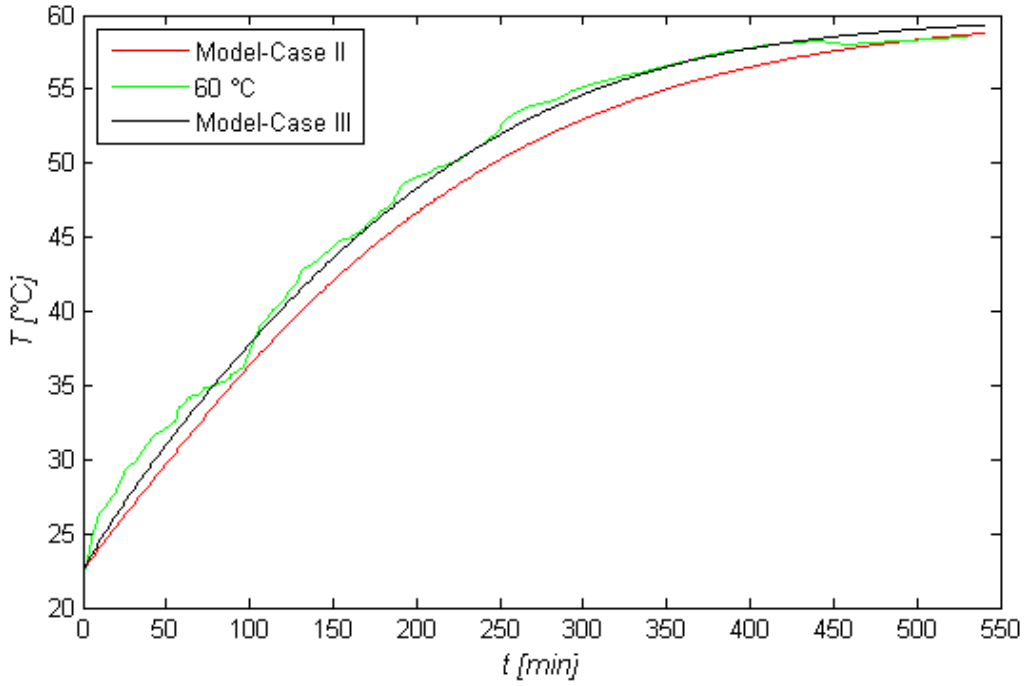

Silva *et al. (*2012) used a methodology for the simultaneous determination of the effective diffusivity and the convective mass transfer coefficient in porous solids, which can be considered as an infinite cylinder during drying. Optimization algorithms based on the inverse method were coupled to the analytical solutions, and these solutions can be adjusted to experimental data of the drying kinetics. The authors found that the mass transfer coefficient was 2.064×10^{-7} $m \cdot s^{-1}$, in that work instead of opting for the numerical solution with boundary condition of equilibrium and variable diffusivity, such boundary condition is discarded using an inverse method. However, the drying conditions are important in the estimation of parameters; the authors used experimental data from Silva *et al.* (2008), the drying air temperature was 50 °C with relative moisture of 20 % and air velocity was maintained at 1.5 $m \cdot s^{-1}$, this shows that the dryer type, the air drying conditions and the air distributions may affect the values for these parameters.

One important factor is the moisture transfer coefficient which affects directly to the moisture transfer during the process, although its determination and especially its concentration dependence, is usually a rather cumbersome and laborious task (TONG; LUND, 1990).

It is worth to remember that the moisture movement is governed by different factors, such as: the properties, form and size of the product and the type of moisture bond in the material (Sander *et al.*, 2003). The major factors affecting the moisture transport during solids drying can be classified as:

i. External factors: these are the factors related to the properties of the surrounding air such as temperature, pressure, humidity, velocity and area of the exposed surface, which correspond to the heat and mass transfer coefficients.
ii. Internal factors: these are the parameters related to the properties of the material such as moisture diffusivity, moisture transfer coefficient, water activity, structure and composition, etc. (DINCER; HUSSAIN, 2003b).

As a comparison, the values of the effective diffusivity (D_e) of the unripe banana system obtained in this work may be compared with those reported by Nogueira (1991) (T_{air} = 70 °C, v_∞ = 0.5 m·s^{-1}, D_e = 4.22×10^{-10} m^2·s^{-1}) and Queiroz (1994) and Queiroz; Nebra (2001) (T_{air} = 68.4 ºC, v_∞ = 0.39 m·s^{-1}, UR = 7.3%, D_e = 5.9×10^{-10} m^2·s^{-1}). In these studies, the banana was considered to be an infinite cylinder. As the diffusive model was used in all the studies mentioned above, the difference between values may be attributed mainly to the following factors: dehydration method, product variety, geometry assumptions, boundary conditions and product physical structure.

Different authors (BAINI; LANGRISH, 2008; NGUYEN; PRICE, 2007; ZABALAGA; CARBALLO, 2014) used the analytical solution of Eq. (5.3) given by Crank (1975) for an infinite slab drying (empirical model), taken the D_e as a constant during the drying process (Eq. 6.5), their results agree with the value founded in this study.

$$M_r = \frac{M_w - M_e}{M_0 - M_e} = \frac{8}{\pi^2}\sum_{n=0}^{\infty}\frac{1}{(2n+1)^2}\exp\left[-\left(\frac{2n+1}{2}\right)^2\frac{\pi^2 D_e}{L^2}t\right] \qquad (6.5)$$

which for long drying times reduces to Eq. 6.6, taken only the first term:

$$M_r = \frac{M - M_e}{M_0 - M_e} = \frac{8}{\pi^2}\exp\left(-\frac{\pi^2 D_e}{4L^2}t\right) \qquad (6.6)$$

The heat transfer coefficient is not a property of a material. It is used to quantify the rate of heat transfer from the surface of the body. It is dependent on the fluid velocity, fluid properties, roughness of the surface and shape of the body, as well as the temperature difference between the surface and the fluid that surrounds the body. In practice, heat flux and temperature on the surface of a material are very difficult to measure without disturbing the heat transfer. In food with high moisture content, mass transfer accompanies heat transfer; this fact is still an additional complication in the measurement of the heat transfer coefficient.

Saravacos; Maroulis (2001), found that the heat transfer coefficients vary from (10 to 200) $W \cdot m^{-2} \cdot K^{-1}$, when the air velocity varies from 0.1 $m \cdot s^{-1}$ (natural convection) to 5.0 $m \cdot s^{-1}$ (forced convection/fluidized bed system). According to Ashrae (1993) the heat transfer coefficient on the apple surface has a value of h = 17.03 $W \cdot m^{-2} \cdot K^{-1}$ for a velocity and temperature of air of 0.39 $m \cdot s^{-1}$ and T_{air} = 27.2 ºC, respectively. Lima; Queiroz; Nebra (2002) found a value of h = 20 $W \cdot m^{-2} \cdot K^{-1}$ for convective drying of bananas with T_{air} = 68.4 ºC, UR = 7.3 %, ν_∞ = 0.39 $m \cdot s^{-1}$ without shrinkage. As it can be noticed the ν_∞ is much lower to the one used in this work (4 $m \cdot s^{-1}$), that is why the heat transfer rate would be much higher.

Hussain; Dincer (2003b) stated that the h for convective drying ranges between (25 to 250) $W \cdot m^{-2} \cdot K^{-1}$ depending on the dryer type, the air control/distribution and the temperature control inside the drying chamber.

6.4.4 Case IV – D_e as a function of moisture content

After making a review of the D_e and its influence in the moisture transfer, it was necessary to consider D_e as a function of moisture content, for instance the h and h_m were estimated once more due to the variation of the D_e.

According to Tong and Lund (1990), Schoeber (1978) was one of the first authors to develop a regular regime method to determine the concentration-dependent diffusion coefficient for systems in which the moisture diffusivity decreases with decreasing moisture content. Tong and Lund (1990) determined an empirical correlation treating the diffusivity as the dependent variable and moisture content as independent variable through the water flux, the driving force, with a mathematical model; they concluded that the D_e decreases exponentially, from 80×10^{-8} to 10×10^{-9} $m^2 \cdot s^{-1}$ for bread at 40 ºC of air-drying temperature.

There is no standard method for experimental determination of moisture diffusivity. Several methods have been proposed in the literature, most of which have been developed primarily for polymeric materials (FRISCH; STERN, 1983). The estimation of moisture diffusivity from drying experiments is a challenging method. A generalized procedure (numerical solution-regression analysis) has been discussed by Marinos-Kouris; Maroulis (2006).

This proposed method uses an experimental drying apparatus and estimates the heat and mass transport properties as parameters of a drying model, which is fitted to experimental data (KIRANOUDIS *et al*., 1993). An important advantage of this method is the determination of effective diffusivity as a function of material moisture content/temperature (Eqs. 3.4 and 5.21), which has been used in this study.

Both approaches were tested in the simulation, the first one considers the dependence of D_e with moisture content and temperature (DMT) described in Eq. 3.4 and the second one considers the D_e as a function of moisture content (DM) (Eq 5.21). The results are shown in Fig. 6.19, as it can be seen that both approaches fit well the experimental data.

Figure 6.19 – Experimental drying curve (green) of the unripe banana slice dried at 60 °C and curves estimation made with moisture content-dependent (red) and moisture content/temperature-dependent diffusivities (black).

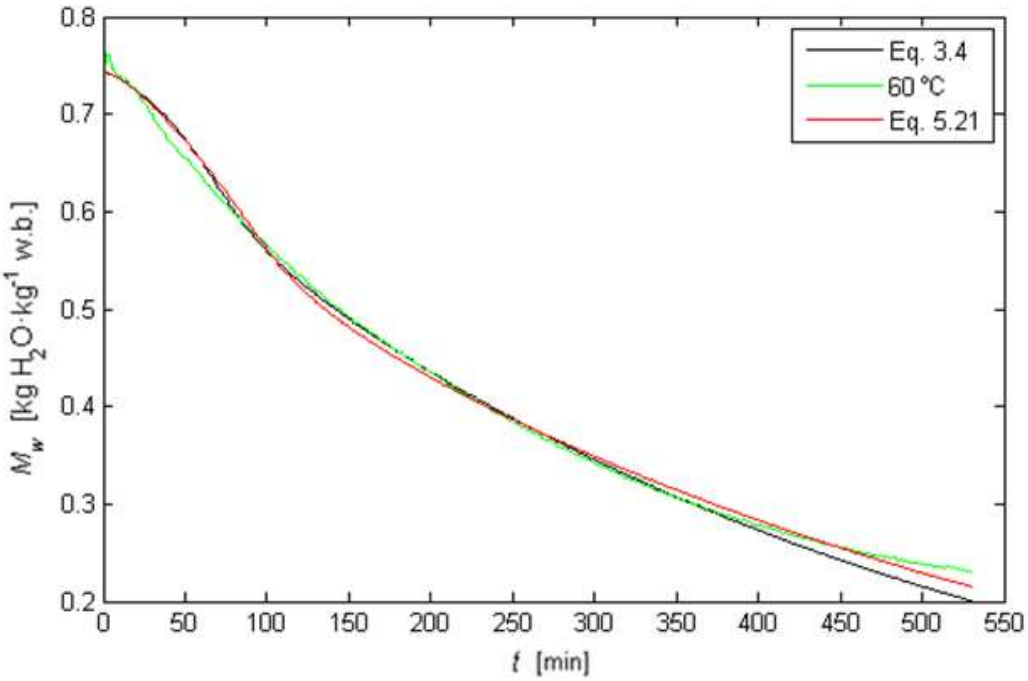

It is proper to make a statistical analysis of both approaches: moisture content-dependent (DM) and the moisture content/temperature dependent (DMT), the model DM has given better results with a highest coefficient of determination and the lowest standard deviation, as shown in Table 6.9.

The evaluation between the experimental drying curve data at 60 °C and the predicted results calculated with the DM (red) and DMT (black) models is given in Fig. 6.20.

Table 6.9 – Determination of the D_e by two approaches DM and DMT along with associated statistics corresponding to the unripe banana slice drying at 60 °C.

Model	Equation	Statistics r^2	Statistics σ
DM	$D_e = \psi_1 M^3 + \psi_2 M^2 + \psi_3 M + \psi_4$	0.993	0.009
DMT	$D_e = D_0 \exp\left(-\frac{A_0}{M}\right)\exp\left(-\frac{B_0}{T}\right)$	0.991	0.011

M Moisture content in dry basis

The comparison between this two approaches, DM and DMT, was performed with the experimental drying curve at 60 °C, to make this comparison it was necessary to standardize the axis between 0 and 1. Therefore, the moisture loss was calculated in its dimensionless form denoted as M_r and treated as a moisture ratio shown in Eq. 6.7.

$$M_r = \frac{M - M_e}{M_0 - M_e} \qquad (6.7)$$

Figure 6.20 - Comparison between experimental moisture ratio (M_r) and modeling results of the DM (red) and DMT (black) approaches during convective drying of unripe banana slice at 60 °C.

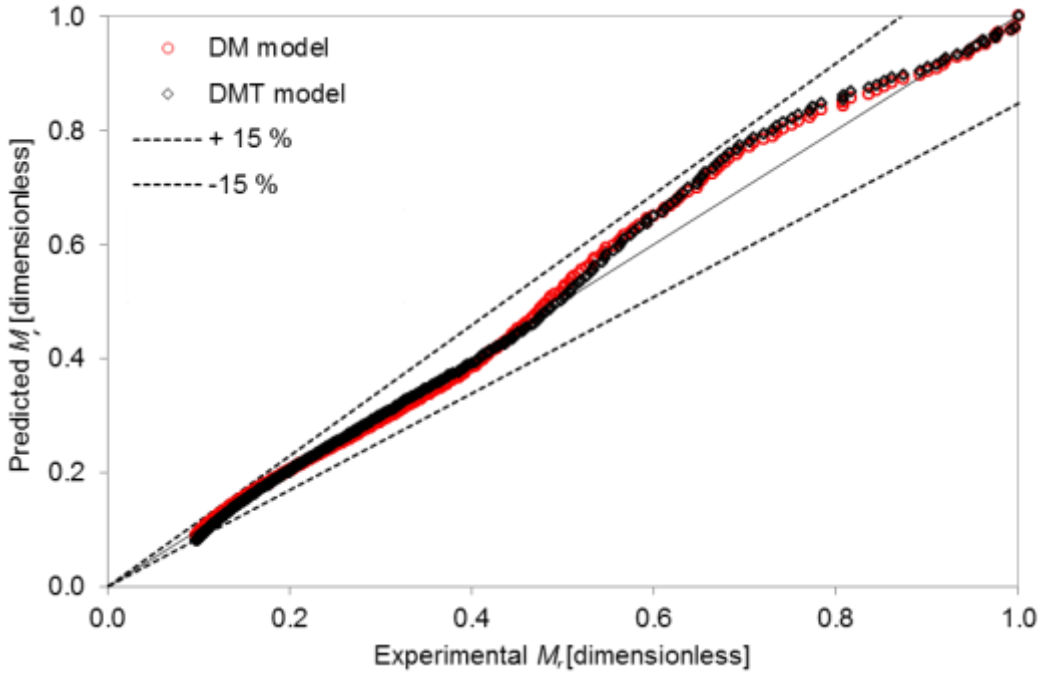

As it can be identified in Fig. 6.20 both approaches show the same behavior, it is interesting to notice that both models present a deviation in the same moisture content (dimensionless) range which corresponds to the first 100 min of drying. The literature recommends incorporating the shrinkage phenomenon in the mathematical model considering porous materials (AZZOUZ *et al.,* 2002; De LIMA; QUIROZ; NEBRA, 2002; HASSINI *et al.,* 2007).

Azzouz *et al.,* (2002) in the study of the drying of grapes, two models of diffusion have been performed to evaluate the effective diffusivity, a simplified one based on Fick's law (analytical method) and a second one that takes account a variable diffusivity (numerical method). Results confirm that the utilization of the analytic method is not justified in the case of the grape which is strongly deformable; in fact, an important gap exists between the coefficient of diffusion identified by the numeric method and the one obtained analytically. This is exactly what happens in the unripe banana drying, in Fig. 6.19 it is possible to note that in the first minutes of drying exists a gap comparing with experimental data, repeating the same behavior in Fig. 6.20.

On the other hand, it is possible to notice that during the last minutes (Fig. 6.19) the decreasing rate of moisture removal estimated by the DM model (red line)

is not as high as the DMT model (black line), this is probably caused by the fact that the combined effect of the decreasing moisture content and the increasing of the temperature inside of the unripe banana slab, resulted in a lower moisture content prediction. This is the main reason why the DM model was chosen for the following mathematical modeling considering the shrinkage effect.

The new founded values for the h and h_m and the parameters of DM model are summarized in Table 6.10. It was necessary to perform a new parameter estimation (heat and mass coefficients), because the variation of D_e had an effect on the resolution of the mathematical model.

Table 6.10 - The new estimated parameters h and h_m along with the DM model

Parameter	Symbol	Value/Correlation	Units
Heat transfer coefficient	H	186	$W \cdot m^{-2} \cdot K^{-1}$
Mass transfer coefficient	h_m	8.45×10^{-5}	$m \cdot s^{-1}$
Effective moisture diffusivity	D_e	$1.46x10^{-11}M^3 - 9.06x10^{-11}M^2 + 7.74x10^{-11}M + 4.04x10^{-10}$	$m^2 \cdot s^{-1}$

M Moisture content in dry basis

Kiranoudis *et al.,* (1993) published the D_e profile as a function of moisture and temperature of carrot and potato, their results showed that the D_e ranged from (2.5 to 20)$\times 10^{-9}$ $m^2 \cdot s^{-1}$ and from (3 to 15)$\times 10^{-9}$ $m^2 \cdot s^{-1}$ for carrot and potato, respectively. The authors worked with a temperature of air-drying of 60 ºC and 80 ºC.

They recognized that the temperature effect is not obvious, but a linear dependence on material moisture content could be considered. They concluded that the effective moisture diffusivity is nearly constant at high moisture content, but it decreases sharply as the moisture content decreases.

The drying of grapes performed by Azzouz *et al.,* (2002) also presented the relationship between the D_e and the moisture content and temperature determined by a numerical method, they concluded that the moisture content (dry basis) affects the D_e evolution compared with the temperature. At 60 ºC of air-drying temperature, the D_e ranged from (0.4 to 9)$\times 10^{-8}$ $m^2 \cdot s^{-1}$.

The unripe banana D_e, estimated from the mathematical model as a function of moisture content (dry basis), represents the evolution of the effective moisture

diffusivity, shown in Fig. 6.21. The D_e is described by different mathematical relationships. The influence of the moisture content is represented by a polynomial law or an exponential law (ZOGZAS; MAROULIS; MARINOS-KOURIS, 1996). In this study the expression of D_e is written under a polynomial law.

The D_e ranged from (4.3 to 2)$\times 10^{-10}$ $m^2 \cdot s^{-1}$ for a moisture content (dry basis) from (3 to 0.02) $kgH_2O \cdot kg^{-1}$ d.b., respectively. The values found seemed to be lower compared with other studies at the same temperatures of air-drying, this might be due to the compact structure of the unripe banana, as it can be verified with the porosity in Fig. 6.4.

Figure 6.21 - Effective moisture content, D_e, of unripe banana as a function of moisture content (dry basis) calculated by the mathematical model at 60 ºC of air-drying temperature.

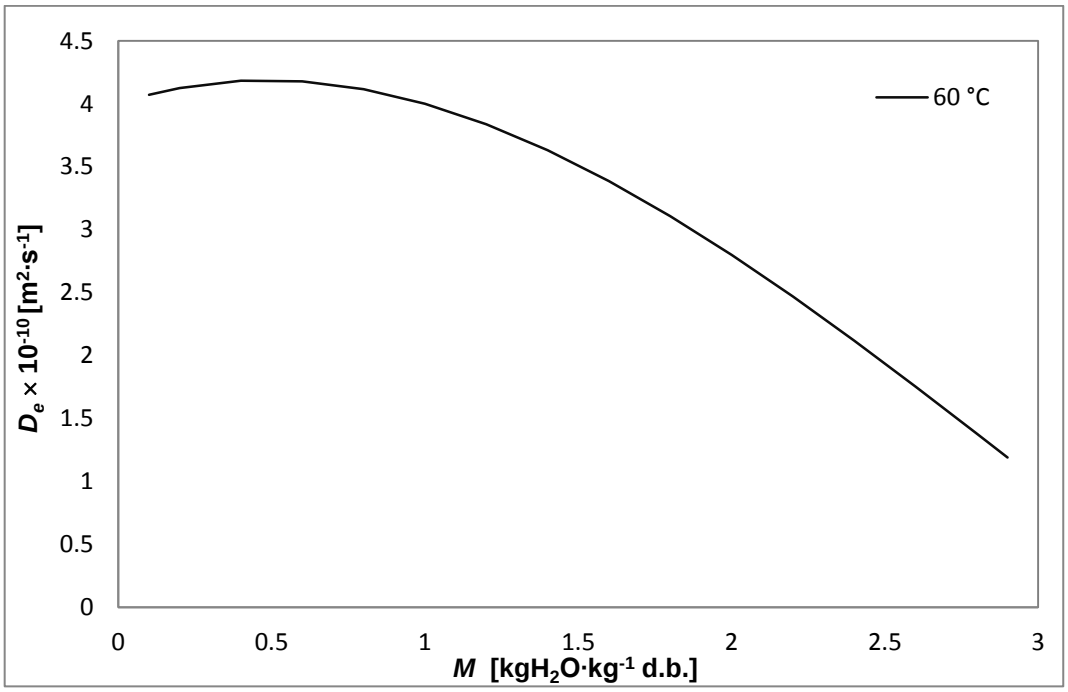

An interesting approach was made under Kumar; Millar; Karim (2015), they recently proposed to integrate the shrinkage inside the D_e correlation, three simulations were performed with: moisture-shrinkage dependent, temperature dependent and the average from the previous approaches.

The results showed that the first minutes of drying (200 min) the predicted moisture content (dry basis) which closely agreed with the experimental moisture data corresponds to the temperature dependent. On the other hand, for the moisture-shrinkage dependent diffusivity model exhibited a faster drying rate in the initial stage but followed experimental data closely in the final stage of drying. This higher drying

rate during the initial stage can be attributed to the higher diffusion coefficient or the diminution in terms of volume/area of the product being dried.

Golestani *et al.,* (2013) also found a higher drying rate compared to the experimental results for both models obtained from two effective diffusivities with and without shrinkage. Therefore, a more complex and physics-based formulation is necessary to calculate effective diffusivity and predict the moisture content more accurately. This leads us to get back to Fig. 6.19 in which at the beginning of the process, as discussed previously, it exists a gap between the predicted model and the experimental data.

6.4.5 Shrinkage condition

During drying, the banana shrinks and this modifies the shape of the body, decreases the area of heat transfer and increases the superficial roughness of the material. This last characteristic provides an increase of the turbulence level in the boundary layer, favoring therefore, the change of energy between air and material (de LIMA; QUEIROZ; NEBRA, 2002).

Tribess (2009) described that the predominant mechanism moisture removal occurred in the decreasing drying rate period (DDR), according to Demirel; Turhan (2003) several authors consider that drying of banana slices is controlled by the DDR, which is divided in two periods (DDR I and DDR II).

The first period DDR I corresponds to the phase in which the material has partially wet surface, the internal resistance overlaps the diffusion mass transfer. The hypothesis at this point is that the shrinkage phenomenon has a great influence on the drying behavior, at the beginning of the drying process.

The second period (DDR II) takes place when the product surface is completely dry and the internal diffusion resistance controls the drying of the material.

Johnson *et al.,* (1998) observed a short time of constant drying rate (CDR) followed by two periods of DDR (I and II) during the drying of the slices of banana (plantain) at temperatures between (40 and 70) °C.

According to Tribess (2009) to identify the transition between the two periods (DDR I and II) the Eq. (6.6) is linearized, specifically the dimensionless moisture

content (M_r). Figure 6.22 shows the plots of the natural logarithm of M_r versus time for the drying of unripe banana slices. A first straight line adjusted well the experimental data during the first 150 min of drying. Thus, a first drying period is identified as DDR I in which the diffusion and the shrinkage phenomenon are the mechanism that describes the drying behavior. A second drying period, observed by the change in the slope, may be due to the combination of transport mechanisms, such as, internal diffusion, capillarity.

Figure 6.22 - The natural logarithm of dimensionless moisture content (M_r) versus drying time of unripe banana slices dried at 60 °C and fitted lines for both periods (DDR I and DDR II).

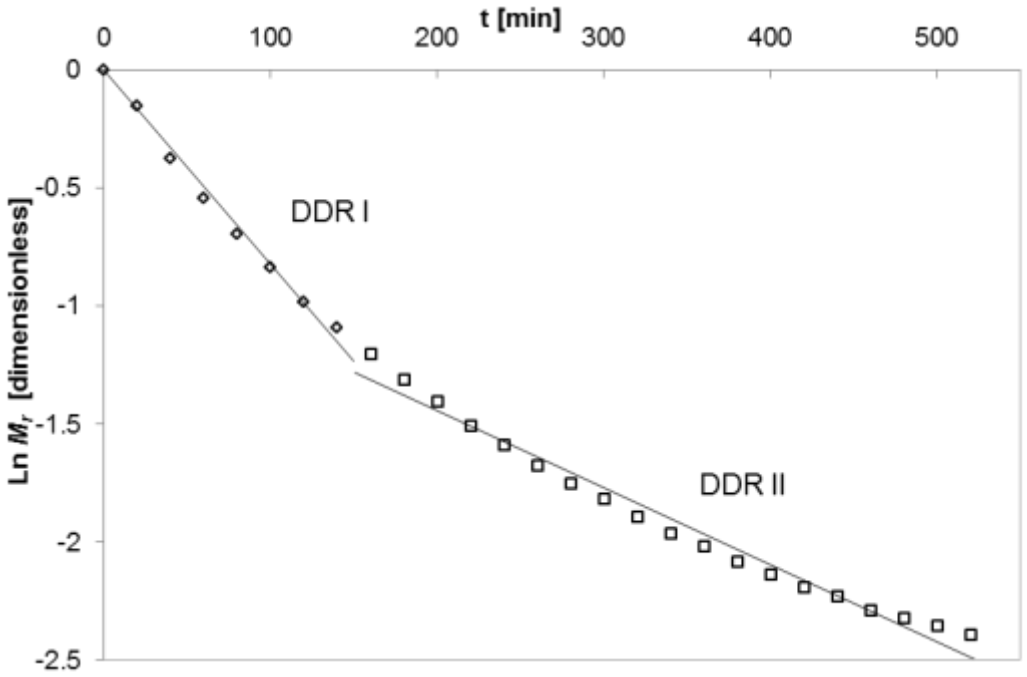

This method was developed to estimated two effective moisture diffusivities, Tribess (2009) concluded that the first period (DDR I) lasted 2 h approximately. In this study, the DDR I lasted 150 min, after that there was a change in the slope. These first 150 min are important because the measurement of the shrinkage phenomenon with the stereoscope showed that an important reduction in the thickness (dL) of the unripe banana slices takes place in the first hours of process, as can be observed in Figure 6.23 the shrinkage measured every hour.

Figure 6.23 - Thickness reduction of unripe banana slices during air-drying at 60 ºC.

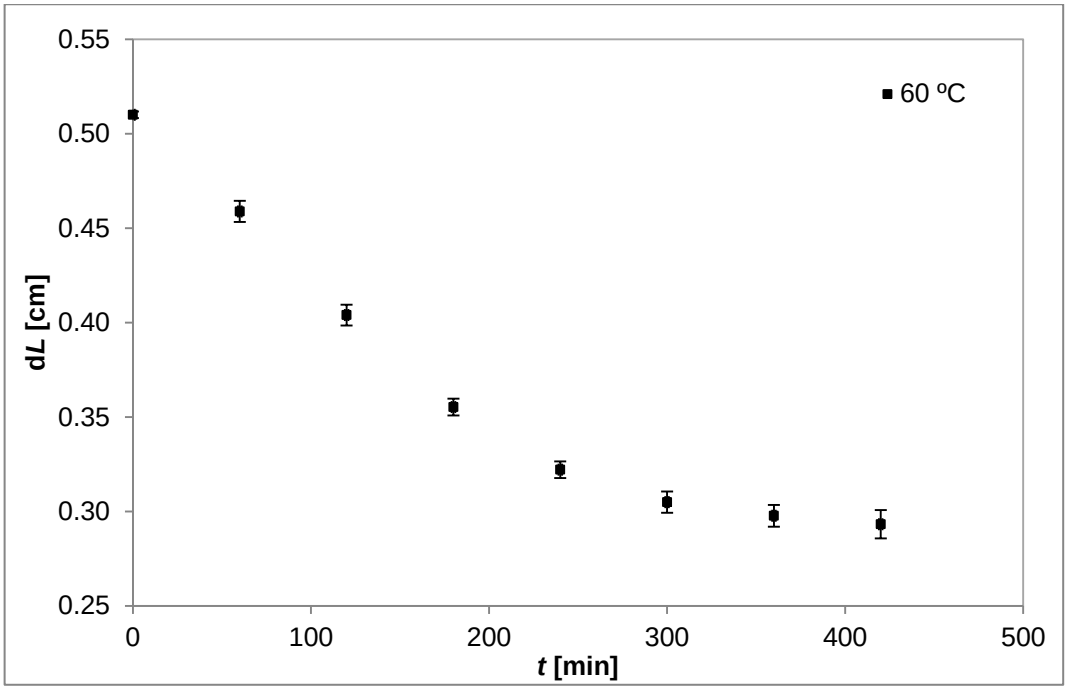

It was possible to measure the reduction of the thickness and also the diameter. It is interesting to observe that at the beginning of the process, the unripe banana surface is completely wet and after one hour of drying the water evaporated and the enzymatic browning had an important effect on the unripe banana color, as it can be seen in Fig. 6.24.

The reduction of the diameter was compared with the thickness reduction; it was found that in the three first hours of drying the thickness experienced a contraction of about (30.34 ± 1.29) % out of the initial thickness (L_0). On the other hand, the reduction of the diameter was only (12.39 ± 1.11) % out of the initial diameter.

Figure 6.24 - Variation of the diameter of the unripe banana slab during the convective drying at 60 °C, 4 $m \cdot s^{-1}$ of air-drying and *RH* of 10 % within the first five hours of process.

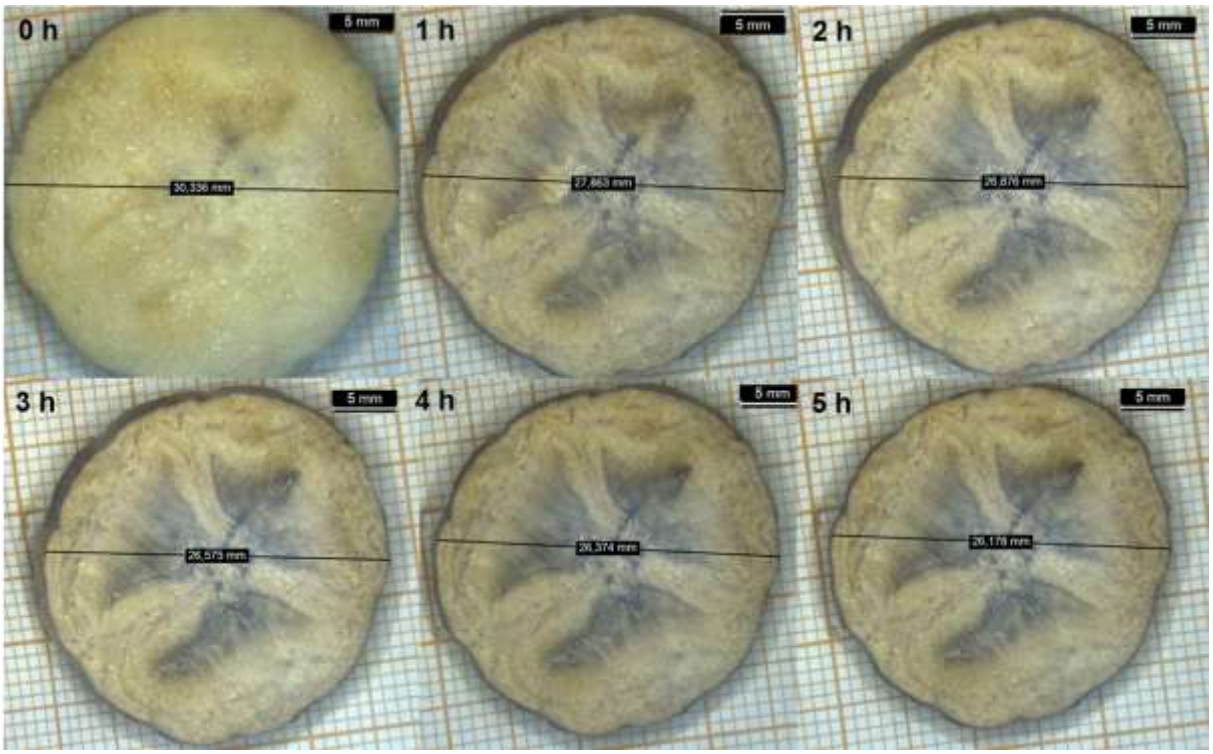

Kumar; Millar; Karim, (2015) studied the porosity and shrinkage of dried food in microscope level and provided a better insight to attain energy effective drying process and quality of dried food. The hypothesis of the pore formation and its evolution during the drying process is shown in Fig. 6.25.

Figure 6.25 - Hypothesized relationships among the drying parameters pore formation and evolution.

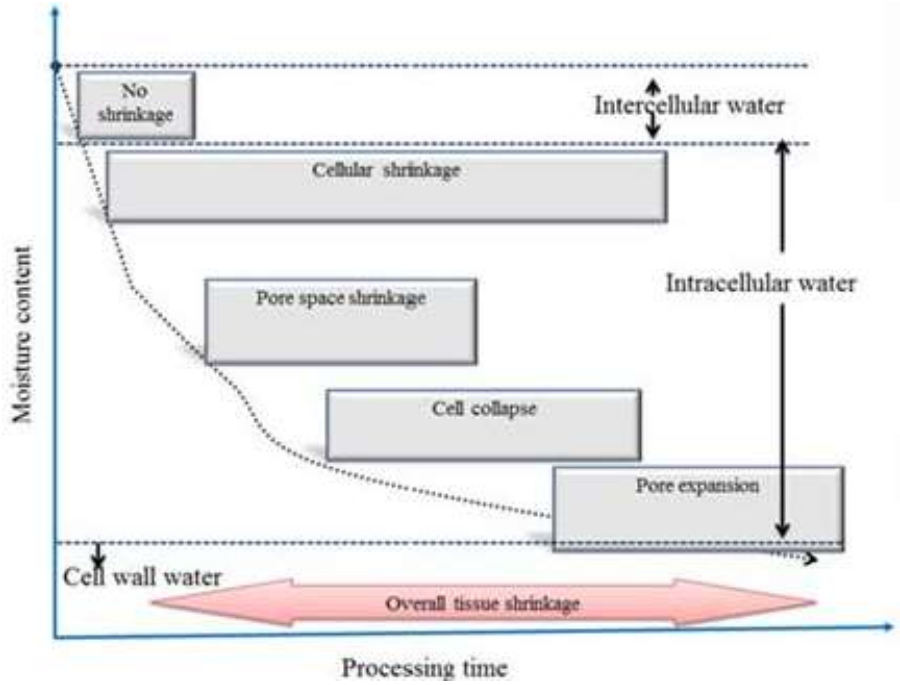

Source: KUMAR (2012)

As food materials has complex structural nature, it is quite impossible to set a generic relationship regardless of types of food. However, an approximate relationship between process parameters and product quality can be achieved through pore characteristics. The unripe banana structure presents higher bound water in cell walls causing low porosity; it is interesting to notice the pores formation as the process is being carried out, as illustrated previously in Fig. 6.25 after the pore formation comes the cell collapsing and pore expansion, as denoted in Fig. 6.26 after of seven hours of drying.

Figure 6.26 – Changes in the unripe banana structure during drying, after 0h, 3 h, 5 h and 7 h of processing.

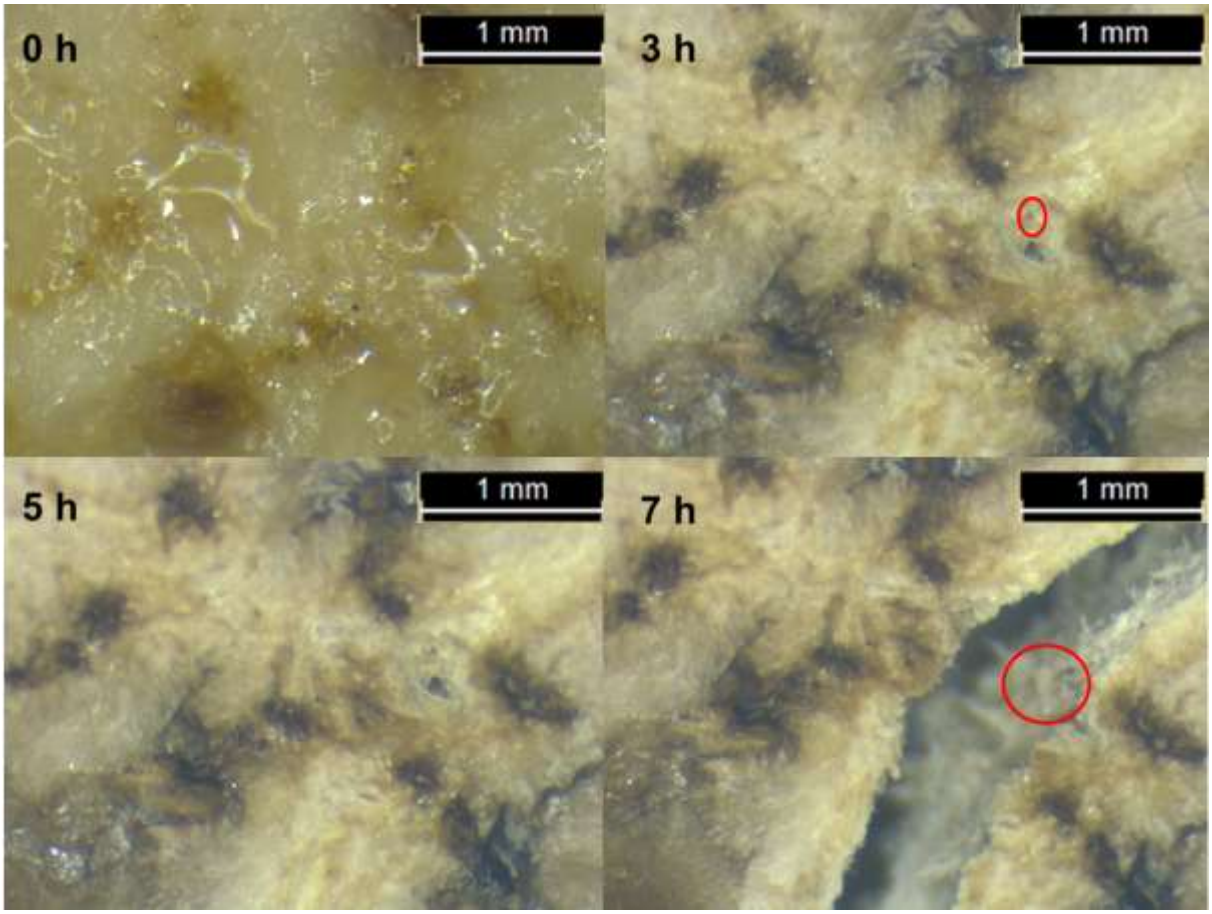

It can be noticed that after 3 h of drying (approximately), the shrinkage in the thickness of the unripe banana slab is not as important as in the first hours of process. Thus, for the shrinkage condition it was necessary to introduce this phenomenon, into Eqs. 5.12 and 5.13, as $\frac{dL}{dt}$ (thickness reduction)

$$\rho\frac{\partial M}{\partial t}=\frac{1}{L^2(t)}\frac{\partial}{\partial\xi}\left(D_0\,\rho\frac{\partial M}{\partial\xi}\right)+\frac{1}{L_0}\frac{dL}{dt}\frac{\partial M}{\partial\xi};\qquad(5.12)$$

$$\rho C_p\frac{\partial T}{\partial t}=\frac{1}{L^2(t)}\frac{\partial}{\partial\xi}\left(k\frac{\partial T}{\partial\xi}\right)+\frac{1}{L_0}\frac{dL}{dt}\frac{\partial T}{\partial\xi};\qquad(5.13)$$

The boundary conditions were also modified for the mass and heat transfer. Eqs. 5.14 and 5.15 described the boundary conditions at the surface.

The computational iterations consider the problem every second, in this way, it was necessary to find an empirical correlation, which described the behavior of the thickness reduction every second. This correlation was derived as a function of time and then introduced into the mathematical modeling, with the restriction of being utilized only during the first 150 min.

Therefore, there will be two D_e estimated by the mathematical model, one for the first and other for the second decreasing drying rate periods (DDR I and II), these parameters are listed in Table 6.11.

Table 6.11 - Effective moisture diffusivity (D_e) of unripe banana for the two DDR (I and II) at 60 ºC of air-drying temperature.

T [°C]	***D*$_e$ [m^2·s^{-1}]**	
	DDR I	**DDR II**
60	3.28×10^{-10}	1.77×10^{-10}

As expected the D_e at the beginning of the process (DDR I) is considerably higher than the second period (DDR II), this could be explained in the Fig. 6.27. It is shown the plot of the moisture content [dimensionless] versus the drying time [min], it is possible to observe that the first period (150 min) of the process the moisture content drops up to 30%, this means that the most part of the moisture is taken from the structure in the first hours of drying. Therefore, the D_e in this period would have to be higher compared with the second period as shown in Table 6.11.

Figure 6.27 – The dimensionless moisture content (M_r) as a function of drying time of unripe banana convective drying slices at 60 °C, 4 m·s^{-1} of air-drying and *RH* of 10 %.

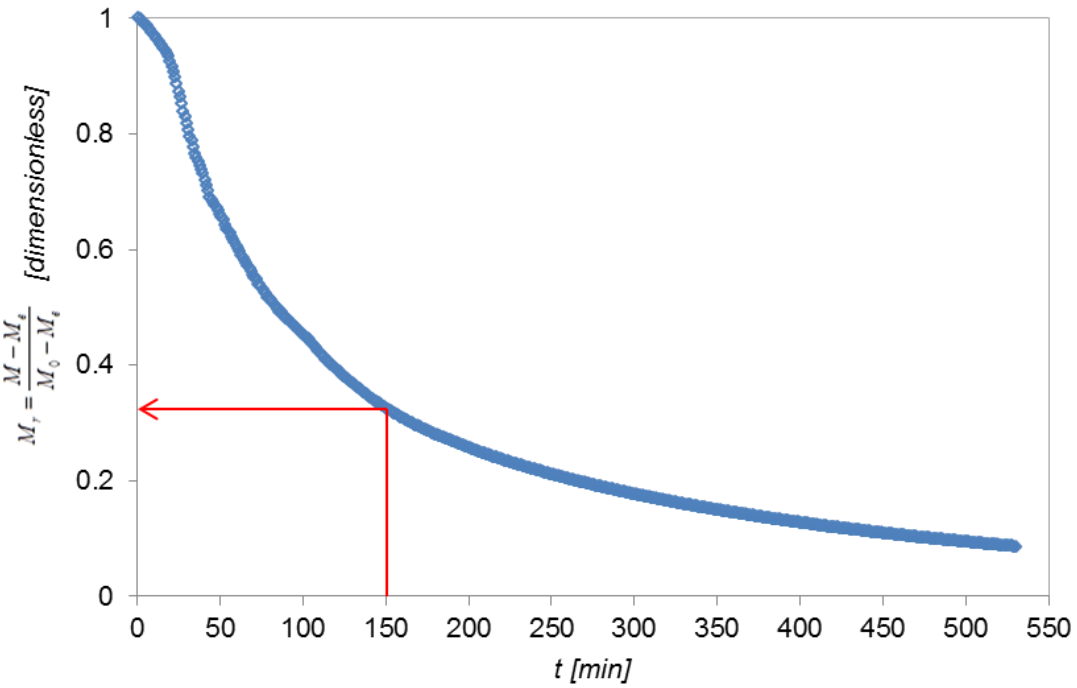

The predicted and the experimental drying curve is plotted as a function of time in Fig. 6.28, as expected, the combined model described accurately the drying behavior; however the last minutes of drying the predicted moisture content decreased (red line), even though the optimized D_e was estimated for this second period.

According to Bennamoun; Fraikin; Léonard (2013), the mathematical modeling must show a mathematical approach more than a physical one. They declared that it is necessary to keep in mind that the objective is not to model the drying curves but to study heat and mass transfer inside the convective dryer, as it is applied in this study.

Figure 6.28 - Experimental drying curve (green) of the unripe banana slice dried at 60 °C and average curve estimation of moisture content (wet basis) estimated by shrinkage model (red).

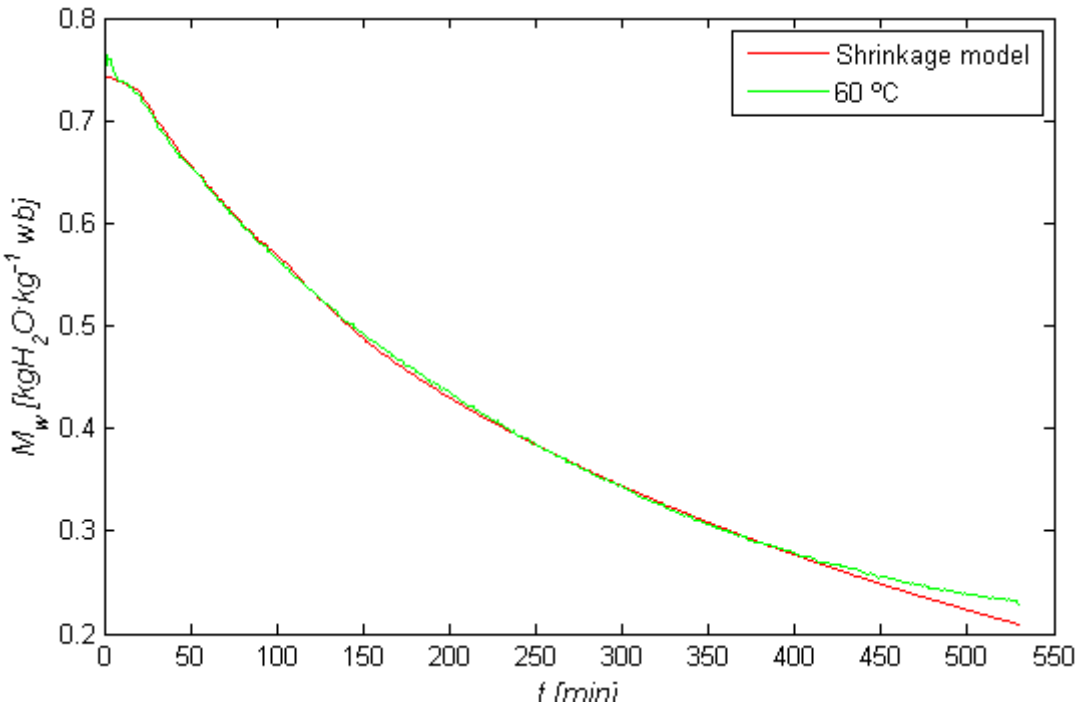

Fig. 6.29, presents the product temperature during the different phases of the process and then a comparison between experimental and the average of modeling results. It is difficult to notice that closed to the changing period towards to DDR II (150 min), there is a little change in the slope (red curve); however, this will not affect the performance of the shrinkage model.

As for the other cases, the temperature inside the unripe banana slab was also predicted but now with the shrinkage model, the first period (DDR I) the temperature inside the unripe banana rises rapidly, which represents the adaptation of the product to the applied drying conditions. It should be a very short period with high increase of temperature as described by Bennamoun; Fraikin; Léonard (2013).

Thus, received energy serves both evaporation of the product water and increasing of its temperature. At the end of the drying process, the most important part of the water are still evaporated and energy almost exclusively serves to increase the product temperature until almost attaining the constant value of the heated air temperature, as observed in Fig. 6.29

.

Figure 6.29 - Experimental average temperature curve (green) of the unripe banana slice dried at 60 °C in comparison with the average temperature estimated by the shrinkage model (red).

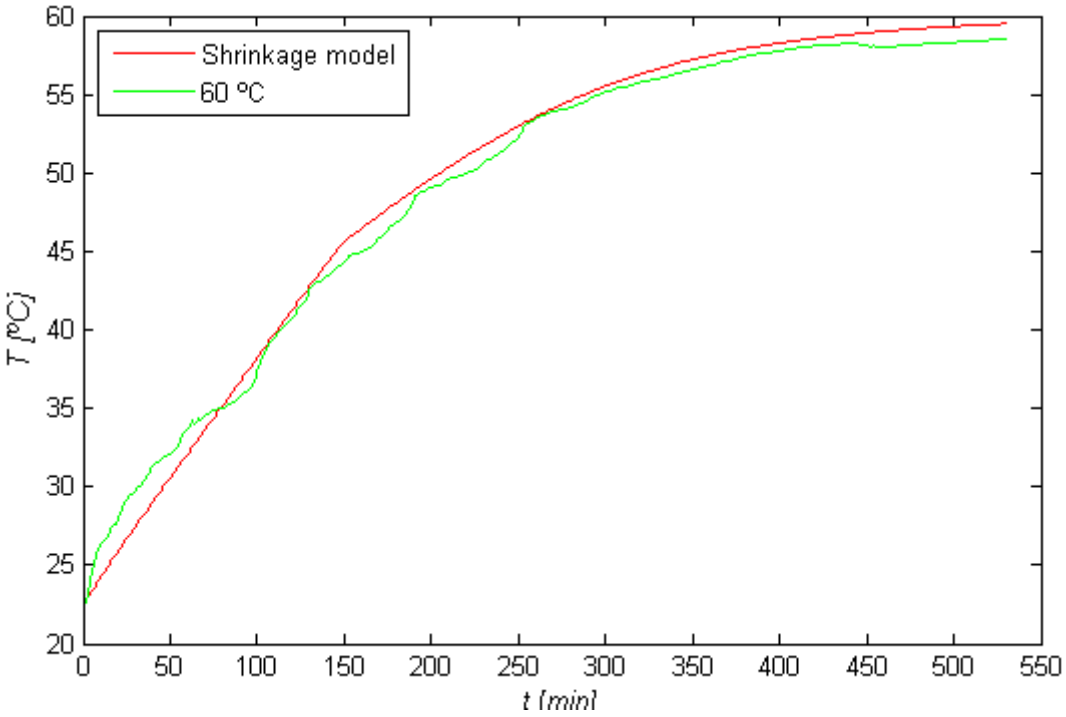

Rahman; Kumar (2007) and Tripathy; Kumar (2009) have shown that, during convective drying, coefficient of heat transfer is not constant and varies with the passage from one drying phase to another. Also, they have shown that shrinkage has an influence on the heat transfer coefficient as a function of moisture content in dried products.

To demonstrate the model-approach presents an accurate description of the drying behavior, it was calculated the coefficient of determination (r^2 = 0.999). The comparison between the experimental and predicted results calculated using the shrinkage model is given in Fig. 6.30, it gives the best representation of the obtained drying curves with the highest coefficient of determination.

As it was possible to measure the thickness during the process experimentally (Fig. 6.23), it was confirmed that the shrinkage is an evident phenomenon that takes place during the process with an important decrease in the thickness of the sample.

Figure 6.30 - Comparison between experimental and modeling results of the product moisture content during convective drying of unripe banana slices at 60 °C.

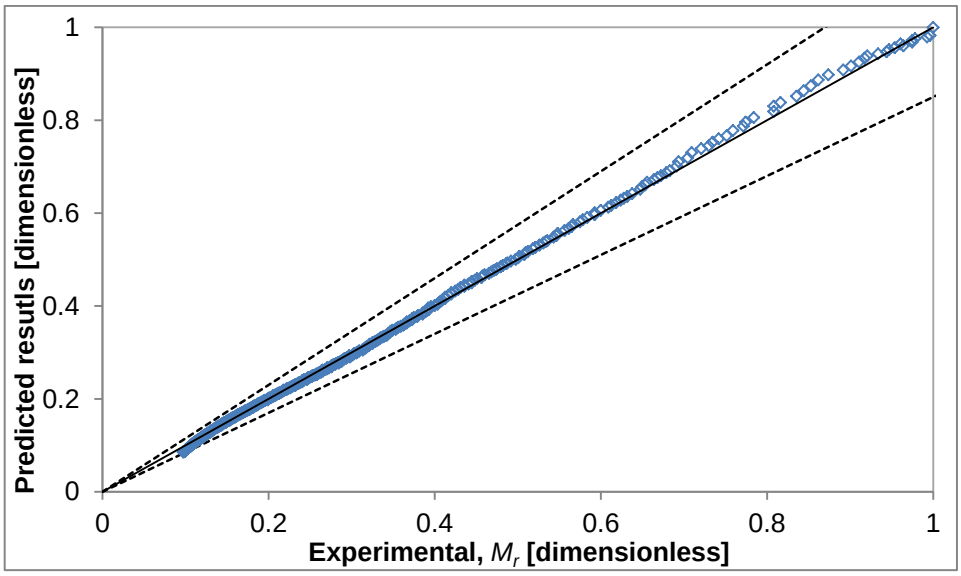

For better visualization, the moisture and temperature profiles within the unripe banana slice as a function of position and time were plotted and presented in Figs. 6.31 and 6.32. As it can be observed, the water content of the upper exposed surface layer of the product gradually decreased with the drying process, and the accumulation phenomenon of local humidity was found in deeper part of the product. As time goes on, the increased range of local moisture content of the deep layer would decrease.

Figure 6.31 - Distribution of moisture content (dimensionless) as a function of drying time and position (dimensionless) of unripe banana convective drying at 60 °C, 4 m·s^{-1} of air-drying and *RH* of 10 %.

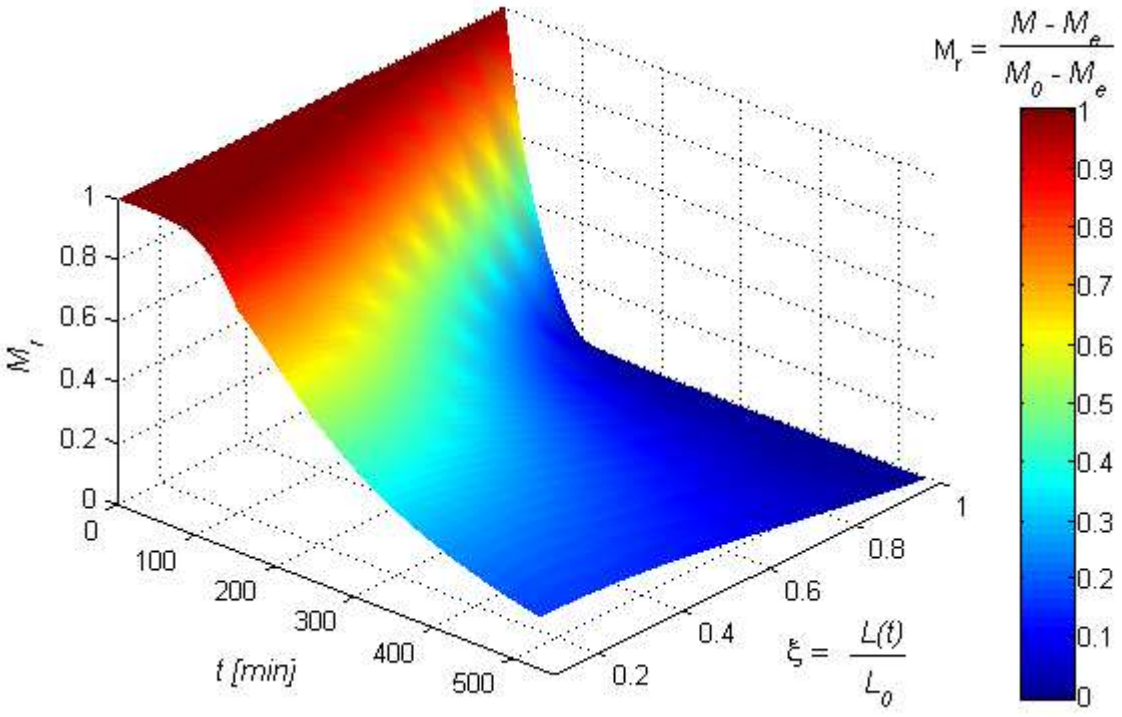

Figure 6.32 - Distribution of moisture content (dimensionless) as a function of drying time and position (dimensionless) of unripe banana convective drying at 60 °C, 4 m·s^{-1} of air-drying and *RH* of 10 %.

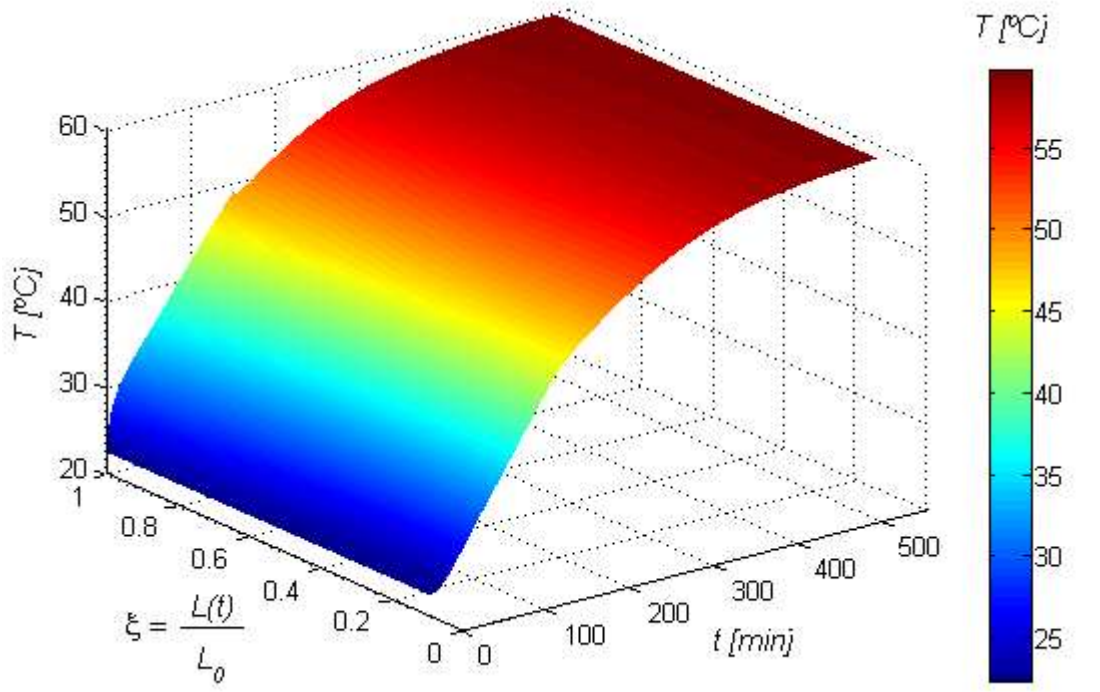

It can be found in Fig. 6.31, that the humidity of the product is rapidly decreasing and the water vapor migrates much easily through the upper exposed surface of the material and then quickly evaporated into the atmosphere. These findings imply that effective diffusivity coefficient (D_e) affects mass transfer and moisture content distribution. Thus, it was possible to find two behaviors (DDR I and DDR II) with two different D_e. However, it was verified during the simulations that the D_e had no obvious influence on the temperature distribution in the unripe banana slab.

It is worth to noticed that the shrinkage effect in Fig. 6.29 and 6.30 is not presented. Returning to the section 5.2 wherein it was explained how the shrinkage phenomenon would be introduced in the mass and heat equations, fixing the location within a changing coordinates grid using the ξ, considered as a moving boundary problem or a lagrangian representation: it is possible to track the location moving along with the system, as the phenomenon is taking place in the solid. This means that the phenomenon in this study the shrinkage is moving together with the system coordinates during the drying process.

6.5 COMSOL modeling

The input parameters are listed in Table 6.12 and the variable thermophysical properties were considered as described in sections 6.3.1 to 6.3.3, it was not possible, as for the mathematical modeling performed in Matlab, to include the porosity as part of the simulation. Kumar; Millar; Karim, (2015) stated that the understanding of porosity and shrinkage would have to be studied as inter and intracellular cell heat and mass transfer.

Table 6.12 - Input parameters considered in the COMSOL Multiphysics simulations.

Parameter	Symbol	Value	Units
Heat transfer coefficient	h	186	$W \cdot m^{-2} \cdot K^{-1}$
Mass transfer coefficient	h_m	8.45×10^{-5}	$m \cdot s^{-1}$
Effective moisture diffusivity	D_e	3.278×10^{-10}	$m^2 \cdot s^{-1}$
Initial slab temperature	T_0	295.15	K
Initial moisture content	C_0	45528	$mol \cdot m^{-3}$
Molar latent heat of vaporization	λ	42480	$J \cdot mol^{-3}$
Air drying temperature	T_{air}	60	°C

It is required to mention that COMSOL Multiphysics works with water concentration in $mol \cdot m^3$, the experimental moisture content calculated through the loss of mass during the drying process is expressed in $kg \cdot kg^{-1}$ db. In order to perform the simulation, the initial moisture content was express in terms of molar concentration $mol \cdot m^{-3}$ using the Eq. (6.8)

$$C_0 = \frac{M_w \rho}{MW_{H_2O}} \qquad (6.8)$$

6.5.2 COMSOL results

COMSOL Multiphysics results are shown as curves of the moisture concentration and temperature as a function of time, but it is necessary to take into consideration that these diagrams are acquired as a point graphs, in this case it was possible to obtain four curves out of four points (edges of the unripe banana slab) shown in Fig. 6.35.

The first figures obtained showed the moisture concentration $mol \cdot m^{-3}$ and the temperature [°C] at the four edges, these results are presented in Figures 6.33 and 6.34.

Figure 6.33 - Moisture concentration at the four edges of unripe banana slice as a function of drying time at 60 °C, 4 m·s^{-1} of air-drying and *RH* of 10 %, obtained by simulation using the COMSOL.

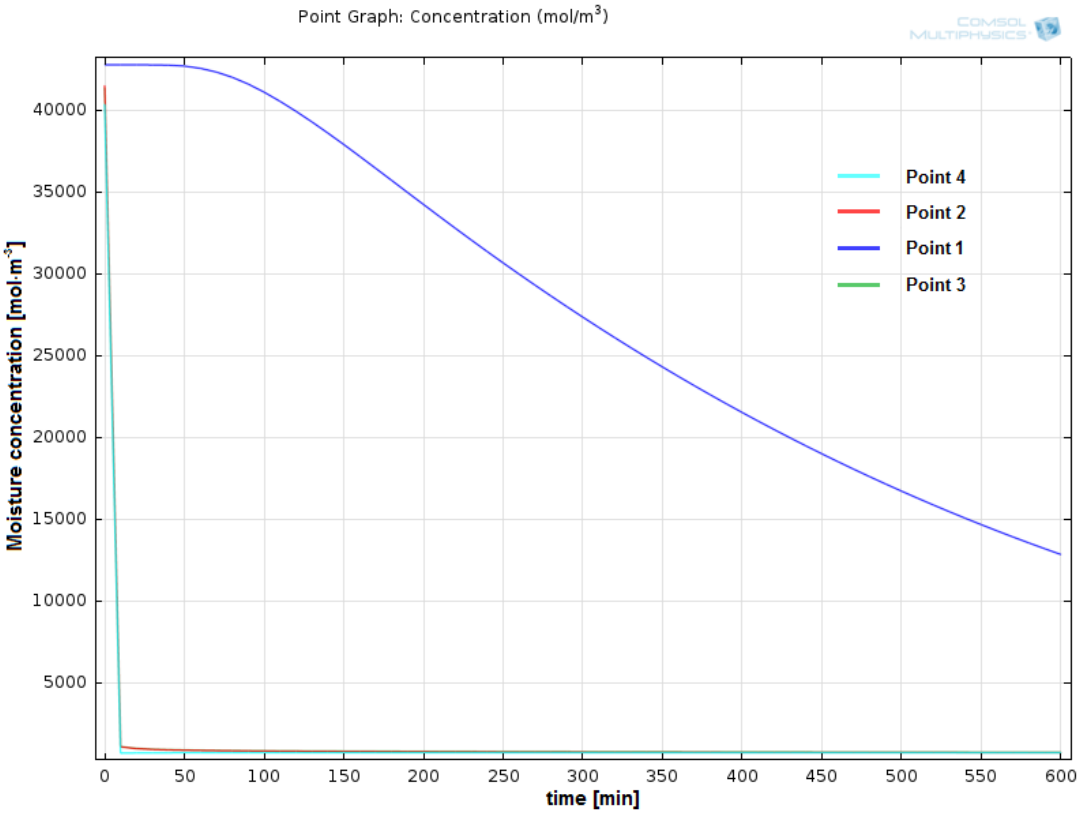

Figure 6.34 - Temperature profile at the four edges of unripe banana slice as a function of drying time at 60 °C, 4 m·s^{-1} of air-drying and *RH* of 10 %, obtained by simulation using the COMSOL.

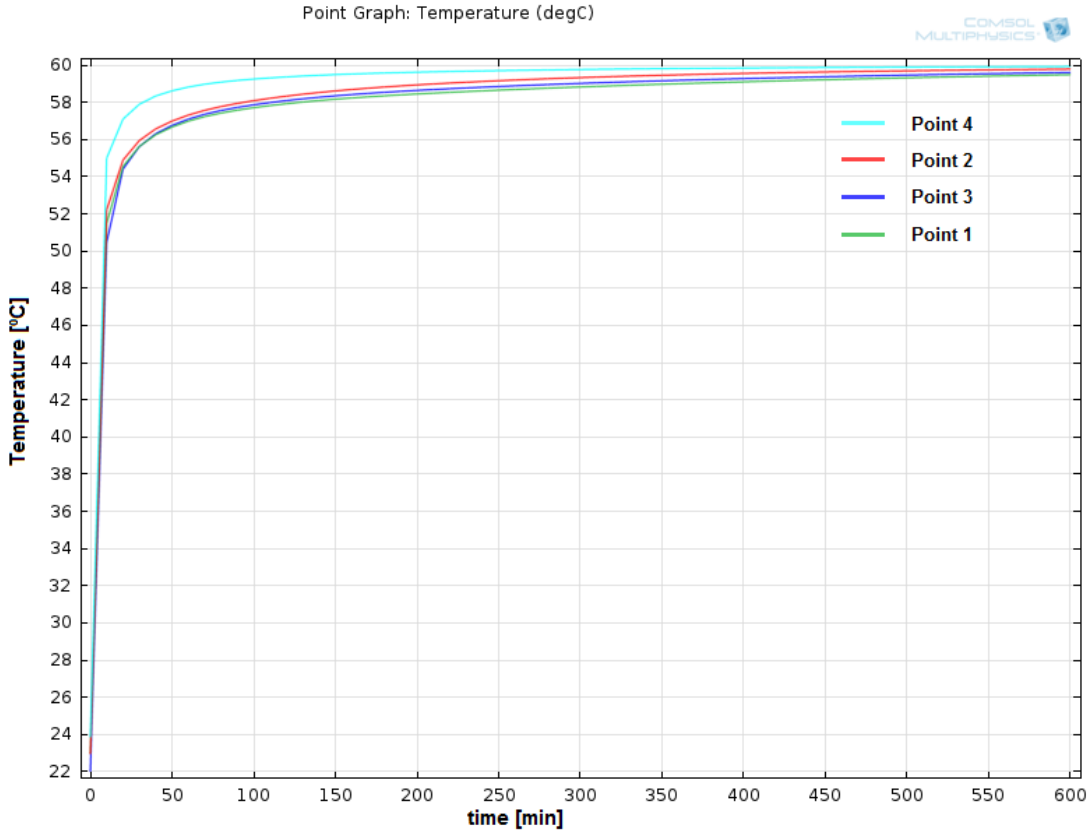

The C_b considered in this simulation it is not equal to the C_{sup} calculated by the mathematical modeling performed by Matlab in previous sections; it was not considered thermodynamic equilibrium relationship between the air humidity and the moisture surface of the slab. It is difficult to know how COMSOL considered the moisture and heat transfer during the drying process. As noticed in Fig. 5.5 in section 5.5.1, points 2, 3 and 4 which are in contact with the air-drying corresponding to the three surface edges dried instantaneously.

It was only possible to get the results in four points calculated by COMSOL, it is hard to make a comparison with the experimental results and it was considered as an approximation, because the points where it can be taken the results seemed to dry faster than it actually occurred. However, this approximation allows to visualize the behavior of the mass and heat transfer in 3D throughout the banana slab.

The interesting part of the COMSOL results are the figures shown in 2D with the contour curves shown as a temperature and moisture profiles followed with the gray arrows indicating the direction of the heat flux and how the water is leaving the food solid matrix, as can be seen in Fig. 6.35.

Figure 6.35 - Moisture concentration and temperature profile of unripe banana slab after 600 min of drying (left) and contour curves (right).

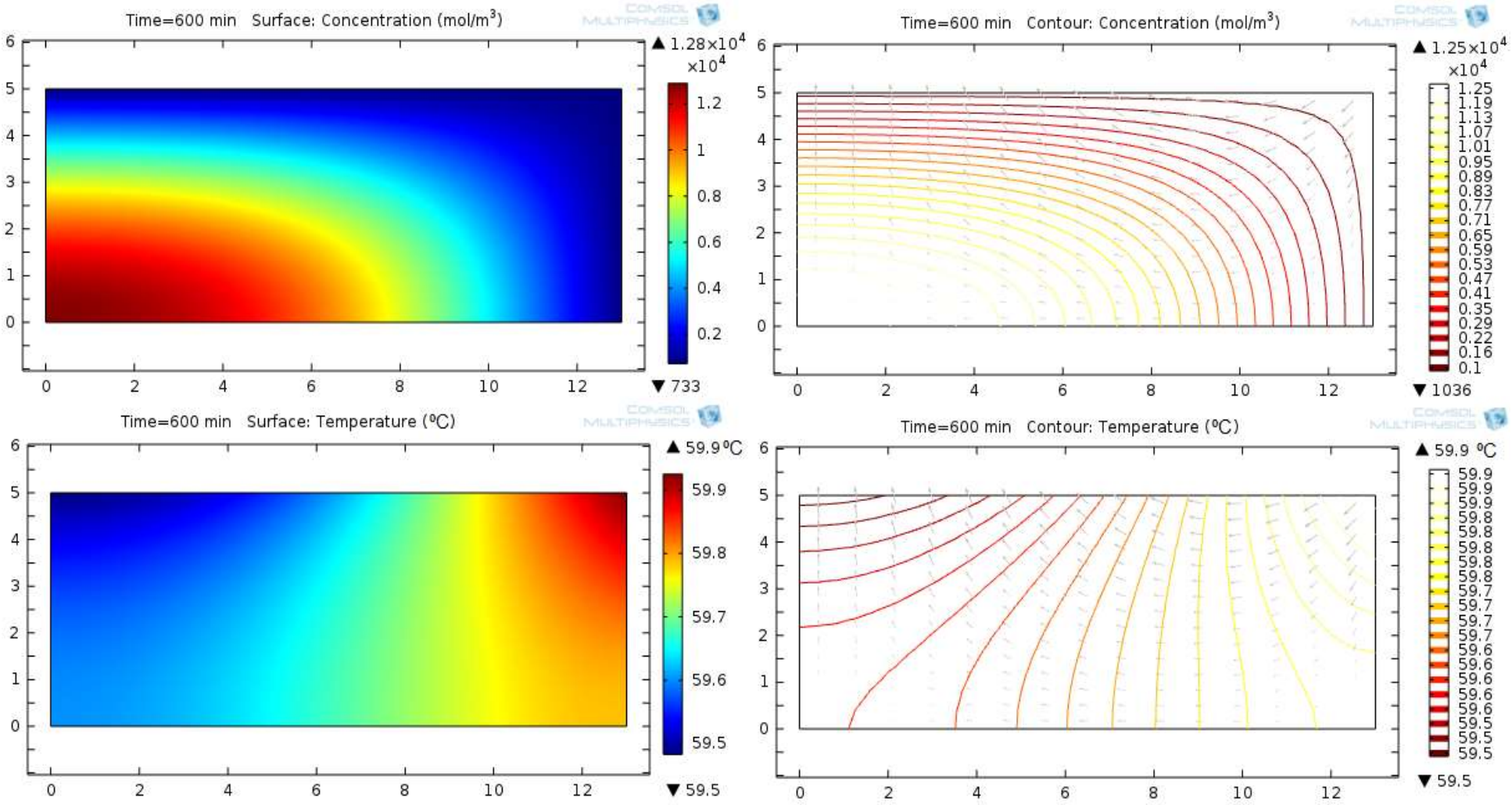

After 600 min of drying the center of the banana slab (Point 1) presents 0.2 $kg \cdot kg^{-1}$ wb, according to Eq. 6.8; comparing this result with the estimated by the model with shrinkage (550 min of drying) phenomenon, this value was closed to 0.3 $kg \cdot kg^{-1}$ w.b. The temperature at the same point (Point 1) calculated by COMSOL was 59.6 ºC approximately, comparable this with that estimated by the model considering shrinkage phenomenon (59.8 ºC), as can be seen in Fig. 6.35. It can be concluded that the COMSOL results at this point are reliable.

All these results can be verified as a 2D-Axisymmetry and being observed as 3D results (Figs. 6.36 and 6.37), as denoted by Perussello *et al.,* (2013) using the COMSOL program, it is possible to perform innumerous simulations changing the air-drying temperature, relative humidity, thermophysical properties, etc.

Figure 6.36 - Moisture content profile of the banana slices after 600 min of convective drying conducted at 60 ºC.

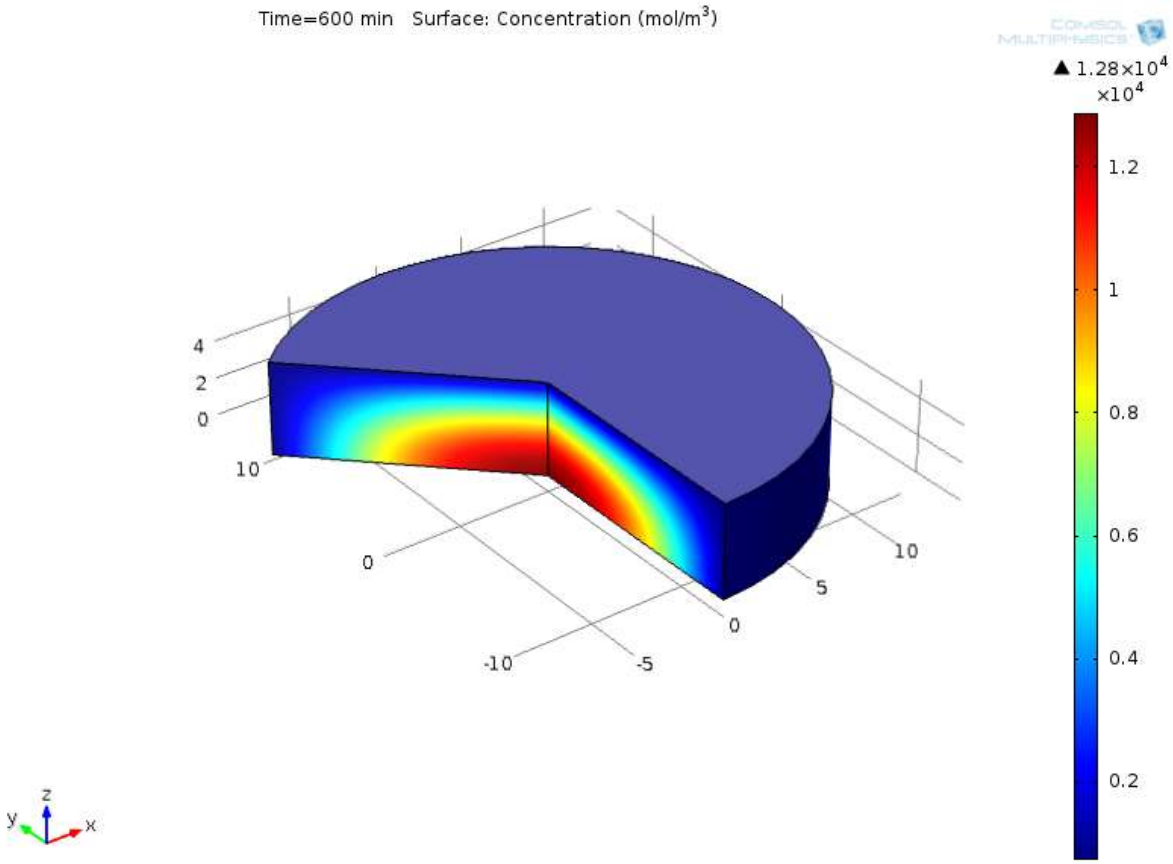

Figure 6.37 - Temperature profile of the banana slices after 600 min of convective drying conducted at 60 ºC.

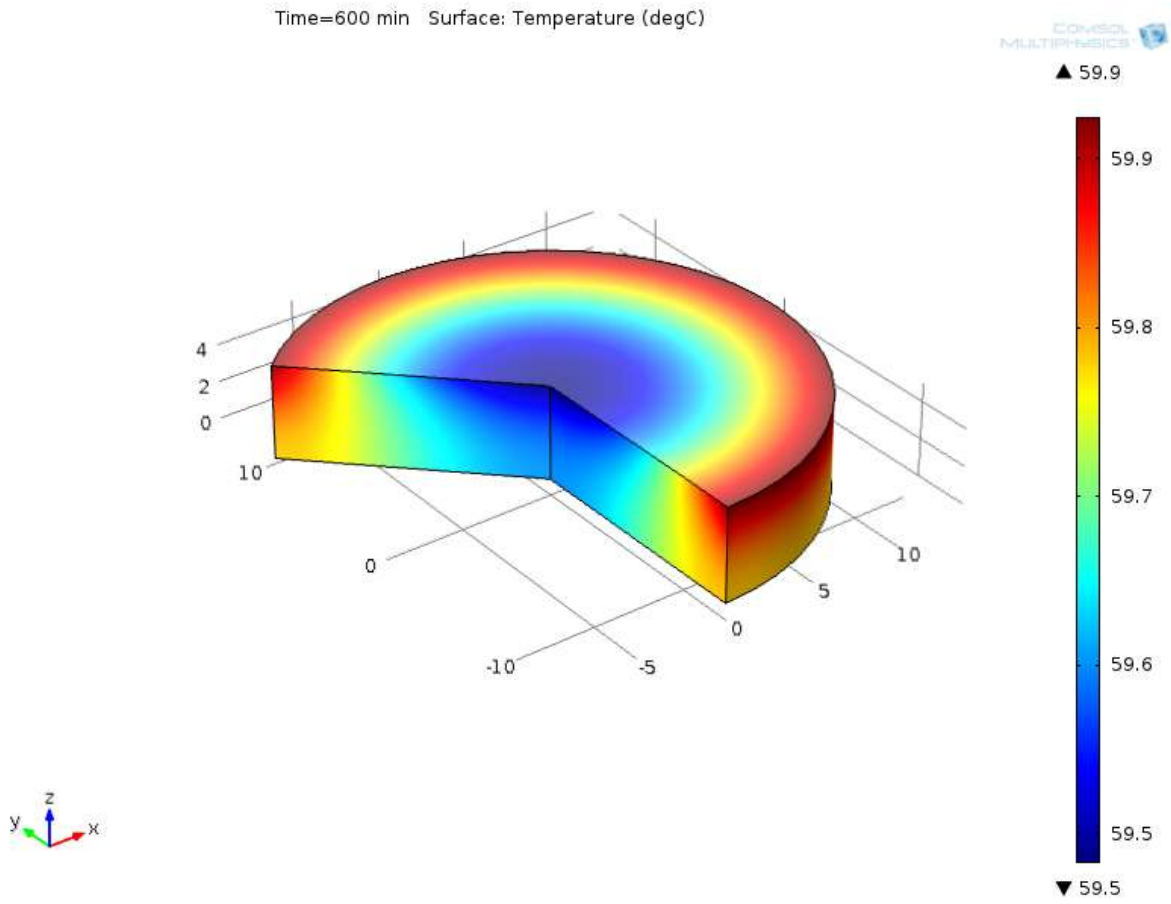

It is important to remember that the total thickness of the unripe banana slice is 10 mm and COMSOL results showed half of thickness due to the symmetry condition. Consequently, the parameters considered in the COMSOL simulation, such as: effective moisture diffusivity, heat and mass transfer coefficients, where taken from the estimation of the mathematical model.

6. CONCLUSIONS

It has been developed a mathematical model describing simultaneous heat and mass transfer processes initially with the thermophysical properties constant during the drying of food products with high moisture. It was employed a simple one-dimensional model of heat and mass transfer that assume unripe banana as a homogenous structure, this framework was applied to represent the movement of water. A numerical solution of the model equation was performed, temperature and moisture distribution were predicted. The results reveal that, with the use of the diffusion process alone, the movement of moisture can simulate the drying process.

In spite of its weaknesses, the model was improved on the basis of more sophisticated mathematical modeling with the incorporation of the variable thermophysical properties, estimation of heat and mass transfer coefficients, the effective moisture diffusivity as a function of moisture content and shrinkage phenomenon, such formulations improved the model consistency.

The model validation was performed to make a parameter estimation, with an optimization technique, it was found that the heat transfer is 186 $W \cdot m^{-2} \cdot K^{-1}$ and the mass transfer is 8.45×10^{-5} $m \cdot s^{-1}$ agreeing with others published in the literature at the same conditions.

Two periods were identified during drying process, decreasing drying rate period I and II (DDR I and II), it was demonstrated that shrinkage phenomenon has a great influence on the drying behavior in the first drying period DDR I. The second period (DDR II) takes place when the product surface is completely dry and the internal diffusion resistance controls the drying of the material.

For instance, it was found the (D_e) for each drying period, for the (DDR I) was around 3.28×10^{-10} $m^2 \cdot s^{-1}$ and for the (DDR II) 1.77×10^{-10} $m^2 \cdot s^{-1}$ considerably lower than the first period, it was possible to observe that the first period (150 min) of the process the moisture content drops up to 30% meaning that the most part of the moisture is taken from the structure in the first hours of drying.

The shrinkage phenomenon was measured successfully, monitoring the reduction of the slab thickness and verifying that the reduction of thickness was higher than the reduction of the radius.

The mathematical modeling considering the shrinkage phenomenon with the variable properties described adequately the drying behavior, this model was validated with the experimental data: the drying kinetics and the temperature at the center and the surface of the unripe banana slice.

The COMSOL Multiphysics simulations were possible to perform through the heat and mass transfer coefficient estimated previously by the mathematical modeling. As it was possible to obtain only four curves corresponding to the four edges of the slab, it was difficult to make a good comparison and to validate these simulations with the experimental data. Nevertheless, the results showed a good behavior especially with the temperature profile inside the unripe banana slice.

7. SUGGESTIONS FOR FUTURE WORKS

The study developed in this thesis showed that the Fick's Second Law describes satisfactorily the drying process performed through the model validation with the drying kinetics and the temperature of the product. In this way, it will be interesting to study this process after other mechanisms for the transport of water during drying, such as pressure driven flow and capillary flow, transport mechanisms of drying of porous media, Darcy's law, evaporation condensation theory, etc.

Within this work, it was demonstrated same benefits of different theoretical frameworks for studying: the movement of moisture with the measurement of the sorption isotherms and the energy transfer inside the solid through the measurement of the thermophysical properties. Although it was generated some interesting results, there are many model extensions we could consider, this includes simulating the models in a more realistic geometry.

It would also be interesting to create a fully three-dimensional model for drying, modelled as three dimensional shapes. With a three-dimensional model, it could be modeled the movement of water more accurately and it will be possible to calculate the contact area and the shrinkage volume.

The present model describes the behavior of one unripe banana slice, it could be performed a model beginning from the dryer operation, particular characteristics of the equipment, creating a more general model. In which, it could be used the COMSOL Multiphysics permitting us to perform innumerous simulations with different foodstuffs, it would only be enough to inform some properties of the product, such as: thermal conductivity, apparent density and heat capacity.

Consequently, it will be possible to save energy, time and work, performing simulations and evaluate the drying time, the quality of the product and the final moisture content with any foodstuff.

REFERENCES

AGRIANUAL 2012. Banana. *Anuario da Agricultura Brasileira*. São Paulo. FNP. Informa economics. South America, p.177-188, 2013.

AGUIRRE, A.; ALVAREZ, A.; CASTREJON, T.; CAROMNA, R.; BELLO, L.A. Moisture adsorption behavior of banana flours (*Musa paradisiaca*) unmodified and modified by acid-treatment. *Starch*, v.62, p.658–666, 2010.

AL-MUHTASEB, A. H.; MCMINN, W. A. M.; MAGEE, T. R. A. Water sorption isotherms of starch powders. Part 1: Mathematical description of experimental data. *Journal of Food Engineering*, v.61, p.297–307, 2004.

ALVARADO, J. D. D. Specific heat of dehydrated pulps of fruits. *Journal Food Process Engineering*, v.14, p.189, 1991.

ANDERSON R., Modifications of the BET equation. *Journal of the American Chemical Society*, v.68, p. 686–691, 1946.

ANDRIEU, J.; GONNET, E.; LAURENT, M. Pulse method applied to foodstuffs: thermal diffusivity determination. *Food Engineering and Process Applications.* Elsevier Applied Science, London, v.1, p. 447-455, 1986.

ASHRAE Handbook. Fundamentals. American society of heating, refrigeration and air-conditioning engineers, Inc., Chapter 30: Thermal properties of foods. pp. 30.1-30.26, 1993.

AUGUSTO, P. E. D.; CRISTIANINI, M. Determining the Convective Heat Transfer Coefficient (h) in Thermal Process of Foods. *International Journal of food Engineering*, v. 7, article 15, p. 54-75, 2011.

AVERSA, M., CURCIO, S., CALABRÒ, V., IORIO, G. Experimental evaluation of quality parameters during drying of carrot samples. *Food and Bioprocess Technology,* v.5, p. 118-129, 2012.

AZZOUZ, S.; GUIZANI, A.; JOMAA, W.; BELGHITH, A. Moisture diffusivity and drying kinetic equation of convective drying of grapes. *Journal of Food Engineering*, v.55, p. 323-330, 2002.

BAINI, R.; LANGRISH, T. A. G. Choosing an appropriate drying model for intermittent and continuous drying of bananas. *Journal of Food Engineering* v.79, p.330-343, 2007.

BATISTA, L. M.; DA ROSA, C.A.; PINTO, L. A. A. Diffusive model with variable effective diffusivity considering shrinkage in thin layer drying of chitosan. *Journal of Food Engineering*, v.81, p. 127–132, 2007.

BARATI, E., ESFAHANI, J.A. Mathematical simulation of convective drying: Spatially distributed temperature and moisture in carrot slab. *International Journal Thermal Science*, v.56, p. 86–94, 2012.

BENNAMOUN, L.; FRAIKIN, L.; LÉONARD, A. Modeling and simulation of heat and mass transfer during convective drying of wastewater sludge with introduction of shrinkage phenomena. *Drying Technology,* v.32, p. 13-22, 2014.

BIALOBRZEWSKI, I. Determination of the mass transfer coefficient during hot-air-drying of celery root. *Journal of Food Engineering*, v.78, p. 1388–1396, 2007.

BILIADERIS, C. G. The structure and interactions of starch with food constituents. *Canadian Journal of Physiology and Pharmacology*. v.69, p. 60–78, 1991.

BIRD, R.; STEWART, W.; LIGHTFOOT, E. Transport phenomena. John Wiley, 2002.

BRUNAUER, S.; DEMING, L.S.; DEMING, W.E.; TELLER, E. On a theory of the Van der Waals adsorption of gases. *Journal of the American Chemical Society*, v.62, p.1723–1732, 1940.

CARDOSO, J. M.; PENA, R. S. Hygroscopic behavior of banana (Musa ssp. AAA) flour in different ripening stages. *Food and Bioprocess Technology*, v.92, p. 73-79, 2014.

CARSLAW, H. S.; JAEGER, J. C. Conduction of Heat in Solids. Clarendon Oxford-Sciences Publication, 2th edition, 1959.

CARSON, E. M. Functional properties of banana starch. Master of Science Thesis. Massachusetts Institute of Technology, US. 1972.

CHEMKHI, S.; ZAGROUBA, F.; BELLAGI, A. Modelling and simulation of drying phenomena with rheological behavior. *Brazilian Journal of Chemical Engineering*, v.22, p. 153-163, 2005.

CHANDRA MOHAN, V. P.; TALUKDAR, P. Three dimensional numerical modeling of simultaneous heat and moisture transfer in a moist object subjected to convective drying*. International Journal of Heat and Mass Transfer*, v.53, p. 4638–4650, 2010.

CHEN, X. D. Simultaneous heat and mass transfer. In: SABLANI, S. S.; RAHMAN, M. S.; DATTA, A. K.; MUJUMDAR, A. S. *Handbook of food and bioprocess modeling techniques*. Boca Raton. CRC Press 2007.

CHOI, Y., OKOS, M.R. Thermal properties of liquid foods - Review. In: Physical and Chemical Properties of Food. *American Society of Agricultural Engineers* ASAE, New York, US, p. 35-77, 1986.

CHRISTELOVÁ, P.; VALÁRIK, M.; HŘIBOVÁ, E.; LANGHE, E.; DOLEZEL, J. A multi gene sequence-based phylogeny of the *Musaceae* (banana) family. *BMC Evolutionary Biology,* v.11, p.103-107, 2011.

CIHAN, A.; KAHVECI, K.; HACIHAFIZOGLU, O. Modelling of intermittent drying of thin layer rough rice. *Journal of Food Engineering*, v.79, p.293–298, 2007.

CORZO, O., BRACHO, N., PEREIRA, A., VÁSQUEZ, A. Weibull distribution for modelling air drying of coroba slices. *Food Science and Technology*, v.41, p. 2023-2028, 2008.

CRANK, J. The mathematics of diffusion. Oxford: Clarendon Press, 1995.

CUI, Z.; XU, S.; SUN, D. Microwave–vacuum drying kinetics of carrot slices. *Journal of Food Engineering*, v.65, p. 157–164, 2004.

CURCIO, S.; AVERSA, M.; CALABRÒ, V.; IORIO, G. Simulation of food drying: FEM analysis and experimental validation. *Journal Food Engineering*, v.87, p. 541–553, 2008.

DATTA, A. K. Heat transfer. In: SABLANI, S. S.; RAHMAN, M. S.; DATTA, A. K.; MUJUMDAR, A. S. *Handbook of food and bioprocess modeling techniques*. Boca Raton. CRC Press 2007.

DATTA, A. K. Status of physics-based models in the design of food products, processes, and equipment. Comprehensive Review *In Food Science and Food Safety*, v.7, p. 121–129, 2008.

DE BOER, J. H. The dynamical character of adsorption. Clarendon Press, Oxford, 1946.

DEFRAEYE, T. Advanced computational modelling for drying processes - a review. *Applied Energy*, v.131, p. 323–344, 2014.

DELGADO, J. M. P. Q.; BARBOSA DE LIMA, A. G. Transport phenomena and drying of solids and particulate materials. Springer Int Swtizerland, 2014.

De LIMA, A. G. B.; QUIROZ, M. R.; NEBRA, S. A. Simulteneous moisture transport and shrinkage during drying of solids with ellipsoidal configuration*. Chemical Engineering Journa*l, v.86, p. 85-93, 2002.

DITCHFIELD, C.; TADINI, C. C. Acompanhamento do processo de amadurecimento da banana nanicão (*Musa cavendishii Lamb.*) In: XVIII Congresso Brasileiro de Ciência e Tecnologia de Alimentos, 2002, Porto Alegre, RS. Anais do XVIII CBCTA. Porto Alegre: SBCTA, 2002. p. 1629-1632.

DITCHFIELD, C. Estudo do processamento continuo do purê de banana. Ph.D. Thesis. Escola Politécnica, São Paulo University. 2004.

ERBAY, Z.; ICIER, F. A review of thin layer drying of foods: Theory, modeling, and experimental results. *Critical reviews in food science and nutrition*, v.50, p. 441-464, 2010.

ERDOĞDU, F. Mathematical approaches for use of analytical solutions in experimental determination of heat and mass transfer parameters. *Journal of Food Engineering*, v.68, p. 233–238, 2005.

ERDOĞDU, F. A review on simultaneous determination of thermal diffusivity and heat transfer coefficient. *Journal of Food Engineering*, v.86, p. 453-459, 2008.

ERDOĞDU, F., LINKE, M., PRAEGER, U., GEYER, M., SCHLÜTER, O. Experimental determination of thermal conductivity and thermal diffusivity of whole green (unripe) and yellow (ripe) Cavendish bananas under cooling conditions. *Journal of Food Engineering*, v.128, p. 46-52, 2014.

FAISANT, N.; BULÉON, A.; COLONNA, P.; MOLIS, C.; LARTIGUE, S.; GALMICHE, J. P.; CHAMP, M. Digestion of Raw Banana Starch in the Small Intestine of Healthy Humans: Structural Features of Resistant Starch. *British Journal of Nutrition*, v.73, p. 111-123, 1995.

FAO (Food and Agriculture Organization of the United Nations). FAOSTAT statistics database (last updated Feb 2014), Agriculture, 2014.

FELDER, R. M.; ROUSSEAU, R. W. Elementary Principles of Chemical Processes. 3th ed. John Wiley: New York, 2000.

FERNANDES, F. A. N.; RODRIGUES, S.; LAW, C. L.; MUJUMDAR, A. S. Drying of exotic tropical fruits: A comprehensive review. *Food and Bioprocess Technology*, v.4, p. 163–185, 2011.

FIGURA, L. O.; TEIXEIRA, A. A. Food Physics Physical properties – Measurement and Applications. Springer-Verlag: Berlin, 2007.

FITO, P.; CHIRALT, A.; BARAT, J. M.; ALVARRUIZ, A. An Approach to the Modelling of Osmotic Dehydration Operations. Departamento de Tecnología de Alimentos. Universidad Politécnica de Valencia. *Process Optimisation and Minimal Processing of Foods*, p. 1-17, Valencia, Spain. 1996.

FRISCH, H. L.; STERN, S. A. Diffusion of small molecules in polymers. In CRC *Critical Reviews in Solid State and Materials Science*, v.2, p. 123-187, 1983.

GHIAUS, A. G.; MARGARIS, D. P.; PAPANIKAS, D. G. Mathematical modelling of the convective drying of fruits and vegetables. *Journal of Food Science*, v.62, p. 1154–1157, 1997.

GOLESTANI, R.; RAISI, A.; AROUJALIAN, A. Mathematical modeling on air drying of apples considering shrinkage and variable diffusion coefficient. *Drying Technology*, v.31, p. 40–51, 2013.

GOYAL, R.; KINGSLY, A.; MANIKANTAN, M.; ILYAS, S. Thin layer drying kinetics of raw mango slices. *Biosystems Engineering*, v.95, p. 43–49, 2006.

GUGGENHEIM, E. A. Applications of Statistical Mechanics. Clarendon Press, Oxford, 1966.

GUIMARÃES; J. L.; WYPYCH, F.; SAUL, C. K.; RAMOS, L. P.; SATYANARAYANA, K.G. Studies of the processing and characterization of corn starch and its composites with banana and sugarcane fibers from Brazil. *Carbohydrate Polymers,* v. 80, p. 130-138, 2010.

HALDERA, A.; DATTA, A. K. Surface heat and mass transfer coefficients for multiphase porous media transport models with rapid evaporation. *Food and Bioproducts Processing,* v.90, p. 475–490, 2012.

HANGOS, M. K.; CAMERON, T. I. *Process modeling and model analysis*. *Harcourt Science and Technology Company*, Academic Press, 2001.

HASSINI, L., AZZOUZ, S., PECZALSKI, R., BELGHITH, A. Estimation of potato moisture diffusivity from convective drying kinetics with correction for shrinkage. *Journal Food Engineering*, v.79, p. 47–56, 2007.

HE, X.; LAU, K.A.; SOKHANSANJ, S; LIM, J.C.; BI, T.X.; MELIN, S.; KEDDY, T. Moisture sorption isotherms and drying characteristics of aspen (*Populus tremuloides*). *Biomass and Bioenergy*, v.57, p. 161–167, 2013.

HERNANDEZ, J. A.; PAVON, G.; GARCIA, M. Analytical solution of mass transfer equation considering shrinkage for modelling food-drying kinetics. *Journal of Food Engineering*, v.45, p. 1–10, 2000.

HII, C. L.; LAW, C. L.; CLOKE, M. Modeling using a new thin layer drying model and product quality of cocoa. *Journal of Food Engineering*, v.90, p. 191–198, 2009.

HOLMAN, J. P. Experimental methods for engineers, fifth ed., McGraw-Hill Books, New York, 1986.

HUSSAIN, M. M.; DINCER, I. Two-dimensional heat and moisture transfer analysis of a cylindrical moist object subjected to drying: A finite-difference approach. *Journal of Heat and Mass Transfer*, v.46, p. 4033–4039, 2003a.

HUSSAIN, M. M.; DINCER, I. Analysis of two-dimensional heat and moisture transfer during drying of spherical objects. *International Journal of Energy Research*, v.27, p. 703-713, 2003b.

IGLESIAS, H. A.; CHIRIFE, J. Technical note: Correlation of BET monolayer moisture content in foods with temperature. *Journal of Food Technology,* v.19, p. 503–506, 1994.

INCROPERA, F. P.; DEWITT, D. P. Fundamentals of Heat and Mass Transfer, 3d. ed., J. Wiley & Sons, New York, 1990.

INFORME AGROPECUARIO. Produção, Colheita e Pós-colheita. EPAMIG. v.26, n. 228, 2005.

JAYAS, D. S.; CENKOWSKI, S.; PABIS, S.; MUIR, W. E. Review of thin layer drying and wetting equations. *Drying Technology,* v.9, p. 551–558, 1991.

JOHNSON, P. N. T.; BRENNAN, J. G.; ADDO-YOBO, F. Y. Air-drying characteristics of plantain (Musa AAB). *Journal Food Engineering,* v. 37, p. 233- 242, 1998.

JUAREZ-GARCIA, E.; AGAMA-ACEVEDO, E., SÁYAGO-AYERDI, S. G., RODRIGUEZ-AMBRIZ, S. L.;BELLO-PEREZ, L. A. Composition, digestibility and application in bread-making of banana flour. *Plant Foods for Human Nutrition*, v.61, p. 131–137, 2006.

KARIM, M. A.; HAWLADER, M. N. A. Drying characteristics of banana: theoretical modelling and experimental validation. *Journal Food Engineering,* v. 70, p.35 – 35. 2005a.

KARIM, M. A.; HAWLADER, M. N. A. Mathematical modelling and experimental investigation of tropical fruits drying. *International Journal of Heat and Mass Transfer*, v.48, p. 4914–4925, 2005b.

KATEKAWA, M. E.; SILVA, M. A. On the influence of glass transition on shrinkage in convective drying of fruits: a case study of banana drying. *Drying Technology*, v.25, p. 1659–1666, 2007.

KAYISU, K.; HOOD, L. F. Molecular structure of banana starch. *Journal of Food Science*, v.46, p. 1894–1897, 1981.

KIRANOUDIS, C. T.; MAROULIS, Z. B.; MARINOS-KOURIS, D.; SARAVACOS, G. D. Estimation of the effective moisture diffusivity from drying data. Application to some vegetables. Proceedings of the Sixth International Congress on Engineering and Food, 23-27 May, 1993, Makuhari Messe, Chiba, Japan.

KIRANOUDIS, C.T.; TSAMI, E.; MAROULIS, Z.B.; MORUNOS-KOURIS, D. Equilibrium moisture content and heat of desorption of some vegetables*. Journal of Food Engineering*, v.20, p. 55–74, 1993.

KOWALSKI, S. J. Mathematical modeling of shrinkage during drying. *Drying Technology,* v.14, p. 307–331, 1996.

KUMAR, C.; KARIM, M.A.; JOARDDER, M.U.H. Intermittent drying of food products: A critical review. *Journal of Food Engineering*, v.121, p. 48–57, 2014.

KUMAR, C.; KARIM, A.; JOARDDER, M.U.H.; MILLER, G.J. Modeling heat and mass transfer process during convection drying of fruit. In 4th International

Conference on Computational Methods, Gold Coast, Australia, November 25–28, 2012.

KUMAR, C.; KARIM, A.; SAHA, S.C.; JOARDDER, M.U.H.; BROWN, R.J.; BISWAS, D. Multiphysics modelling of convective drying of food materials. In Proceedings of the Global Engineering, Science and Technology Conference, Dhaka, Bangladesh, December 28–29, 2012.

KUMAR, C.; MILLAR, J. G.; KARIM, M. A. Effective diffusivity and evaporative cooling in convective drying of food material. *Drying Technology*, v.33, p. 227-337, 2015.

KURNIA, J.C., SASMITO, A.P., TONG, W., MUJUMDAR, A.S. Energy-efficient thermal drying using impinging-jets with time-varying heat input – a computational study. *Journal of Food Engineering*, v.114, p. 269–277, 2013.

LEWICKI, P.P. Data and Models of Water Activity. II: Solid Foods. In Food Properties Handbook, 2ed.; Rahman, M.S., Ed.; CRC Press: Boca Raton, 68-153, 2009.

LEMUS-MONDACA, R., BETORET, N., VEGA-GALVÉZ, A., LARA, E. Dehydration characteristics of papaya (*Carica pubenscens*): determination of equilibrium moisture content and diffusion coefficient. *Journal of Food Process Engineering*, v.32, p.645–663, 2009.

LEMUS-MONDACA, R.A., VEGA-GÁLVEZ, A., MORAGA, N.O. Computational simulation and developments applied to food thermal processing. *Food Engineering Reviews*, v.3, p. 121–135, 2011.

LEMUS-MONDACA R. A.; ZAMBRA, C. E.; VEGA-GÁLVEZ, A.; MORAGA, N. O. Coupled 3D heat and mass transfer model for numerical analysis of drying process in papaya slices. *Journal of Food Engineering,* v. 116, p.109-117, 2013.

LII, C. Y.; CHANG, S. M.; YOUNG, Y. L. Investigation of the physical and chemical properties of bananas starches. *Journal of Food Science*, v. 47, p.1493-1497, 1982.

LIMA, A. G. B.; QUEIROZ, M. R.; NEBRA, S. A. Heat and mass transfer model including shrinkage applied to ellipsoidal products: case study for drying of bananas. *Developments in Chemical Engineering and Mineral Processing,* v.10, p. 281-304, 2002.

LOZANO, J. E.; ROTSTEIN, E.; URBICAIN, M. J. Total porosity and open-pore porosity in the drying of fruits. *Journal of Food Science,* v.45, p. 1403-1407, 1980.

MAROUSIS, S. N.; SARAVACOS, G. D. Density and porosity in drying starch materials. *Journal of Food Science,* v.55, p. 1367-1372, 1990.

MARIANI, V.C., BARBOSA DE LIMA, A.G., DOS SANTOS COELHO, L. Apparent thermal diffusivity estimation of the banana during drying using inverse method. *Journal of Food Engineering,* v.85, p. 569-579, 2008.

MARIANI, V.C., BARBOSA DE LIMA, A.G., DOS SANTOS COELHO, L. Estimation of the apparent thermal diffusivity coefficient using an inverse technique. *Inverse Problems in Science and Engineering.* v. 17, p. 568-589, 2009.

MARINOS-KOURIS, D.; MAROULIS, Z. B. Transport properties in the drying of solids. In Handbook of Industrial Drying, 3ed.; Mujumdar, A.S., Ed.; CRC Press: Boca Raton, p. 82-119, 2006.

MATTEA, M.; URBICAIN, M. J.; ROTSTEIN, E. Prediction of thermal conductivity of vegetable foods by the Effective Medium Theory. *Journal of Food Science,* v.51, p. 113-115, 1986.

MAYOR, L.; SERENO, A. M. Modelling shrinkage during convective drying of food materials: a review. *Journal of Food Engineering*, v.61, p. 373-386, 2004.

MENDEZ, L. M. *Processo de aglomeração de farinha de banana verde com alto conteúdo de amido resistente em leito fluidizado pulsado.* Escola Politécnica, Universidade de São Paulo, São Paulo, 2013.

MENEZES, E. W.; MELO, A. T.; LIMA, G. H.; LAJOLO, F. M. Measurement of carbohydrate components and their impact on energy value of foods*. Journal of Food Composition and Analysis*, v.17, p. 331-338, 2004.

MENEZES, E.W.; DAN, M.C.; CARDENETTE, G.H.; GOÑI, I.; BELLO-PÉREZ, L.A.; LAJOLO, F.M. In Vitro Colonic Fermentation and Glycemic Response of Different Kinds of Unripe Banana Flour. *Plant Foods for Human Nutrition*, v.65, p. 379-385, 2010.

MIKETINAC, M. J.; SOKHANSANJ, S.; TUTEK, Z. Determination of heat and mass transfer coefficients in thin layer drying of grain. *Transactions of the ASAE*, v.35, p. 1853–1858, 1992.

MOHSENIN, N.N. Structure, Physical Characteristics and Rheological Properties. *Physical Properties of Plant and animal Materials*, v.1, part I (2 ed.), p. 73-84, 1968.

MOHSENIN, N.N. Thermal properties of Foods and Agricultural Materials, Gordon Breach, Science Publishers, 1980.

MOTA, R. V.; LAJOLO, F. M.; CORDENUNSI, B. R.; CIACCO, C. Composition and functional properties of banana flour from different varieties. *LWT-Food Science Technology,* v.52, p. 63–68, 2000.

MUJUMDAR, A. S. International drying symposium series (IDS): A personal perspective, *Drying Technology,* v.17, xi – xx, 1999.

MUSTAFFA, R.; OSMAN, A.; YUSOF, S.; MOHAMED, S. Physicochemical changes in Cavendish banana (Musa cavendishii, var. Montel) at different positions within a bunch during development and maturation. *Food Science and Agriculture*, v. 78, p. 201-207, 1998.

NELSON, C. S.; PLOETZ, R. C.; KEPLER, K. A. Musa species (banana and plantain) Musaceae (banana family). In: Species Profile for Pacific Island Agroforesty, v. 2.2, 2006. Available: www.agroforesty.org

NILNONT, W., THEPA, S., JANJAI, S., KASAYAPANAND, N., THAMRONGMAS, C., BALA, B. Finite elements simulation for coffee (Coffea arabica) drying. *Food and Bioproduct Processing,* v.90, p. 341-350, 2011.

NOGUEIRA, R. I. Processo de secagem de banana (Musa acuminata subgrupo *Cavendish* cultivar nanica) parametros ótimos na obtenção de banana-passa. Master Thesis, State University of Campinas, Campinas, Brazil, 1991.

OKOS, M.R.; NARSIMHAN, G.; SINGH, R.K.; WEITNAUER, A.C. Food Dehydration. In Handbook of Food Engineering, Heldman, D.R.; Lund, D.B., Eds.; New York: Marcel Dekker, 1992.

OZTOP, H., AKPINAR, E. Numerical and experimental analysis of moisture transfer for convective drying of some products. *International Communications in Heat and Mass Transfer* v.35, p. 169–177, 2008.

PERUSSELLO, C.A.; MARIANI, V.C.; MASSON, M. L.; CASTILHOS, F. Determination of thermophysical properties of yacon (*Smallanthus sonchifolius*) to be used in a finite element simulation. *International Journal of Heat and Mass Transfer*, v.67, p. 1163-1169, 2013.

PERUSSELLO, C.A.; MARIANI, V.C.; MENDES, L.A. Development of a linear heat source probe and determination of banana thermal conductivity. *International Journal of Food Engineering*, v.6, p. 1–15, 2010.

PLOETZ, R. C.; KEPLER, A. K.; DANIELLS, J.; NELSON, S. Banana and Plantain – an overview with emphasis on Pacific island cultivars. v.1, 2007. Available: www.agroforesty.org

PORNCHALOEMPONG, P., BALABAN, M.O., TEIXEIRA, A.A.; CHAU, K.V. Numerical simulation of conduction heating in conically shaped bodies. *Journal of Food Process and Engineering*, v.25, p. 539–550, 2003.

QUEIROZ, M. R. Theoretical and experimental study of the drying kinetics of banana. Doctor Thesis, State University of Campinas, Campinas, Brazil, 1994.

QUEIROZ M. R. NEBRA, S. A. Theoretical and experimental analysis of the drying kinetics of banana, *Journal of Food Engineering*, v.47 p. 127-132, 2001.

RAHMAN, M. S. Food Properties Handbook. CRC Press, 1995.

RAHMAN, N.; KUMAR, S. Thermal analysis of natural convective air drying of shrinking bodied. *International Journal of Energy Research*, v.31, p. 204–217, 2007.

RAHMAN, M. S.; POTLURI, P.L. Thermal conductivity of fresh and dried squid meat by line source thermal conductivity probe, *Journal of Food Science,* v.56, p. 582-583, 1991.

REID, R. C.; PRAUSNITZ, J. M.; SHERWOOD T. K. The properties of gases and liquids. 3th ed. McGraw-Hill, 1977.

RIEDEL, L., Measurements of thermal diffusivity on foodstuffs rich in water, *Kaltetechnik*, v.21, p. 315, 1969.

SABAREZ, H.T. Computational modelling of the transport phenomena occurring during convective drying of prunes. *Journal Food Engineering*. v.11, p. 279–288, 2012.

SAGILATA, M.G.; SINGHAL, R. S.; KULKARNI, P. R. Resistant starch – a review. *Comprehensive Reviews in food Science and Food Safety,* Chicago, v.5 p. 1-17, 2006.

SANDER, A.; SKANSI, D.; BOLF, N. Heat and Mass Transfer Models in Convection Drying of Clay Slabs. *Ceramics International*, v. 29, p. 641-653, 2003.

SANTOS, F. S. A.; FIGUEIREDO, R. M. F., QUEIROZ, A. J. M. Moisture adsorption isotherms of spiced cassava flour. *Rev. Bras. Prod Agroind*, v.6, p. 149–155, 2004.

SANTANA, F. F.; AUGUSTO, P. E. D.; CRISTIANINI, M. Determination of the convective heat transfer Coefficient (h) in the sterilization of retortable pouches. *International Journal of Food Engineering*, v.7, issue 1, articule 10, 2011.

SARAVACOS, G. D.; MAROULIS, Z. B. Transport properties of food. Marcel Decker, Inc. New York, US, 2001.

SCHIESSER, W. E. The Numerical Method of Lines. Academic Press, San Diego, 1991.

SCHOEBER, W. J. A. H. In *Proceedings of the first international symposium on drying;* Mujumdar, A. S., Ed.; Science Press: Princeton, NJ, p. 1-9, 1978.

SHAHARI, N.; HIBBERD, S. Mathematical Modelling of Shrinkage Effect During Drying of Food. *IEEE Colloquium on Humanities, Science & Engineering Research,* Kota Kinabalu, Sabah, Malaysia. p. 249-254, 2012.

SILVA, C. M. D. P. S.; SILVA, W. P.; FARIAS, V. S.; GOMES, J. P. Effective diffusivity and convective mass transfer coefficient during the drying of bananas,

Journal of the Brazilian Association of Agricultural Engineering, v.32, p. 342-353, 2012.

SILVA, C. S.; PEROSA, J. M. Y.; RUA, P. S.; ABREU, C. L. M.; PÂNTANO, S. C.; VIEIRA, C.R.Y.; BRIZOLA, R. M. O. Economic evaluation of the banana's losses in retail trade: a case study. *Revista Brasileira de Fruticultura*, v.25, p. 229-234, 2003.

SILVA, W. P.; HAMAWAND, I.; SILVA, C. M. D. P. S. A liquid diffusion model to describe drying of whole bananas using boundary-fitted coordinates. *Journal of Food Engineering*, v.137, p. 32–38, 2014.

SILVA, W. P.; PRECKER, J. W.; SILVA, C. M. D. P. S.; GOMES, J. P. Determination of effective diffusivity and convective mass transfer coefficient for cylindrical solids via analytical solution and inverse method: Application to the drying of rough rice. *Journal of food engineering,* v. 98, p. 302-308, 2010.

SILVA, W.P.; SILVA, C.M.D.P.S.; GAMA, F. J. A. An improved technique for determining transport parameters in cooling processes. *Journal of food engineering,* v. 111, p. 394-402, 2012.

SILVA, W. P.; SILVA, C. M. D. P. S.; SILVA, D. D. P. S.; SILVA, C. D. P. S. Numerical simulation of the water diffusion in cylindrical solids. *International Journal of Food Engineering*, v.4, p. 1-16, 2008.

SIMAL, A.; ROSSELLÓ, C.: BERNA, A.; MULET, A. Drying of shrinking cylinder shaped bodies. *Journal of Food Engineering*, v.37, p. 423–435, 1998.

SINGH, R. P. Thermal diffusivity in food processing. *Journal of Food Technology*, v.36, p. 87, 1982.

SPRICIGO, C. P. Perdas Pós-Colheita de Frutas e Hortaliças. Perdas Pós-Colheita de Frutas e Hortaliças. 2011. EMBRAPA. www.poscolheita.cnpdia.embrapa.br.

SOUZA, S. L.; BORGES, A. L. O cultivo da bananeira. Cruz das almas: EMBRAPA Mandioca e Fruticultura, 2004.

SUNTHARALINGAM, S; RAVINDRAM, G. Physical and biochemical properties of green banana flour. *Plant Food for Human Nutrition,* v. 43*,* p. 19 – 27, 1993.

SWEAT, V.E. Thermal properties of foods. *Engineering Properties of Foods,* Eds., Marcel Dekker, Inc., 1986.

SWEAT, V.E*. Engineering Properties of Foods*; Marcel Dekker: New York, 1994.

TONG, C. H.; LUND, D. B. Effective moisture diffusivity in porous materials as a function of temperature and moisture content. *Biotechnology programming,* v.6, p. 67-75, 1990.

TRIBESS, T. B. *Processo de obtenção de farinha de banana verde com alto conteúdo de amido resistente.* 2009. Tese (Doutorado em Engenharia Química) – Escola Politécnica, Universidade de São Paulo, São Paulo, 2009.

TRIBESS T.B.; HERNANDEZ-URIBE, J.P.; MENDEZ-MONTEALVO, M.G.C.; MENEZES, E.W.; BELLO-PEREZ, L.A.; TADINI; C.C. Thermal properties and resistant starch content of unripe banana flour (Musa cavendishii) produced at different drying conditions. LWT - Food Science and Technology, v.42, p. 1022–1025, 2009.

TRIPATHY, P.P.; KUMAR, S. Modeling of heat transfer and energy analysis of potato slices and cylinders during solar drying. *Applied Thermal Engineering*, v.29, p. 884–891, 2009.

VAGENAS, G. K.; KARATHANOS, V. T. Prediction of the effective moisture diffusivity in gelatinized food systems. *Journal of Food Engineering*, v.18, p. 159–179, 1993.

VERBOVEN, P., NICOLAI, B.M., SCHEERLINCK, N., DE BAERDEMAEKER, J. The local heat transfer coefficient in thermal food process calculations: A CFD approach. *Journal of Food Engineering,* v.33, p. 15–35, 1997.

VILLA-CORRALES, L., FLORES-PRIETO, J.J., XAMÁN-VILLASEÑOR, J.P., GARCÍA-HERNÁNDEZ, E. Numerical and experimental analysis of heat and moisture transfer during drying of Ataulfo mango. *Journal of Food Engineering*, v.98, p. 198–206, 2010.

VITRAC, O., TRYSTRAM, G. A method for time and spatially resolved measurement of convective heat transfer coefficient (h) in complex flows. *Chemical Engineering Science,* v.60, p. 1219–1236, 2005.

WANG, N.; BRENNAN, J.G. Moisture sorption isotherm characteristics of potatoes at four temperatures. Journal of Food Engineering, v.14, p. 269–282, 1991.

WANG, N.; BRENNAN, J. Changes in structure, density and porosity of potato during dehydration. *Journal of Food Engineering*, v.24, p. 61-76, 1995.

WANG, Z.; SUN, J.; LIAO, X.; CHEN, F.; ZHAO, G.; WU, J.; HU, X. Mathematical modeling on hot air drying of thin layer apple pomace. Food Research International, v.40(1), p. 39–46, 2007.

YAN, Z., SOUSA-GALLAGHER, M.J., OLIVEIRA, F. Shrinkage and porosity of banana, pineapple and mango slices during air-drying. Journal of Food Engineering 84, p. 430–440, 2008.

ZABALAGA, R.F.; CARBALLO, S. C. Convective Drying and Water Adsorption Behavior of Unripe Banana: Mathematical Modeling. *Journal of Food Processing and Preservation*. In press. DOI: 10.1111/jfpp.12352

ZARE, D.; MINAEI, S.; MOHAMAD ZADEH, M.; KHOSHTAGHAZA, M.H. Computer simulation of rough rice drying in a batch dryer. *Journal Energy Conversion and Management*, v.47, p. 3241-3254, 2006.

ZENEBON, O.; PASCUET, N. S. Métodos físico-químicos para análises de alimentos do Instituto Adolfo Lutz. 4a. ed, Brasília: IAL – Instituto Adolfo Lutz, p. 1018, 2005.

ZHANG, P; WHISTLER, R. L.; BEMILLER, J. N.; HAMAKER, B. R. Banana starch: production, physicochemical properties, and digestibility-a review. *Carbohydrate Polymers,* v. 59, p. 443-458, 2005.

ZHENGYONG, Y.; SOUSA-GALLAGHER, M.; OLIVEIRA, F. A. R. Shrinkage and porosity of banana, pineapple and mango slices during air-drying. *Journal of food engineering,* v.84, p. 430-440, 2008.

ZOGZAS, N. P.; MAROULIS, Z. B.; MARINOS-KOURIS, D. Moisture diffusivity data compilation in foodstuffs. *Drying Technology*, v.14, p. 2225–2253, 1996.

Appendix A

Algorithm

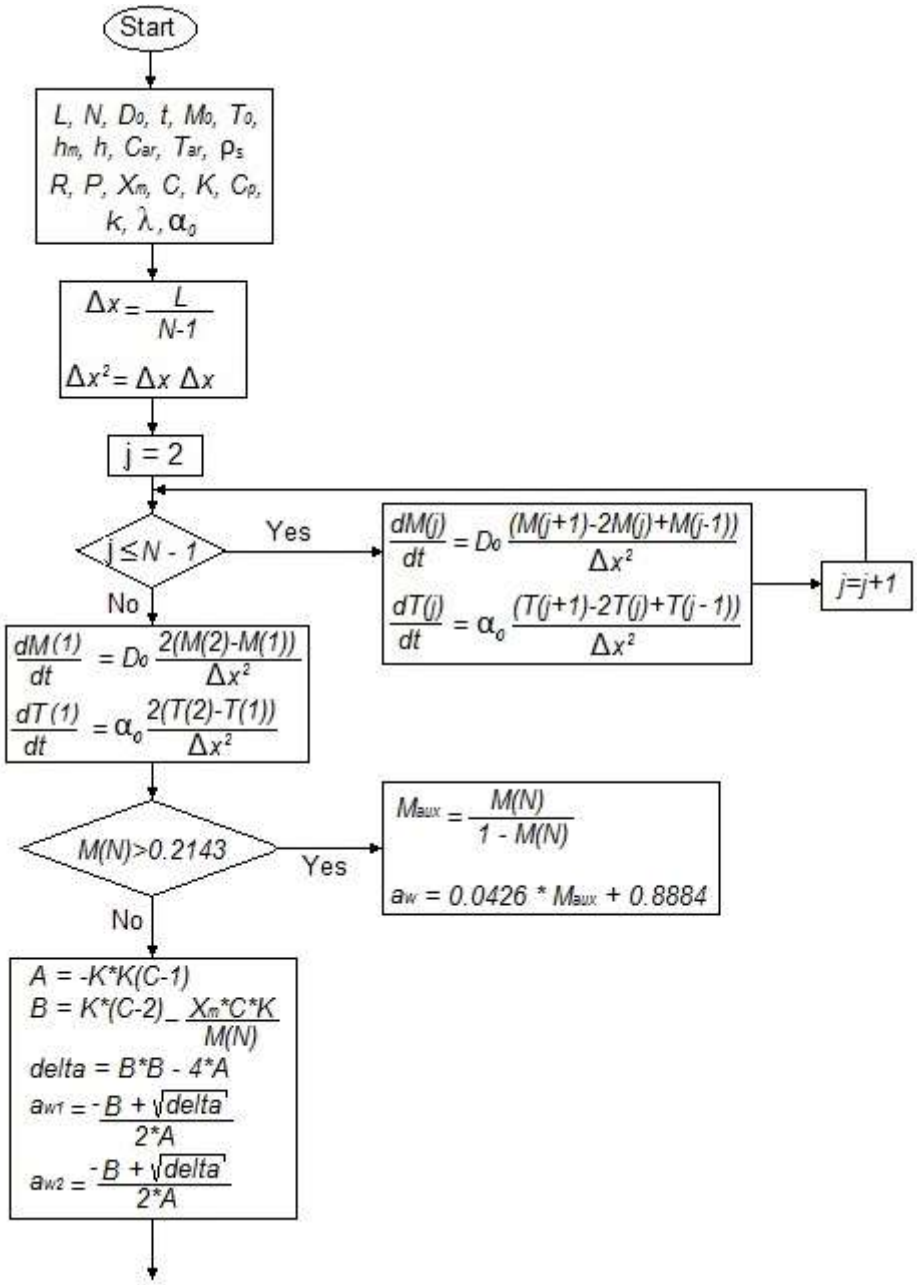

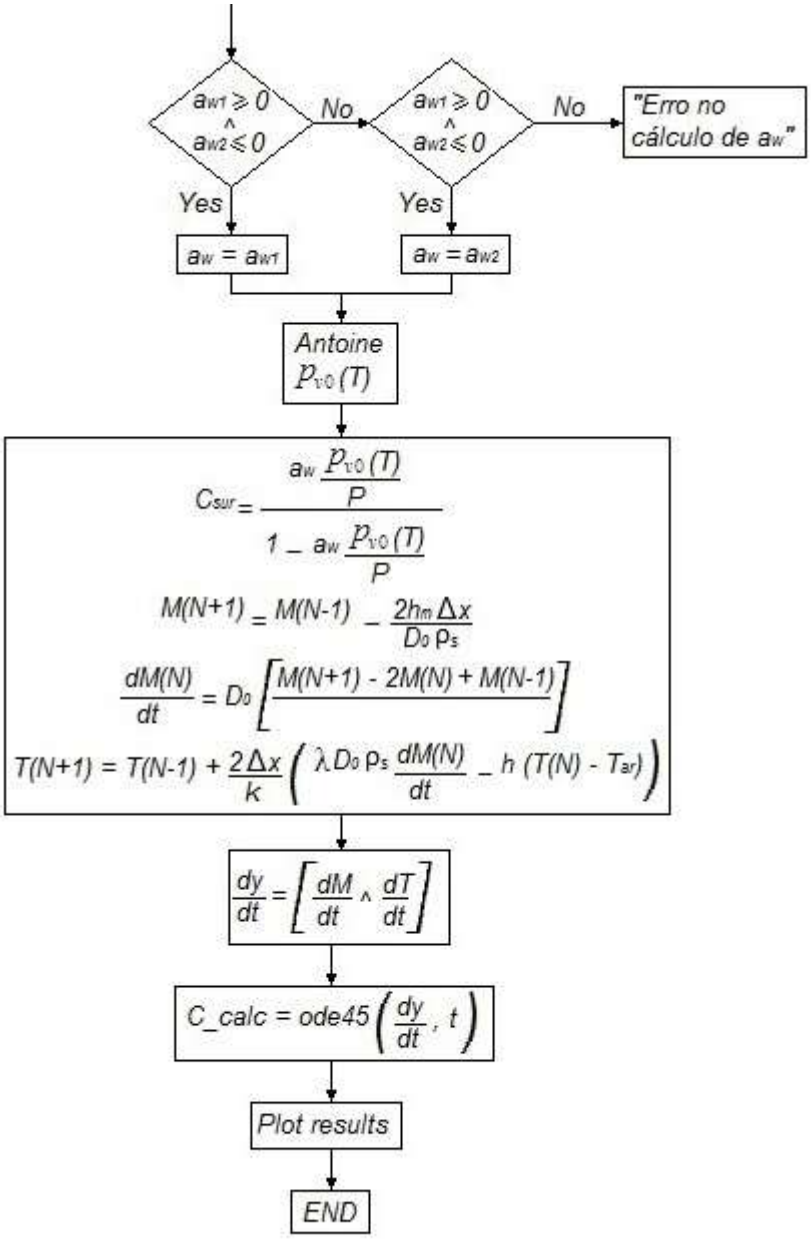
$a_{w1} \geq 0 \wedge a_{w2} \leq 0$
No
$a_{w1} \geq 0 \wedge a_{w2} \leq 0$
No
"Erro no cálculo de a_w"
Yes
Yes
$a_w = a_{w1}$
$a_w = a_{w2}$
Antoine
$P_{v0}(T)$
$C_{sur} = \frac{a_w \frac{P_{v0}(T)}{P}}{1 - a_w \frac{P_{v0}(T)}{P}}$
$M(N+1) = M(N-1) - \frac{2h_m \Delta x}{D_0 \rho_s}$
$\frac{dM(N)}{dt} = D_0 \left[\frac{M(N+1) - 2M(N) + M(N-1)}{}\right]$
$T(N+1) = T(N-1) + \frac{2\Delta x}{k}\left(\lambda D_0 \rho_s \frac{dM(N)}{dt} - h\,(T(N) - T_{ar})\right)$
$\frac{dy}{dt} = \left[\frac{dM}{dt} \wedge \frac{dT}{dt}\right]$
C_calc = ode45 $\left(\frac{dy}{dt}, t\right)$
Plot results
END

Appendix B

Experimental data of thermophysical properties

B-1. Thermal conductivity of unripe banana slices during process drying

Drying time [min]	k [W·m^{-1}·K^{-1}]					k average [W·m^{-1}·K^{-1}]	X_w [wb]	X [db]
	Slice 1	Slice 2	Slice 3	Slice 4	Slice 5			
0	0.758	0.705	0.796	-	-	0.753	0.7275	2.6695
30	0.359	1.171	0.578	0.635	0.895	0.728	0.6945	2.2736
60	0.61	0.62	0.651	0.494	0.524	0.580	0.6583	1.9268
120	0.408	0.351	0.282	0.354	0.432	0.365	0.5712	1.3321
150	0.288	0.379	0.372	0.264	0.303	0.321	0.5379	1.1642
180	0.219	0.299	0.368	0.219	0.235	0.268	0.4921	0.9689
210	0.201	0.208	0.369	0.187	0.299	0.253	0.4555	0.8365
240	0.191	0.261	0.242	0.2	0.247	0.228	0.4138	0.7059
270	0.167	0.28	0.18	0.197	0.233	0.211	0.3760	0.6026
300	0.162	0.19	0.158	0.114	0.102	0.145	0.3307	0.4942

B-2. Specific heat of unripe banana slices during process drying

Drying time [min]	C_p [MJ·m^{-3}·K^{-1}]					C_p average [MJ·m^{-3}·K^{-1}]	X_w [wb]	X [db]
	Slice 1	Slice 2	Slice 3	Slice 4	Slice 5			
0	4.800	4.194	4.520	-	5.369	4.721	0.7275	2.6695
30	2.987	5.635	3.898	4.354	5.369	4.449	0.6945	2.2736
60	4.349	4.284	5.101	3.318	3.898	4.190	0.6583	1.9268
120	3.163	2.889	2.423	3.083	3.454	3.002	0.5712	1.3321
150	2.569	3.156	3.188	2.246	2.556	2.743	0.5379	1.1642
180	1.992	2.485	2.892	2.036	2.133	2.308	0.4921	0.9689
210	1.871	2.065	3.050	1.647	2.494	2.225	0.4555	0.8365
240	1.755	2.361	2.217	1.764	2.055	2.030	0.4138	0.7059
270	1.534	2.298	1.364	1.613	2.017	1.765	0.3760	0.6026
300	1.525	1.601	1.352	1.128	0.994	1.320	0.3307	0.4942

B-3. Thermal difusivity of unripe banana slices during process drying

Drying time [min]	α [$mm^2 \cdot s^{-1}$]					α average [$mm^2 \cdot s^{-1}$]	X_w [wb]	X [db]
	Slice 1	Slice 2	Slice 3	Slice 4	Slice 5			
0	0.186	0.168	0.158	-	-	0.171	0.7275	2.6695
30	0.120	0.176	0.148	0.146	0.160	0.150	0.6945	2.2736
60	0.140	0.140	0.128	0.149	0.134	0.138	0.6583	1.9268
120	0.129	0.122	0.116	0.115	0.125	0.121	0.5712	1.3321
150	0.112	0.120	0.118	0.117	0.119	0.117	0.5379	1.1642
180	0.110	0.120	0.127	0.108	0.110	0.115	0.4921	0.9689
210	0.107	0.101	0.121	0.114	0.120	0.113	0.4555	0.8365
240	0.109	0.111	0.109	0.113	0.120	0.112	0.4138	0.7059
270	0.109	0.112	0.112	0.112	0.116	0.112	0.3760	0.6026
300	0.106	0.119	0.117	0.101	0.103	0.109	0.3307	0.4942

B-3. Porosity of unripe banana slices during process drying

Moisture content X_w [wb]	ε
0.7698	0.10 ± 0.01
0.6821	0.11 ± 0.01
0.6139	0.12 ± 0.01
0.6098	0.12 ± 0.02
0.5938	0.12 ± 0.01
0.5477	0.13 ± 0.01
0.5392	0.13 ± 0.02
0.4676	0.13 ± 0.02
0.4183	0.12 ± 0.01
0.3790	0.12 ± 0.01
0.3568	0.12 ± 0.02
0.3441	0.12 ± 0.03
0.2952	0.10 ± 0.02
0.2439	0.10 ± 0.02
0.2128	0.09 ± 0.01
0.1772	0.09 ± 0.01
0.1532	0.08 ± 0.01